

AN ABSTRACT OF THE THESIS OF

JOSEPH J. KARNIEWICZ for the degree of DOCTOR OF PHILOSOPHY

in PHYSICS presented on August 10, 1979

Title: DE-HAAS VAN-ALPHEN EFFECT IN THE QUANTUM LIMIT

Abstract approved: Redacted for privacy

Allen Wasserman

In this work we apply the finite temperature formulation of quantum statistical mechanics to an analysis of the de Haas-van Alphen effect in the quantum limit. A new expression is derived for the differential magnetic susceptibility which clearly shows the individual contributions of zero-temperature and non-zero temperature terms.

Interactions have been included in a linearized approximation and contact is made with more heuristic approaches.

Approximations in the form of algebraic expressions are made to the temperature correction terms and these are compared to the exact result for the various values of the parameters. The results, which are valid at very low temperatures, may be regarded as the quantum limit analog of the usual DHVA algebraic result.

Finally, the self-energy is calculated in Landau level states using a Yukawa potential in the Born approximation. Suggestions are made for a possible extension to a self-consistent Born approximation which would retain full quantum number information as well as incorporate range effects in a realistic fashion.

de-Haas van-Alphen Effect in the Quantum Limit

by

Joseph J. Karniewicz

A THESIS

submitted to

Oregon State University

in partial fulfillment of  
the requirements for the  
degree of

Doctor of Philosophy

Completed August 10, 1979

Commencement June 1980

APPROVED:

Redacted for privacy

\_\_\_\_\_  
Associate Professor of Physics

in charge of major

Redacted for privacy

\_\_\_\_\_  
Chairman of Department of Physics

Redacted for privacy

\_\_\_\_\_  
Dean of Graduate School

Date thesis is presented August 10, 1979

## ACKNOWLEDGEMENT

I would like to take this opportunity to thank all those who have provided help and encouragement throughout various aspects of this work.

In particular, concerning the technical aspects of this project, I would like to thank Professor Allen Wasserman who unfailingly gave of his time, insight, and expertise in matters of theoretical physics.

On a more personal note, I would like to thank my very special friend, Ruby Moon, who provided the initial encouragement to undertake the Ph.D. and who supplied moral support well above and beyond the call of duty throughout our stay in Corvallis.

I would also like to thank my parents whose confidence and encouragement were always present.

And finally, on a slightly metaphysical note, I would like to thank the Creator for providing such a fascinatingly constructed universe for us to play in and ponder.

## TABLE OF CONTENTS

I.	Introduction.....	1
II.	Magnetic Susceptibility for a Pure System	
	A. Lifshitz-Kosevitch Region.....	12
	B. Quantum Limit Region.....	19
III.	Magnetic Susceptibility for an Impure System.....	25
IV.	Temperature Corrections	
	A. Mathematical Analysis.....	40
	B. Graphical Analysis.....	42
V.	Self-Energy Calculation	
	A. Introduction.....	68
	B. Born Approximation.....	74
VI.	Summary and Conclusion	
	Discussion.....	89
	Bibliography.....	93
	Appendix A.....	94
	Appendix B.....	95
	Appendix C.....	98
	Appendix D.....	102
	Appendix E.....	105
	Appendix F.....	112

LIST OF ILLUSTRATIONS

<u>Figure</u>		<u>Page</u>
1	DHVA effect in the quantum limit for Bismuth at $T=.6^{\circ}\text{K}$	4
2	DHVA effect in the LK limit for Rhenium and Silver	4
3	Relationships among $E_n$ , $\bar{E}_n$ , and $\mu$ .	24
4	Magnetic field dependence of $\mu$ .	35
5	Effect of the magnetic field dependence of $\mu$ on the magnetic susceptibility of Bismuth for the $n=2$ level	35
6A	XT and XTA vs B	47
6B	XO and XT vs B	48
6C	X and XA vs B	49
	$T=.3 \quad T_d=.6 \quad N=3$	
7A	XT and XTA vs B	50
7B	XO and XT vs B	51
7C	X and XA vs B	52
	$T=.4 \quad T_d=.6 \quad N=3$	
8A	XT and XTA vs B	53
8B	XO and XT vs B	54
8C	X and XA vs B	55
	$T=.5 \quad T_d=.6 \quad N=3$	
9A	XT and XTA vs B	56
9B	XO and XT vs B	57
9C	X and XA vs B	58
	$T=.7 \quad T_d=.6 \quad N=3$	
10A	XT and XTA vs B	59
10B	XO and XT vs B	60
10C	X and XA vs B	61
	$T=.2 \quad T_d=.3 \quad N=3$	
11A	XT and XTA vs B	62
11B	XO and XT vs B	63
11C	X and XA vs B	64
	$T=.8 \quad T_d=1.2 \quad N=3$	
12A	XT and XTA vs B	65
12B	XO and XT vs B	66
12C	X and XA vs B	67
	$T=.3 \quad T_d=.1 \quad N=3$	

# de-Haas van-Alphen Effect in the Quantum Limit

## I. INTRODUCTION

An oscillatory dependence of the magnetic susceptibility of an electron gas with the applied magnetic field was first predicted under certain conditions by L.D. Landau<sup>(1)</sup>. This effect was observed under the predicted conditions of high magnetic field and low temperature by de-Haas and van-Alphen<sup>(2)</sup> in 1930 and now bears their name. It's real utility however was not appreciated until Lifschitz and Kosevich<sup>(3)</sup> pointed out that the period of the oscillations, when plotted against the reciprocal of the field strength, was directly proportional to the extremal cross-sectional areas of the electron fermi-surface (FS) in directions perpendicular to the magnetic field. This observation has enabled the de-Haas-van-Alphen effect to evolve into a highly sensitive probe of the FS of solids.

Typical DHVA data ( magnetic susceptibility (  $\chi$  ) vs  $1/B$  ) is shown in fig. 1 for both Silver and Rhenium. One should note not only the periodicity of the oscillations but also the fact that two or more oscillations may be present simultaneously depending upon the characteristics of the FS being examined.

As noted previously, the DHVA effect is intrinsically a high field, low temperature effect in which  $\hbar \omega_c \gg K_B T$  where  $\omega_c$  is the cyclotron frequency,  $K_B$  is Boltzmann's constant, and T is the temperature. The Lifschitz-Kosevich analysis<sup>(3)</sup> makes use of the

above conditions on temperature and field but also demands that

$$\hbar\omega_c \ll \mu \quad \text{where } \mu \quad \text{is the chemical potential of}$$

the electrons in the solid. For most metals this is the usual state of affairs even with "high" DHVA fields.

As the field strengths available to the experimentalist increase or equivalently for metals with an unusually small chemical potential, eg. Bismuth, the condition  $\hbar\omega_c \ll \mu$  is not automatically satisfied.

We shall refer to the region  $\hbar\omega_c \sim \mu$  as the quantum limit (QL) in contrast to the Lifschitz-Kosevich (LK) region where  $\hbar\omega_c \ll \mu$ .

In fig.2 we show a typical plot of magnetic susceptibility vs. field for Bismuth in the QL region. The purely sinusoidal oscillations which were present in the LK limit have evolved into a far more complex line shape in the QL. In fig. 2 one can simultaneously observe both LK and QL oscillations since two parts of the FS are involved and the electron surface reaches the QL before the hole surface. One can also observe in fig. 2 the characteristic split in the line shape caused by the two spin states of the electrons.

Although it may in principle be possible to analyze the QL line shapes in terms of LK oscillations and their harmonics ( just as it is possible to analyze a square wave in terms of its Fourier components ) it is both cumbersome and questionable to do so. The LK result is an expansion of  $\chi$  in the assumed small parameter  $\hbar\omega_c/\mu$  and applying it outside of this region raises doubts as to its convergence. It may even be totally inappropriate to attempt to apply the LK analysis to the QL region since the theoretical express-



Figure one shows the DHVA susceptibility oscillations in  
a) Rhenium and b) Silver in the high  $n$  region. (ref. 5)

Figure two shows the last ( $n=0$ ) DHVA oscillation in the differential magnetic susceptibility for Bismuth at  $T=6^{\circ}\text{K}$  with  $B$  along the binary axis. The broken line is a schematic version of what the curve might be at  $T=0$  if there were no broadening and if the fast oscillations due to holes were absent. The pair of arrows indicate spin split peaks. (ref. 4)

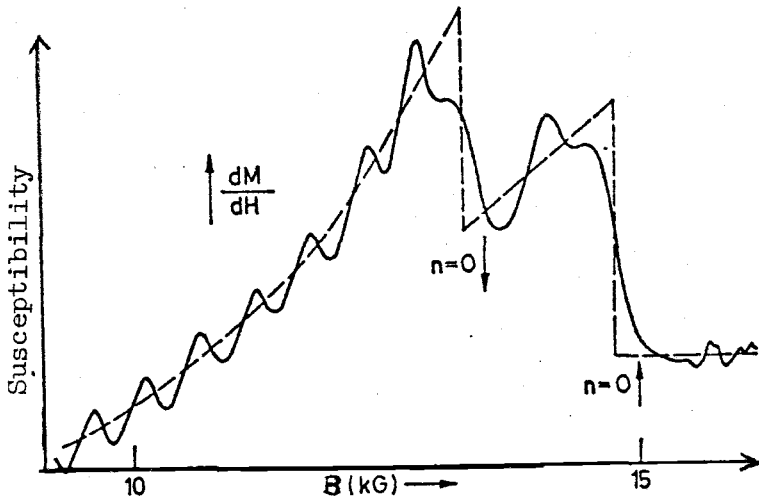


Fig. 2

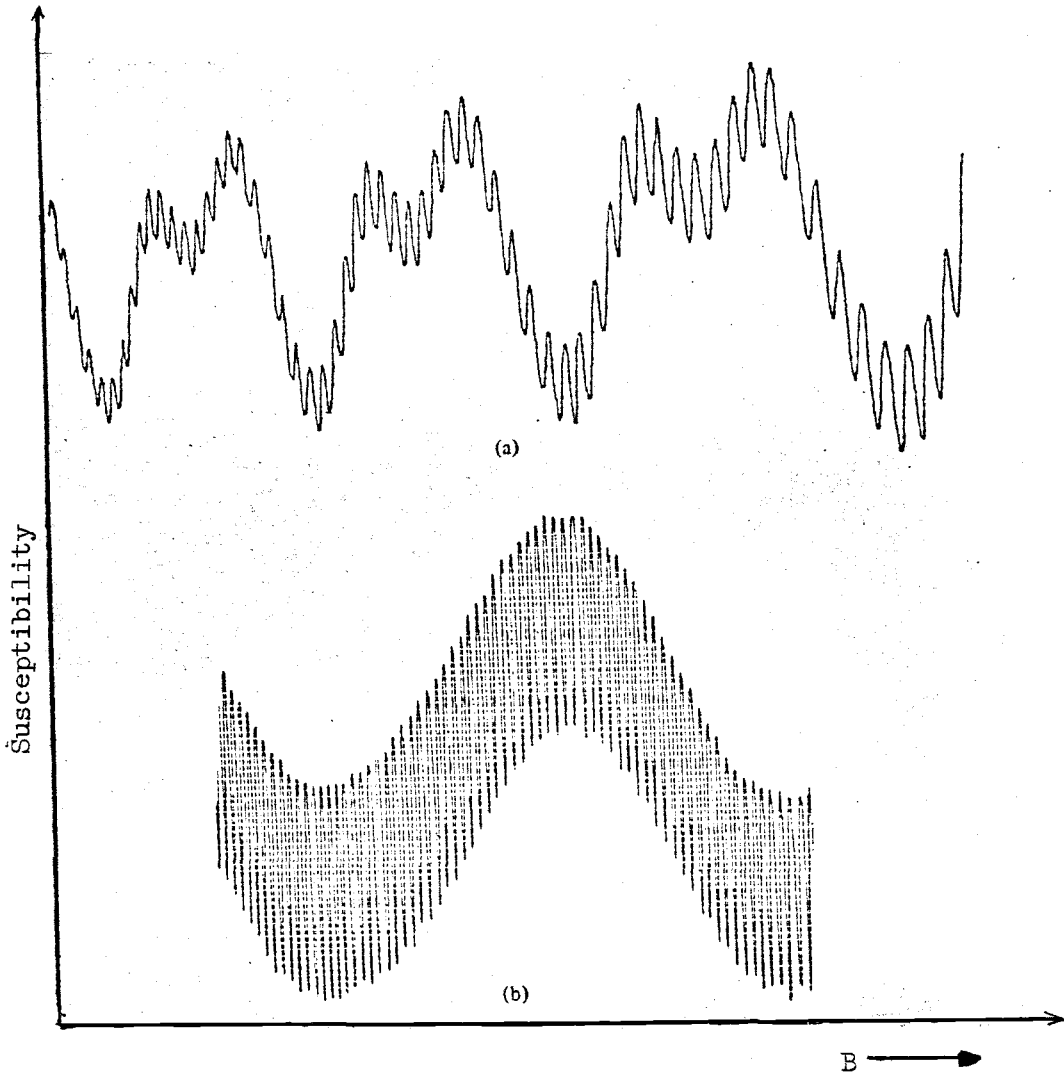


Fig. 1

-ion derived by Lifschitz-Kosevich is not the total susceptibility of the electron gas but rather the oscillatory part of the susceptibility, i.e. the total susceptibility with the Pauli and Landau terms subtracted out. In the QL region on the other hand it is only the total susceptibility which is observed and which is capable of analysis.

The effect of introducing impurities into the lattice in which the electrons are contained also provides another distinction between magnetism in the LK as opposed to the QL region.

Dingle<sup>(6)</sup> showed in a heuristic manner that the introduction of impurity scattering in the LK limit would cause the normal amplitude factor  $\exp[-K_B T / \hbar \omega_c]$  to be modified by a temperature enhancement factor  $T_D = |\Sigma_I| / \pi K_B$  where  $\Sigma_I$  is the zero temperature limit of the self-energy due to impurity scattering.<sup>1</sup> The effect of impurity scattering therefore is to cause a reduction in the amplitude of the oscillations equivalent to increasing the temperature by an amount equal to the Dingle temperature  $T_D$ . Excessive impurity scattering is thus capable of quenching the amplitude of the oscillations if the magnetic field is of insufficient strength.

In the QL however, the predominant effect of impurity scattering is to modify the steep slope on the high field side of any given quantum limit peak. As we shall see in Ch. 2 the differential susceptibility<sup>2</sup>

---

1. Dingle himself did not associate the Dingle temperature with a self-energy.

2. The differential susceptibility is defined as  $dM/dB$  in contrast to the susceptibility which is defined as  $M/B$ .

in the QL for a pure system suffers a discontinuity at certain field values. It diverges as these field values are approached from the low field side and tends to a finite value when approached from the high field side. The introduction of impurities into the lattice removes the divergence and discontinuity in  $\chi$  at these critical values and produces a large but finite slope on the high field side of the critical value.

Although several experiments have already been performed in the QL<sup>(7)</sup>, the only theory available for data analysis has been rather heuristic in its inclusion of impurity scattering and remains incomplete in that the final result for the susceptibility is expressed solely in terms of an integration to be done numerically. Information concerning impurity scattering is then obtained through a trial and error approach in which one searches for those parameters which yield the best fit after numerical integration to the high field slope of the QL peak.

To date, there does not exist in the literature a first principles analysis of the differential susceptibility for an electron gas in an impure lattice which is applicable to the quantum limit. For reasons mentioned above such a derivation would require a completely different mathematical approach from that employed in the LK region and would not be a mere extension of the LK result into the high field region. Furthermore, such a derivation should preferably be grounded in many-body theory and not be forced to include interactions in a heuristic manner.

The main focus of Ch. 3 of the present work is to introduce into

the literature such an analysis.

Experiments in the QL<sup>(7)</sup> have also indicated that the Dingle temperature, which is responsible for the slope on the high field side of the quantum limit peak, may in certain impurity systems actually be dependent upon the strength of the magnetic field.

To understand the origin of such effects, it is necessary to calculate the self-energy due to impurity scattering in the presence of a strong magnetic field.

In even the most favorable of situations, with weak but realistic potentials and no multiple scattering, such a calculation can be extremely difficult. More complex situations require increasingly more sophisticated approximations to the self-energy resulting in increasingly more difficult calculations. In fact, in order to make any progress at all it has become common practice to simplify the nature of the scattering potentials to the ultra short range delta function.

This has the advantage of introducing mathematical simplification into the analysis but only at the expense of losing information concerning the range of the potential as well as any quantum number dependence which the self-energy may have.

Apart from an attempt by Brailsford<sup>(8)</sup>, there has not appeared in the literature a calculation of the self-energy in any approximation which attempts to use a realistic potential with range effects in full magnetic field states. Of course the mathematical difficulties involved in such a calculation would preclude its use in a highly sophisticated self-energy approximation such as a self-consistent T-matrix approach. But it is quite possible that restoring some detail to the scattering

potentials may allow even a Born approximation to the self-energy to adequately account for some of the observed experimental data.

In Ch. 4 of the present work we attempt such a calculation as described above using a screened coulomb potential to calculate the self-energy within the restrictions of a simple Born approximation.

We are aware of the possible inadequacies of such an approximation to the self-energy which ignores multiple scattering and suggest a way to incorporate the above result into a self-consistent Born approximation which even in the delta function model suggests interesting B and impurity concentration dependencies.

The points discussed above are developed according to the following format.

In chapter two we shall discuss the DHVA effect in both the QL and LK limits but shall restrict ourselves to an electron gas in a perfect lattice using the effective mass approximation. Although this chapter is mainly pedagogical much of it is based upon a new approach to the problem which will allow us to clearly focus on the physical and mathematical distinction between the two regimes as well as providing a frame of reference in which to compare the more difficult calculation of chapter three for the impure lattice.

Even though the results for the differential susceptibility for electrons in a perfect lattice in the LK limit are well known <sup>(3)</sup>, the mathematical techniques used to obtain them here are unique to our approach and possess certain logical advantages over other derivations; primarily in the manner in which the analysis allows the susceptibility to be decomposed into its three unique physical components ( Landau,

Pauli, and DHVA) in the LK region.

The result we obtain in chapter two for the zero temperature contribution to the susceptibility in the QL has also appeared in the literature <sup>(9)</sup>. But the methods employed in reference nine require that the susceptibility at non-zero temperature be obtained from the zero temperature susceptibility by means of a numerical integration with a temperature broadening function.

Our derivation proceeds along quite different lines from those now currently appearing in the literature and we find that our derivation allows the susceptibility to be expressed in terms of two distinct components. One which corresponds solely to the zero temperature contribution and on which clearly shows in an additive fashion the corrections which temperature will introduce. Our form has the further advantage that one can focus on the mathematically more complex temperature correction terms and perhaps approximate them with simple useable functions.

In chapter three, which is the main focus of this work, we present for the first time a rigorous derivation for the low temperature differential magnetic susceptibility in the quantum limit of an electron gas in an impure lattice. The starting point of the derivation is Luttinger's theorem <sup>(10)</sup> which expresses the thermodynamic potential for an interacting system in terms of the Fourier coefficients of the Matsubara Green's function for the system.

Just as for the non-interacting case, the result for the susceptibility shows the individual contribution of zero-temperature and non-zero temperature terms. These terms are more complex than

those for the non-interacting case discussed in chapter two, but it is shown that they reduce properly to the non-interacting result (derived from the more familiar starting point of chapter two) in the limit that the self-energy approaches zero.

In chapter four we turn our attention to the non-zero temperature terms and attempt to find those physical regions in which they may be approximated by certain asymptotic forms. We present there a series of computer generated plots which compare the asymptotic approximations to the  $T \neq 0$  terms with their "exact" values as obtained through a numerical integration. We also compare the graphs generated for the contribution to the total susceptibility ( temperature + zero-temperature) of a single LL using both the exact temperature and approximate temperature forms and try to determine those regions in which the replacement causes a negligible difference in the observed line shapes for the total susceptibility.

In chapter five we briefly review some of the approaches and inherent difficulties involved in calculating the self-energy caused by impurity scattering in an impure lattice. We present there for the first time a calculation of the self-energy in the Born approximation using a realistic Yukawa potential in full magnetic field states.

We find that the result is capable of detailed analysis in certain regions of the parameters but would require numerical evaluation in others. We conclude our investigation at this point since numerical work on the self-energy would begin to pave the way for an extensive investigation of how the simple Born approximation which we discuss may be incorporated into a more sophisticated self-consistent Born



approximation. The task would certainly be non-trivial but would include multiple scattering events in a manner which hopefully would be adequate to show the interplay between range, field strength, and quantum numbers which would give rise to a field dependent Dingle temperature under the appropriate conditions, eg. weak but long range scattering potentials.

In chapter six we review what has been accomplished in this work and make certain suggestions as to how the analysis of the QL which we have presented may be used to provide alternate and complementary methods for analyzing quantum limit experiments in addition to those which are currently in use.

## II. MAGNETIC SUSCEPTIBILITY FOR A PURE SYSTEM

### A. LIFSHITZ-KOSEVITCH REGION

The analysis begins with the calculation of the thermodynamic potential ( $\Omega$ ) which may be defined as <sup>(11)</sup>,

$$\Omega = -\frac{1}{\beta} \ln \text{Tr} e^{-\beta [\hat{H} - \mu \hat{N}]} \quad (2-1)$$

where the symbols and notation used are defined in appendix A.

Once  $\Omega$  is calculated, the magnetization  $M$ , the susceptibility  $\bar{\chi}$ , and the differential susceptibility  $\chi$ , may be found from the following prescriptions,

$$M = -\left(\frac{\partial \Omega}{\partial B}\right)_{\mu}, \quad \bar{\chi} = \frac{M}{B}, \quad \chi = \frac{dM}{dB} \quad (2-2)$$

For a non-interacting system of particles the expression for  $\Omega$  simplifies considerably to the form <sup>(11)</sup>,

$$\Omega = -\frac{1}{\beta} \sum_j \ln [1 + e^{-\beta(\epsilon_j - \mu)}] \quad (2-3)$$

The single particle eigenvalues are found by solving the eigenvalue equation,  $H \psi_j = \epsilon_j \psi_j$ , where for the system under consideration  $H$  has the form,

$$H = (\bar{p} + e\bar{A}/c)^2 + V(\bar{r}) - \bar{\mu}_s \cdot \bar{B} \quad (2-4)$$

where,

$\bar{A}(\bar{r})$  is the vector potential and is related to  $\bar{B}$  by  $\bar{B} = \nabla \times \bar{A}$

$\bar{V}(\bar{r})$  is the crystal potential experienced by the electrons.

We shall assume that the effect of the crystal potential may be adequately accounted for by introducing a band effective mass ( $m^*$ ) into the kinetic energy term. The mass which appears in the magneton ( $\mu_B$ ) is left unchanged since the spin potential energy being non-coulombic is not affected by the motion of the electrons in the crystal field (except that the g-factor may be modified by crystal potential effects through spin-orbit coupling).

With these assumptions, the Hamiltonian takes the form,

$$H = \left[ -i\hbar \nabla + e\bar{A}/c \right]^2 - \bar{\mu}_s \cdot \bar{B}$$

(2-5)

There exists some flexibility in the choice of  $\bar{A}$  since only the curl of the vector potential need be specified. Traditionally two gauges are employed in dealing with magnetic problems - the symmetric gauge in which  $A_\phi = B\rho/2$ ,  $A_z = A_\rho = 0$  and the Landau gauge in which  $A_x = -By$ ,  $A_y = A_z = 0$ . Both gauges will yield a constant magnetic field  $B$  in the  $z$  direction.

In the symmetric gauge the eigenfunctions and eigenvalues are found to be <sup>(12)</sup> in the limit of a system of infinite volume,

$$\Psi(\rho, \phi, z) \propto R_n(\rho) e^{im\phi} e^{ik_z z}$$

$$m = 0, \pm 1, \dots; \quad -\infty \leq k_z \leq +\infty; \quad n = 0, 1, 2, \dots; \quad \sigma = \pm 1$$

$$R(\rho) = e^{-\xi/2} \xi^{|m|/2} \omega(\xi) \quad ; \quad \xi = \gamma \rho^2 \quad 14.$$

$$\gamma = m \omega_c / \hbar$$

$$\omega(\xi) = {}_1F_1[-n, |m+1|, \xi]$$

$$\begin{aligned} \sum_{n, m, K_z, \sigma} = & \left[ n + \frac{|m| - m}{2} + \frac{1}{2} \right] \hbar \omega_c^* + \frac{\hbar^2}{2m^*} K_z^2 - \\ & - \sigma G \hbar \omega_c \end{aligned}$$

(2-6)

Some interesting features of these states may be noted. First, as the magnetic field is turned off and  $\omega_c \rightarrow 0$ , the energy spectrum does not reduce to the expected free electron result. The resolution of this apparent discrepancy was first discussed by Rensinck<sup>(13)</sup>, who showed that the order in which one takes the limits  $V \rightarrow \infty$  and  $B \rightarrow 0$  is crucial in recovering the free electron result.

Secondly, we see that there exists an angular momentum dependent energy differential between those states with positive and those with negative angular momentum. It has been shown that this effect will feed back into the Fermi-Dirac distribution function and give rise to a net orbital magnetic moment. If we recall that the classical Bohr-vanLeeuwen<sup>(14)</sup> theorem predicts that the orbital magnetization of an electron gas is identically equal to zero, we may conclude that in all aspects, both spin and orbital, electron magnetism is a purely quantum phenomena.

Thirdly, for  $m > 0$ , the degeneracy in the energy is apparently infinite (or at least proportional to some power of the infinite volume).

In the Landau gauge, the solution to the eigenvalue problem takes the form<sup>(12)</sup>,

$$\Psi_{\alpha}(\vec{r}) = e^{i k_x x} e^{i k_z z} e^{-\gamma/2 (y-y_0)^2} H_n [\sqrt{\gamma} (y-y_0)]$$

$$\varepsilon_{\alpha} = (n + 1/2) \hbar \omega_c^* - \sigma G \hbar \omega_c + \frac{\hbar^2}{2m^*} k_z^2$$

$$\alpha = (n, k_x, k_z, \sigma)$$

where,  $\gamma = m \omega_c / \hbar$  and  $y_0 = k_x / \gamma$ . (2-7)

We again note the apparent infinite degeneracy due to the absence of the  $k_x$  quantum number in the energy. This degeneracy factor may be determined by means of a heuristic argument developed by Landau<sup>(12)</sup>. He argued that the center of oscillation of the harmonic oscillator eigenfunction,  $y_0$ , must lie within the confines of the solid, i.e.  $0 \leq y_0 \leq L_y$ . But since  $y_0$  is related to  $k_x$ , this puts a bound on the range of  $k_x$  such that  $0 \leq k_x \leq \gamma L_y$ . Thus the number of allowed  $k_x$  values we may have is  $\gamma L_x L_y / 2\pi$ . This shows that the degeneracy is proportional to the area of the solid perpendicular to the magnetic field and to the strength of the magnetic field itself. This field dependent degeneracy is crucial to understanding the DHVA and all other oscillatory magnetic phenomena.

Taking the degeneracy factor into account and choosing a unit volume, we find that

$$\Omega = -\frac{D}{\beta} \sum_{\substack{n=0 \\ \sigma=\pm 1}}^{\infty} \int_{-\infty}^{\infty} dk_z \ln [1 + e^{-\beta \varepsilon_{\alpha}}]$$

where,

$$\bar{\epsilon}_\alpha = \epsilon_\alpha - \mu = (n + 1/2) \hbar \omega_c + A k_z^2 - \sigma G \hbar \omega_c - \mu \quad 16.$$

$$D = m \omega_c / 4 \pi^2 \hbar$$

$$A = \hbar^2 / 2 m^*$$

(2-8)

An integration by parts with respect to  $k_z$  yields,

$$\Omega = -2DA \sum_{n,\sigma} \int_{-\infty}^{\infty} dk_z \frac{k_z^2}{1 + e^{\beta \bar{\epsilon}_\alpha}}$$

(2-9)

The identity,

$$\frac{1}{1 + e^z} = \frac{1}{2\pi i} \int_{b-i\infty}^{b+i\infty} \pi \csc \pi s e^{-sz} dz \quad (0 < |b| < 1)$$

(2-10)

may be used to obtain the form,

$$\Omega = -\frac{DA}{i\pi} \int_{-\infty}^{\infty} dk_z \int_{b-i\infty}^{b+i\infty} \sum_{n,\sigma} ds k_z^2 \pi \csc \pi s e^{-\beta s \bar{\epsilon}_\alpha}$$

(2-11)

Finally the  $k_z$  integration may be done to yield

$$\Omega = -\frac{\tilde{C}}{2\pi i} \sum_{n,\sigma} \int_{b-i\infty}^{b+i\infty} \frac{\pi \csc \rho_0 s}{s^{3/2}} e^{-\bar{\epsilon}_n s} ds$$

where,

$$\tilde{C} = \frac{e B \sqrt{2m^* \pi}}{h^2 c \beta}, \quad \rho_0 = \pi / \beta$$

$$\bar{\epsilon}_n = (n + 1/2) \hbar \omega_c^* - \sigma G \hbar \omega_c - \mu$$

(2-12)

It is at this point that the physical distinction between magnetism in the LK and QL regions causes the analysis to take different routes.

In the LK region, the ratio of  $\mu/\hbar\omega_c$  is  $\gg 1$  so that there are many densely packed levels below the FS. As the magnetic field is increased, the Landau levels (LL) start to pass through the FS as a quasi-continuum. Electrons in states above the Fermi energy enter states of lower energy whose degeneracy has been increased enough to accommodate them. It is the combined effect of LL's riding up through the FS and electrons falling down to lower LL's, which are increasing in energy and degeneracy, which gives rise to the oscillatory behavior seen in the DHVA effect.

To mathematically reflect this near continuum of levels in the LK region, it is appropriate to perform the sum of LL's called for in eq. 2-12.

The result of this summation is,

$$R = \frac{-\tilde{C}}{2\pi i} \int_{b-i\infty}^{b+i\infty} ds \frac{\pi \csc \rho_0 s \cosh \lambda s}{\sinh \lambda^* s}$$

where,  $\lambda = G \hbar \omega$ ,  $\lambda^* = \hbar \omega^*/2$ . (2-13)

At this stage the following Mittag-Leffler expansion can be introduced into the integrand<sup>(15)</sup>,

$$\frac{\pi \csc \rho_0 s}{\sinh \lambda^* s} = \frac{\beta}{\lambda^*} + \sum_{n=-\infty}^{+\infty} \frac{(-1)^n \beta}{(s - n\beta) \sinh \beta \lambda^* n} +$$

$$+ \sum_{N=-\infty}^{+\infty} \frac{(-1)^{N+1} i \pi}{\lambda^* (S - N\pi i / \lambda^*) \sinh N\pi^2 / \beta \lambda^*}$$

where  $\sum'$  means omit the  $n=0$  term. (2-14)

Each of the three terms in the above expansion will yield contributions to  $\Omega$  which we call  $\Omega_1$ ,  $\Omega_2$ ,  $\Omega_3$  respectively. For "weak" fields ( $\hbar \omega_c \ll \mu$ ) it has been shown<sup>(15,16)</sup> that the first term gives rise to the familiar Pauli paramagnetic susceptibility, the second to the Landau diamagnetic susceptibility, and the third to the DHVA oscillatory susceptibility.

Specifically  $\Omega_3$  may be put into the form,

$$\Omega_3 = -\tilde{c} \sum_{n,\sigma}' \frac{(-1)^n \pi}{\sinh N\pi^2 / \beta \lambda^*} \frac{\Theta(\delta)}{\beta \lambda^* \Gamma(3/2)} \left[ \int_0^\delta \sqrt{x} \sin \left[ \frac{N\pi}{\lambda^*} (\delta - x) \right] dx \right]$$

where,  $\delta = \beta [\mu - \sigma \lambda]$  (2-15)

It is important to note the appearance of the term  $\sinh N\pi^2 / \beta \lambda^*$  in the denominator. For high temperatures and low fields this term will contribute an amplitude factor which behaves as  $\exp(-K_0 T / \hbar \omega_c^*)$  effectively damping the amplitude of the oscillations. Thus the experiment is intrinsically a low temperature, high field experiment.

Mention should be made at this point of the pioneering work of R.B.Dingle<sup>(6)</sup> in extending the above analysis of the DHVA effect to include electron-impurity interactions. In that case, the LL's are no longer exact eigenstates of the system and electrons will scatter out of the LL's at a rate determined by the interactions. Dingle



incorporated this effect into the analysis by giving each LL a Lorentzian line shape with a width determined by the scattering rate. When this broadening was folded into the calculation for  $\chi$ , he found that the scattering could be viewed as a temperature enhancement effect on the amplitude of the oscillations. Instead of  $\exp(-k_B T / \hbar \omega_c^*)$  there would now be a term  $\exp(-k_B [\tau + \tau_D] / \hbar \omega_c^*)$  where  $\tau_D$  is the so-called Dingle temperature.

In the quantum limit discussed in the next section, the condition  $\hbar \omega_c^* \ll \mu$  no longer applies since the LL's are widely spaced which causes them to pass through the FS as individual spin split levels. As noted by Rode<sup>(7)</sup>, this physical situation has its mathematical consequence in that we refrain from performing the sum over  $n$  in eq. 2-12 anticipating that the susceptibility will be ultimately expressible as a sum of nearly non-overlapping terms whose main contribution at any field strength will come from that LL which is about to pass or has just passed through the FS.

### B. QUANTUM LIMIT REGION

Rather than summing over  $n$  as in the LK limit we now work directly with eq. 2-12 and employ the following Mittag-Leffler expansion,

$$\pi \coth \beta S = \frac{\beta}{S} + 2\beta S \sum_{k=1}^{\infty} \frac{(-1)^k}{[S^2 - k^2 \beta^2]}$$

(2-16)

This produces a decomposition of  $\chi$  into  $\chi_0$  and  $\chi_{\tau}$  where,

$$\Omega_0 = \frac{-\beta \tilde{C}}{2\pi i} \sum_{\substack{n=1 \\ \sigma=\pm 1}}^{\infty} \int_{b-i\infty}^{b+i\infty} ds \frac{e^{-\bar{\epsilon}_n s}}{s^{5/2}}$$

$$\Omega_T = \frac{-\beta \tilde{C}}{i\pi} \sum_{\substack{n, \sigma \\ K}} \int_{b-i\infty}^{b+i\infty} ds \frac{(-1)^K e^{-\bar{\epsilon}_n s}}{s^{1/2} [s^2 - K^2 \beta^2]} \quad (2-17)$$

(2-18)

Here  $\Omega_0$  implies temperature independence while  $\Omega_T$  implies temperature corrections to  $\Omega_0$ . This will become evident as the development continues.

If we make use of the fact that,

$$\frac{1}{[s^2 - K^2 \beta^2]} = \frac{-1}{2K\beta} \left[ \int_0^{\infty} dx e^{(s-K\beta)x} + \int_0^{\infty} dx e^{-(s+K\beta)x} \right]$$

(2-19)

then we may write for either term in the resulting sum for  $\Omega_T$ ,

$$\Omega_T^{\pm} = \frac{\tilde{C}}{2\pi i} \sum_{n, \sigma, K} \frac{(-1)^K}{K} \int_0^{\infty} dx e^{-K\beta x} \int_{b-i\infty}^{b+i\infty} ds \frac{e^{-s[\bar{\epsilon}_n \pm x]}}{s^{1/2}} dx$$

(2-20)

In both  $\Omega_0$  &  $\Omega_T^{\pm}$ , the integrals which appear may be thought of as members of the following class of integrals,

$$C_\nu(\alpha, \Sigma) \equiv \frac{1}{2i} \int_{b-i\infty}^{b+i\infty} \frac{ds}{s^\nu} \cos \Sigma' s e^{\alpha s}$$

(2-21)

which closely resemble the Hankel representation for the reciprocal

$\Gamma$  function, viz. (17)

$$\frac{1}{\Gamma(\nu)} = \frac{1}{2\pi i} \int_{b-i\infty}^{b+i\infty} \frac{e^{\alpha s}}{s^\nu} \frac{ds}{\alpha^{\nu-1}}$$

(2-22)

Although this class of integrals does not appear directly in the free electron case, it does appear in the interacting system and the free electron case may then be thought of as the  $\Sigma' \rightarrow 0$  limit of the more general problem.

With this notation we may now write,

$$\begin{aligned} \Omega_0 &= -\frac{\tilde{C}\beta}{\pi} C_{5/2}(-\bar{\Sigma}_n, 0) \\ \Omega_\tau^\pm &= -\frac{\tilde{C}}{\pi} \int_0^\infty dx L(x) C_{1/2}(-\bar{\Sigma}_n \pm x, 0) \end{aligned}$$

(2-23)

where,

$$L(x) \equiv \ln [1 + e^{-\beta x}]$$

The function  $L(x)$  has come about by explicitly performing the sum over  $k$ .

For the special case of  $\Sigma' = 0$  which defines the free electron case, we can see directly that,

$$C_{1/2}(\alpha, 0) = \frac{\Gamma(1/2)}{\sqrt{\alpha}} \Theta(-\alpha)$$

$$C_{5/2}(\alpha, 0) = \Gamma(-3/2) \alpha^{3/2} \Theta(-\alpha)$$

(2-24)

This enables  $\Omega_0$  and  $\Omega_{\Gamma}^{\pm}$  to be put into the form,

$$\Omega_0 = -\frac{\tilde{c}\beta}{\pi} \cdot \frac{4}{3} \Theta(-\bar{\xi}_n) |\bar{\xi}_n|^{3/2}$$

$$\begin{aligned} \Omega_{\Gamma}^{\pm} &= -\frac{\tilde{c}}{\sqrt{\pi}} \int_0^{\infty} dx \frac{\Theta[-\bar{\xi}_n \pm x] L(x)}{\sqrt{-\bar{\xi}_n \pm x}} \\ &= -\frac{\tilde{c}}{\sqrt{\pi}} \left[ \int_{-\bar{\xi}_n \Theta(-\bar{\xi}_n)}^{\infty} \frac{L(\gamma + \bar{\xi}_n)}{\sqrt{\gamma}} d\gamma + \Theta(-\bar{\xi}_n) \int_0^{-\bar{\xi}_n} \frac{L[-(\gamma + \bar{\xi}_n)]}{\sqrt{\gamma}} d\gamma \right] \end{aligned}$$

(2-25)

where a change of variable has been used to obtain the last expression in 2-25.

These results are not pursued further since they are embodied in the complete analysis for the interacting system which appears in the next chapter.

Nevertheless we can make several observations. The step function  $\Theta(-\bar{\xi}_n)$  implies that as soon as a LL passes through the FS it no longer contributes to  $\Omega_0$ . Furthermore, if we were to calculate the differential susceptibility  $\chi$ , a second derivative in B would introduce a

$|\bar{\xi}_n|^{-1/2}$  dependence which diverges as  $\bar{\xi}_n \rightarrow 0$ . This is to be expected since the LL's are infinitely sharp in energy and their passing through the FS introduces discontinuities in  $M$  which are reflected in the infinite derivatives. It can be shown that the differential susceptibility, when calculated for a non-interacting system in the LK limit, also suffers this fate. Of course the introduction of impurities into the system will remove this divergence in both limits.

We also note that as expected, the main contribution to  $\chi$  in the QL is due to a single LL - that one which is currently passing through the FS and producing a zero in  $\bar{\xi}_n$ .

In the next chapter we shall repeat the calculation for  $\Omega$  in the quantum limit with the inclusion of interactions between the electrons and impurity scatterers in the lattice. Although the method used is of necessity quite different from that of the non-interacting system, the mathematics is surprisingly similar.

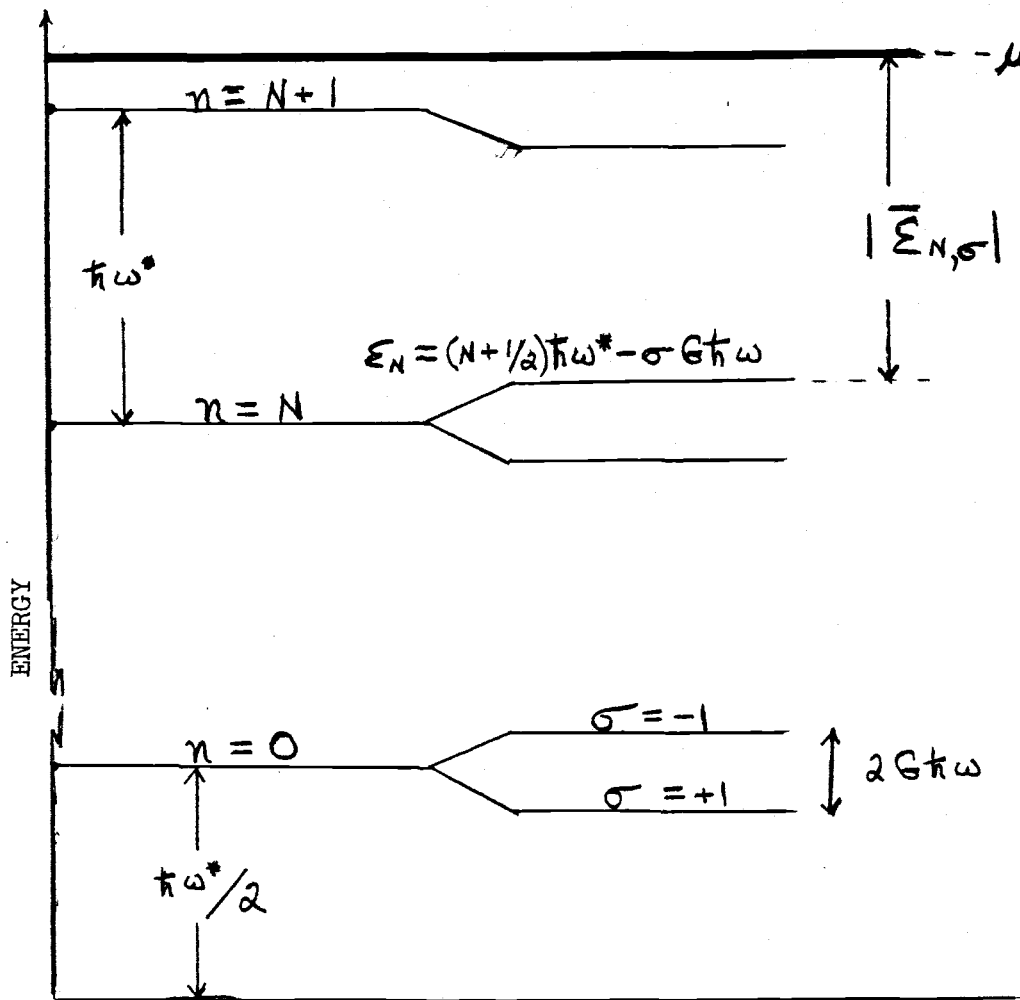


Fig. 3

Figure three illustrates the relationship among,

$$\epsilon_n = (n + 1/2)\hbar\omega_c^* - \sigma G\hbar\omega,$$

$$\bar{\epsilon}_n = (n + 1/2)\hbar\omega_c^* - \sigma G\hbar\omega - \mu, \text{ and}$$

$\mu$ .

### III. MAGNETIC SUSCEPTIBILITY FOR AN IMPURE SYSTEM

In order to calculate  $-\Omega$  for an interacting system, we will use the formalism of non-zero temperature quantum statistical mechanics.

The central quantity in this formalism is the Green's function which is defined as<sup>(18)</sup>,

$$G(\bar{x}, \tau, \bar{x}', \tau') = -T_{\tau} \left\{ \hat{\rho}_G T_{\tau} [\Psi_{\kappa}(\bar{x}, \tau) \Psi_{\kappa}^{\dagger}(\bar{x}', \tau')] \right\} \\ = G(\bar{x}, \bar{x}', \tau - \tau') \quad \text{if } \frac{\partial H}{\partial \tau} = 0.$$

(3-1)

where  $\Psi(\bar{x}, \tau)$  and  $\Psi^{\dagger}(\bar{x}', \tau')$  are field operators in the complex time Heisenberg picture, i.e.  $\Psi(\bar{x}, \tau) = e^{\hat{K}\tau/\hbar} \Psi(\bar{x}) e^{-\hat{K}\tau/\hbar}$  with  $\hat{K} = \hat{H} - \mu \hat{N}$ .  $\hat{H}$  is the hamiltonian of the system,  $\hat{N}$  is the number operator, and  $\mu$  is the chemical potential.  $\tau$  is the analytically continued complex time variable which is related to the real time through  $\tau = -it$ .  $T_{\tau}$  is an operator which, for purely imaginary time, orders quantities according to decreasing values of  $\tau$ . The quantity  $\hat{\rho}_G$  is the grand canonical density operator which for thermal equilibrium is defined as  $\hat{\rho}_G = e^{\beta[\Omega - \hat{K}]}$ .

A very important property of the temperature Green's function which follows directly from the cyclical property of the trace is its periodic structure in the  $\tau$  variable<sup>(18)</sup>. Specifically we can show that  $G(\bar{x}, \bar{x}', \tau) = -G(\bar{x}, \bar{x}', \tau - \beta\hbar)$ . Because of this property we may expand  $G$  in a Fourier series,

$$G(\bar{x}, \bar{x}', \tau) = \frac{1}{\beta\hbar} \sum_l e^{-i\beta\omega_l \tau} G(\bar{x}, \bar{x}', \beta\omega_l)$$

(3-2)

where,  $f_\alpha = (2l+1)\pi/\beta$ ;  $l = 0, \pm 1, \dots$  for fermions.

One can also show that in the set of states  $|\alpha\rangle$  which diagonalizes the hamiltonian,  $G(\bar{x}, \bar{x}', f_\alpha)$  has the form<sup>(18)</sup>,

$$G(\bar{x}, \bar{x}', f_\alpha) = \sum_\alpha \frac{\langle x|\alpha\rangle \langle \alpha|x'\rangle}{i f_\alpha - \bar{\epsilon}_\alpha/\hbar} \quad (3-3)$$

The  $G(f_\alpha)$  play a central role in the analysis to follow because of the following theorem developed by Luttinger<sup>(10)</sup> which expresses  $\Omega$  in terms of the  $G(f_\alpha)$ ,

$$\Omega = -\frac{1}{\beta} \sum_l \text{Tr} \ln \left[ -\frac{1}{G(f_\alpha)} \right] \quad (3-4)$$

This expression, which is strictly valid for the calculation of the non-analytic parts of  $\Omega$ <sup>(19)</sup>, has also been shown to be valid for the entire thermodynamic potential in the limit of low temperature<sup>(20)</sup>.

The Green's function can also be shown to satisfy a Dyson type integral equation,

$$G = G_0 + G_0 \Sigma G \quad (3-5)$$

where  $G_0$  is the Green's function for the non-interacting system,  $G$  is the Green's function for the fully interacting system, and  $\Sigma$  is the self-energy operator.



From the Dyson equation, we may formally write,

$$G^{-1} = G_0^{-1} - \Sigma \quad (3-6)$$

In terms of the states  $|\alpha\rangle$ , which diagonalize  $G_0$  ( for our considerations these will be the Landau levels ), we have,

$$\langle \alpha | G^{-1} | \alpha' \rangle = \langle \alpha | G_0^{-1} | \alpha \rangle \delta_{\alpha\alpha'} - \langle \alpha | \Sigma | \alpha' \rangle \quad (3-7)$$

At this stage we may note another fundamental distinction between the LK and QL regions which occurs in the manner in which the self-energy may be treated.

It has been demonstrated by Fowler and Prange<sup>(21)</sup> and Soven<sup>(22)</sup> that for short range potentials in the weak field region ( $\hbar\omega_c \ll \mu$ ), it is sufficient as a first approximation to calculate the self-energy in plane wave states as if the magnetic field were absent. The resulting introduction of the false  $k_y$  quantum number, in addition to the expected  $k_x$  and  $k_z$  quantum numbers is dealt with by averaging the self-energy over extremal orbits perpendicular to the  $k_z$  direction.

In the QL we are not at liberty to make a weak field approximation. The self-energy will remain a function of the full set of LL quantum numbers  $(n, k_x, k_z)$  as well as the magnetic field itself and indeed it is expected that some of the interesting features of the QL will arise specifically because of this  $n$  dependence.

In chapter five it is shown that  $\langle \alpha | \Sigma | \alpha' \rangle$  will be diagonal in the Landau level states if we assume that the impurity potentials

have azimuthal symmetry about the z axis - a not too restrictive assumption for a model calculation.

This assumption provides for a considerable simplification in the formalism since<sup>3</sup>,

$$\begin{aligned} \text{Tr} \ln(-1/\hat{G}) &= \sum_{\alpha} \langle \alpha | \ln(-\hat{G}^{-1}) | \alpha \rangle \\ &= \sum_{\alpha} \ln[-\langle \alpha | \hat{G}^{-1} | \alpha \rangle] \end{aligned}$$

(3-8)

Thus we may write that,

$$\Omega = -\frac{1}{\beta} \sum_{\alpha, l} \ln[\bar{\epsilon}_{\alpha} + \Sigma(\alpha, \beta_{\alpha}) - i\beta_{\alpha}]$$

(3-9)

where,

$$\bar{\epsilon}_{\alpha} = (n + 1/2)\hbar\omega_c + \frac{\hbar^2}{2m^*} k_z^2 + \sigma G\hbar\omega_c - \mu$$

(3-10)

With the help of an integral representation for the logarithm

which is reviewed in appendix B, we may write  $\Omega$  as

$$\begin{aligned} \Omega = -\frac{1}{\beta} \sum_{\alpha} \left[ -\sum_{\beta_{\alpha} > 0} \int_b^{b+i\infty} \frac{ds}{s} e^{-s\beta_{\alpha}} \right. \\ \left. + \sum_{\beta_{\alpha} < 0} \int_{b-i\infty}^b \frac{ds}{s} e^{-s\beta_{\alpha}} \right] \quad (0 < |b| < 1) \end{aligned}$$

(3-11)

---

3. In the case that  $\langle \alpha | \hat{\epsilon} | \alpha' \rangle$  is off diagonal, as will occur for example with spin dependent potentials, the Green's function becomes a matrix and must be diagonalized prior to all subsequent manipulations.

where,

$$g(\rho_q) = \bar{\Sigma}_\alpha + \Sigma^1(\alpha, \rho_q) - i \rho_q. \quad (3-12)$$

It is at this point that this theory distinguishes itself from other approaches. The closed form sum over  $\rho_q$  in eq. 3-11 is in practice impossible to perform. Some authors<sup>(21)</sup> have been able to use only the leading term as in the special case of electron-phonon interactions in which a high temperature result permits just the  $\rho_0$  term to be taken while others<sup>(23)</sup> have attempted a numerical evaluation of the sum. The approach we shall follow, first developed by Bharatiya and Wasserman<sup>(24,25)</sup>, consists in expanding  $g(\rho_q)$  about  $\rho_0$ , retaining the first two terms in the expansion and then summing over all  $Q$ . It has been applied to the impurity and electron-phonon problem<sup>(24)</sup> and has been able to turn the imaginary axis formulation of statistical mechanics into a practical quasi-particle approach for dealing with interacting systems.

Mathematically this approximation to the exact result is dependent upon  $\Sigma^1(\rho_q)$  being a slowly varying function of  $\rho_q$ . Alternatively one may conceive of the approach as attempting to develop a one or more parameter approximation to an otherwise unassailable problem. The approach will ultimately stand or fall on its ability to describe the experimental data.

We proceed with the analysis by using the Poisson sum formula to accomplish the sum over  $Q$ . That is,

$$\sum_{\rho_q > 0} e^{-s g(\rho_q)} = \sum_{\nu=-\infty}^{+\infty} \int_0^{\infty} dy e^{-2\pi i \nu y} e^{-s g(y)} \quad (3-13)$$

As discussed previously, we shall assume that

$$g(y) = g(0) + y \left. \frac{dg(y)}{dy} \right|_{y=0} \quad (3-14)$$

Performing the summations and integrations called for in eq. 3-13 will require the use of the following properties of  $\Sigma'$ , all of which are easily derivable from the spectral relation<sup>(18)</sup>,

$$\Sigma'(p_e) = \frac{1}{2\pi} \int_{-\infty}^{\infty} \frac{\Gamma(\omega)}{i p_e - \omega} d\omega ; \quad \Gamma(\omega) \gg 0$$

$$\text{Im } \Sigma'(p_e) > 0 \quad \text{For } p_e < 0$$

$$\text{Im } \Sigma'(p_e) < 0 \quad \text{For } p_e > 0$$

$$\Sigma'(-p_e) = \Sigma'^*(p_e)$$

(3-15)

We shall also employ the identity,

$$\sum_{\nu=-\infty}^{\infty} \frac{1}{2\pi i \nu + z} = \frac{1}{1 - e^{-z}} \quad (\text{Re } z > 0)$$

(3-16)

By using relations 3-15 and 3-16, eq. 3-11 reduces to

$$\Omega = \frac{1}{\beta} \sum_{\alpha} \int_b^{b+i\infty} \frac{ds}{s} \frac{e^{-s g(0)}}{[1 + e^{-s g'(0)}]} - \frac{1}{\beta} \sum_{\alpha} \int_{b-i\infty}^b \frac{ds}{s} \frac{e^{-s g^*(0)}}{[1 + e^{-s g'^*(0)}]}$$

(3-17)

Making use of the actual form of  $g(0)$ , we can write after some algebraic simplification,

$$\Omega = \frac{-1}{2i\beta} \sum_{\alpha} \int_b^{b+i\infty} \frac{e^{-s[\bar{\epsilon}_{\alpha} + \epsilon'(p_0, \alpha) - \epsilon'(p_0, \alpha)/2]}}{\sin[s(p_0 + i\epsilon'(p_0)/2)]} + \frac{1}{2i\beta} \sum_{\alpha} \int_{b-i\infty}^b \frac{e^{-s[\bar{\epsilon}_{\alpha} + \epsilon^*(p_0, \alpha) - \epsilon'^*(p_0, \alpha)/2]}}{\sin[s(p_0 - i\epsilon'^*(p_0)/2)]}$$

$$\epsilon'(p_0) = \left. \frac{d}{dy} \epsilon'(y) \right|_{y=0}$$

(3-18)

Although we could continue using the above form and develop a two parameter theory involving  $\epsilon'$  and  $\epsilon'^*$  we shall henceforth assume that,

$$\epsilon'(p_0) \ll \epsilon(p_0) ; \quad \epsilon'(p_0) \ll p_0 = \pi/\beta$$

(3-19)

Thus we may finally write  $\Omega$  as

$$\Omega = \frac{-1}{2i\beta} \sum_{\alpha} \left[ \int_b^{b+i\infty} \frac{ds}{s} \frac{e^{-s[\bar{\epsilon}_{\alpha} + \epsilon(p_0)]}}{\sin p_0 s} + \int_{b-i\infty}^b \frac{ds}{s} \frac{e^{-s[\bar{\epsilon}_{\alpha} + \epsilon^*(p_0)]}}{\sin p_0 s} \right]$$

(3-20)

In eq. 3-20 the sum over states is of the form,

$$\sum_{\alpha} = \mathcal{D} \int_{-\infty}^{\infty} dk_z ; \quad \mathcal{D} = \frac{m\omega_c}{4\pi^2 \hbar}$$

(3-21)

We now further assume that  $\Sigma'(k_z)$  is a slowly varying function of

$k_z$  so that,

$$\int_{-\infty}^{\infty} e^{-Ask_z^2} f(\Sigma'(k_z)) dk_z \approx f(\Sigma'(0)) \left[ \frac{\pi}{AS} \right]^{1/2}$$

$$A = \hbar^2/2m^*$$

(3-22)

With this assumption we may now write,

$$\begin{aligned} n = \frac{-\tilde{c}}{2\pi i} \Sigma'_{n,0} \left[ \int_b^{b+i\infty} \frac{ds}{s^{3/2}} \pi \operatorname{csc} \rho_0 s e^{-s[\bar{\epsilon}_n + \Sigma'(p_0)]} \right. \\ \left. + \int_{b-i\infty}^b \frac{ds}{s^{3/2}} \pi \operatorname{csc} \rho_0 s e^{-s[\bar{\epsilon}_n + \Sigma'(p_0)]} \right] \end{aligned}$$

$$\tilde{c} = \frac{eB}{h^2 c} \frac{\sqrt{2m^* \pi}}{\beta}$$

(3-23)

Contact may now be made with the results which were derived from a more conventional point for the non-interacting system by letting

$\Sigma' = 0$  in eq. 3-23 and comparing the result with eq. 2-12.

Making use of the expansion <sup>(26)</sup>,

$$\pi \operatorname{csc} \rho_0 s = \frac{\beta}{s} + 2s\beta \sum_{k=1}^{\infty} \frac{(-1)^k}{[s^2 - k^2\beta^2]}$$

(3-24)

as well as the relations <sup>(26)</sup>,

$$\frac{1}{[s^2 - k^2 \beta^2]} = \frac{-1}{2k\beta} \left[ \int_0^\infty e^{(s-k\beta)x} dx + \int_0^\infty e^{-(s+k\beta)x} dx \right] \quad 33.$$

$$\sum_{k=1}^{\infty} \frac{(-1)^k}{k} e^{-kx} = -\ln [1 + e^{-x}] \quad (3-25)$$

(3-26)

allows us to write,  $\Omega = \Omega_0 + \Omega_T^+ + \Omega_T^-$  where

$$\Omega_0 = -\frac{\tilde{C}\beta}{2\pi i} \sum_{n,\sigma} I_{5/2}(\alpha, \Sigma_I) \quad (3-27)$$

$$\Omega_T^\pm = -\frac{\tilde{C}}{2\pi i} \sum_{n,\sigma} \int_0^\infty dx L(x) I_{5/2}(\alpha \pm x, \Sigma_I) \quad (3-28)$$

and,

$$I_\nu(\alpha, \Sigma_I) = \int_b^{b+i\infty} ds \frac{e^{-st}}{s^\nu} + \int_{b-i\infty}^b ds \frac{e^{-st^*}}{s^\nu}$$

$$t = \bar{\Sigma}_n + \Sigma_I = \bar{\Sigma}_n + \Sigma_{R'} + i \Sigma_I = \alpha + i \Sigma_I \quad (3-29)$$

These integrals are evaluated in appendix C where it is shown that

$$I_\nu(\bar{z}, \Sigma_I) = 2i S_\nu(\bar{z}, |\Sigma_I|) \quad (3-30)$$

with

$$S_{1/2}(z, |\mathcal{E}_I|) = \sqrt{\pi/2} \frac{[G(z) - z]^{1/2}}{G(z)}$$

$$S_{5/2}(z, |\mathcal{E}_I|) = -\frac{4}{3} \frac{\sqrt{\pi}}{\sqrt{2}} [|\mathcal{E}_I| [G(z) + z]^{1/2} + \alpha [G(z) - z]^{1/2}]$$

(3-32)

and

$$G(z) = [z^2 + \mathcal{E}_I^2]^{1/2}$$

(3-33)

Before we proceed to calculate the susceptibility, there are still some points to resolve.

First is that  $M$  depends explicitly upon  $B$  through all the obvious dependencies as well as through the not so obvious dependence contained in the chemical potential as well as the self-energy. Therefore, the expressions for  $M$  and  $\chi$  are of the form

$$M = -\left(\frac{\partial \Omega}{\partial B}\right)_{\mu, \mathcal{E}} dB - \left(\frac{\partial \Omega}{\partial \mathcal{E}}\right)_{\mu, B} d\mathcal{E}$$

(3-34)

$$\chi = \left(\frac{\partial M}{\partial B}\right)_{\mu, \mathcal{E}} dB + \left(\frac{\partial M}{\partial \mu}\right)_{B, \mathcal{E}} d\mu + \left(\frac{\partial M}{\partial \mathcal{E}}\right)_{\mu, B} d\mathcal{E}$$

(3-35)

This implies that one needs explicit knowledge of the field dependence of both the chemical potential and the self-energy in order to calculate the differential magnetic susceptibility.

For the LK limit,  $\mu$  is known to vary with  $B$  according to  $(\hbar \omega_c / \mu_0)^{2/3}$  where  $\mu_0$  is the chemical potential at zero field.<sup>(3)</sup> Taking this correction term into account introduces terms of negligible effect into the calculation of  $\chi$  in the LK limit.



In the QL however,  $\mu$  may show a less than negligible variation with B, particularly for the n=0,1,2 peaks.

In fig. four we show some numerical estimates obtained by Rode<sup>(9)</sup> of the  $\mu$  vs B variation for the n=2 level in pure Bismuth.

Figure five shows the effect that including this  $\mu(\beta)$  dependence has on the shape of the differential susceptibility curve. The outer curve is computed with a  $\mu(\beta)$  dependence included while the inner curve excludes it. It should be noted that the inner curve is scaled down slightly from its  $\mu \neq$  constant counterpart but is essentially unaltered in shape by the exclusion of the  $\mu(\beta)$  dependence.

Experimentalists have found that the most useful characteristic of the line shape for extraction of Dingle temperature information is the slope on the high field side of the peaks<sup>(4)</sup>. As one can see, this slope remains essentially unaltered by inclusion of a B dependence in  $\mu$ . The  $\mu(\beta)$  dependence will however be important in determining the location in B of any particular peak even though it will not appreciably affect the shape of any peak.

It should also be noted that  $\mu$  will not be the only parameter which will affect the location of a peak but will appear in the theory inseparable linked with the real parts of the n and possible B dependent self-energy through the expression,

$$\alpha_{n,\sigma} = (n + 1/2) \hbar \omega_c^* - \sigma G \hbar \omega_c + \Sigma_R^I(\beta) - \mu(\beta)$$

(3-36)

whose zero determines the position of the T=0 peak on the B axis.

Figure four shows the variation in electron Fermi energy as a function of magnetic field strength for a model calculation for Bismuth. The magnetic field is in the binary direction and covers the range over which the  $n=2$  level empties. ( ref. 9 )

Figure five shows a comparison of the differential magnetic susceptibility calculated with and without the Fermi energy fluctuations. The inner (narrower) waveform is for constant Fermi energy. The constant Fermi energy waveform has been displaced in field by a few percent in order to facilitate comparison of the curves. ( ref. 9 )

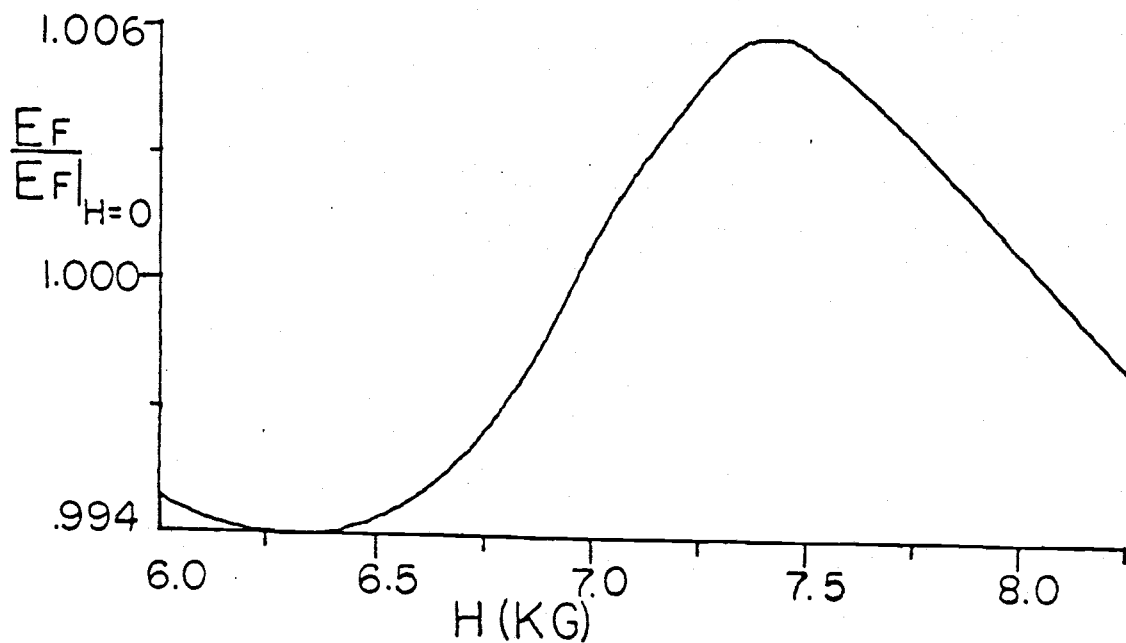


Fig. 4

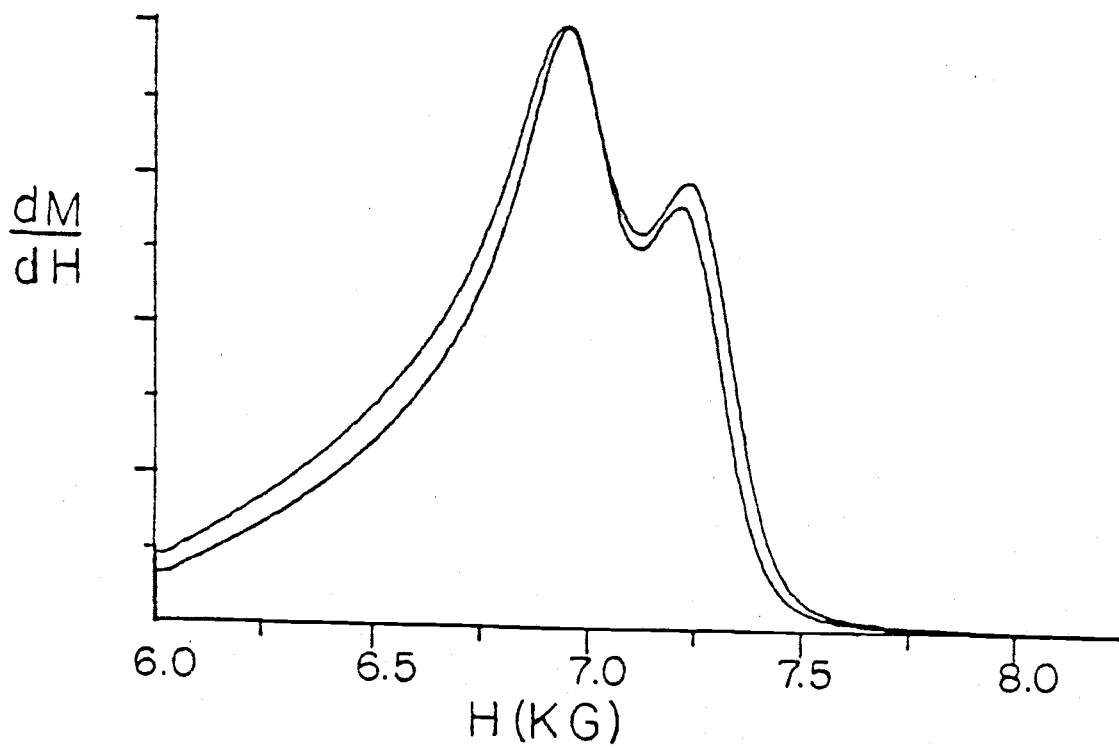


Fig. 5

The real part of the self-energy terms will in general consist of contributions from impurity scattering centers and from crystal potential effects. In lieu of a specific band model, we shall determine our total effective  $\bar{\mu}$  ( $\bar{\mu} = \mu - \Sigma'_R$ ) from the available experimental data on peak positions and neglect the internal variations of  $\mu$  within any peak. We shall also assume that  $\Sigma(B)$  is a sufficiently slowly varying function of B so that its derivatives with respect to B may be neglected.

With these points in mind, the calculation of  $M$  and  $\chi$  proceeds in a straight forward manner and we find that,

$$M = \sum_{n,\sigma} M(n,\sigma) \quad (3-37)$$

$$\chi = \sum_{n,\sigma} \chi(n,\sigma) \quad (3-38)$$

$$M(n,\sigma) = -2C_n DB \left\{ [G(\alpha) - \alpha]^{1/2} - \frac{1}{2} I_1(\alpha) \right\} - \frac{4}{3} D \left\{ [|\mathcal{A}_I| [G(\alpha) + \alpha]^{1/2} + \alpha [G(\alpha) - \alpha]^{1/2}] - \frac{3}{4} I_2(\alpha) \right\}$$

$$\chi(n,\sigma) = C_n^2 DB \left\{ \frac{[G(\alpha) - \alpha]^{1/2}}{G(\alpha)} - \frac{1}{2} I_3(\alpha) \right\} - 4C_n D \left\{ [G(\alpha) - \alpha]^{1/2} - \frac{1}{2} I_1(\alpha) \right\} \quad (3-39)$$

$$(3-40)$$

$$G(z) = [z^2 + |\mathcal{A}_I|^2]^{1/2} \quad (3-41)$$

$$L(z) = \ln [1 + e^{-\beta z}]$$

$$E(z) = \frac{1}{1 + e^{\beta z}}$$

$$D = \frac{e^{\sqrt{m^*}}}{h^2 c}$$

$$F_1(z) = \frac{[G(z) - z]^{1/2}}{G(z)}$$

$$C_n = [(n+1/2)M - \sigma G] d\mu_B$$

$$\alpha = C_n \beta + \sum_R -\mu$$

$$F_2(z) = \frac{F_1(z)}{G(z)} \left[ 1 + \frac{\lambda z}{G(z)} \right]$$

$$I_1(\alpha) = \int_0^\infty E(x) [F_1(\alpha+x) - F_1(\alpha-x)] dx$$

$$I_2(\alpha) = \frac{1}{\beta} \int_0^\infty L(x) [F_1(\alpha+x) + F_1(\alpha-x)] dx$$

$$I_3(\alpha) = \int_0^\infty E(x) [F_2(\alpha+x) - F_2(\alpha-x)] dx$$

(3-42)

Equation 3-40 should be compared to eq. D-12 which will show the equivalence between the  $T=0$  susceptibility as derived from our formalism and from Rode's<sup>(9)</sup>.

Equation 3-40, which is the main result of this work, expresses the magnetization and differential susceptibility in the QL for an impure system as a sum of individual terms each of which corresponds to a particular set of the LL quantum numbers  $(n, \sigma)$ .

The quantity  $\alpha(n, \sigma)$  plays a role similar to that of  $\bar{\xi}(n, \sigma)$  in the non-interacting system but includes the renormalization of the LL energies caused by the introduction of the real part of the self-energy.

The divergence which occurred in the non-interacting case has now been eliminated because the function  $G^{-1}(\alpha) = [\alpha^2 + \Sigma_I^2]^{-1/2}$  does not diverge as  $\alpha \rightarrow 0$  due to the fact that  $\Sigma_I$  is not zero.

It is also apparent that the contribution of any particular LL to  $M$  or  $\chi$  no longer abruptly ceases when  $\alpha$  becomes positive (i.e. as the LL passes through the FS) but now contributes a steep but finite slope on the high field side of the peak (approximately at  $\alpha = 0$ ).

The sharp discontinuities of the non-interacting case can be regained by noting that

$$[G(\alpha) - \alpha]^{1/2} \xrightarrow{\Sigma_I \rightarrow 0} [|\bar{\xi}_n| - \xi_n]^{1/2} = \sqrt{\alpha} |\bar{\xi}_n|^{1/2} \Theta(-\bar{\xi}_n)$$

We again note the distinct separation between  $T=0$  and  $T \neq 0$  ( $I_1$  and  $I_2$ ) terms which allows their relative importance to be determined and which facilitates further analysis of the temperature contributions.

Of crucial importance is the fact that  $\Sigma_I$  in each term is a function of  $n, \sigma$ , and  $B$ . This fact is capable of producing substantial modifications in the observed line shapes from those found

on the basis of a strict Lorentzian broadening for all levels.

In chapter four we shall turn our attention to an analysis of the  $T \neq 0$  terms and in chapter five we shall discuss the calculation of a realistic  $\xi(\eta, \sigma, \mathcal{B})$  in the Born approximation.

## IV. TEMPERATURE CORRECTIONS

## A. MATHEMATICAL ANALYSIS

Unlike ordinary Fermi gas problems where the low temperature corrections are usually negligible, both the quantum and LK limits require the inclusion of temperature effects in order to fully reproduce the observed line shapes.

The only other theoretical treatment of the QL previous to this one<sup>(9)</sup> did not attempt to isolate the temperature from the zero-temperature terms nor was that theory cast in such a way as to facilitate such a decomposition.

In the present work however we see that the temperature correction terms are expressed as integrals of the form,

$$I(\alpha) = \int_0^{\infty} \frac{1}{1+e^{\beta x}} [f(\alpha+x) - f(\alpha-x)] dx \quad (4-1)$$

The rapid decay in  $x$  of the function  $[1+e^{\beta x}]^{-1}$  at low temperature suggests an approximation technique based on Laplace's method of asymptotic expansions in which the function  $[f(\alpha+x) - f(\alpha-x)]$  is expanded about  $x=0$ . It is hoped that if and when the expansion is forced to leave its region of convergence, the function  $[1+e^{\beta x}]^{-1}$  will be small enough to render the errors incurred negligible.

The functions to be expanded both contain terms of the form

$$\left[ (\alpha \pm x)^2 + \frac{1}{4} \right]^{-1/2} \quad (4-2)$$



which have branch points at  $\chi = \pm \alpha \pm i \Sigma_{\Gamma}^4$ . These branch points limit the region of convergence of the expansions to  $|\chi| < [\alpha^2 + \Sigma_{\Gamma}^2]^{1/2}$ . Thus we expect that the asymptotic approximations will be accurate if

$$\frac{k_B T}{[\alpha^2 + \Sigma_{\Gamma}^2]^{1/2}} < 1 \quad (4-3)$$

These conditions will hold far to the right or left of any particular LL crossing (i.e.  $|\alpha| > k_B T$ ) or near the crossing region itself ( $|\alpha| < k_B T$ ) provided that the scattering is strong enough or the temperature is low enough so that  $k_B T < |\Sigma_{\Gamma}|$ .

Keeping these points in mind and retaining only the first terms in the expansion of the integrands, we find that

$$I_1(\alpha) \simeq 2 F_1'(\alpha) \int_0^{\infty} x E(x) dx = \frac{\pi^2}{6\beta^2} F_1'(\alpha)$$

$$I_3(\alpha) \simeq 2 F_2'(\alpha) \int_0^{\infty} x E(x) dx = \frac{\pi^2}{6\beta^2} F_2'(\alpha)$$

$$F_1'(\alpha) = -\frac{1}{2} \frac{F_1(\alpha)}{G(\alpha)} \left[ 1 + 2 \frac{\alpha}{G(\alpha)} \right]$$

$$F_2'(\alpha) = +6 \frac{F_1(\alpha)}{G^2(\alpha)} \left[ \frac{1}{4} - \frac{\alpha}{G(\alpha)} - \left[ \frac{\alpha}{G(\alpha)} \right]^2 \right]$$

---

4. Recall that  $\alpha$  may be thought of as the field dependent distance of any LL from the FS and that the dominant contributions of that LL occur in the region  $\alpha \sim 0$ .

Higher order terms in the expansion have been investigated ( up to three terms have been examined ) and we find that although the absolute deviation between the exact and the approximate results becomes smaller on a point for point basis, the introduction of more terms causes the line shape to become distorted in such a way that one might mistake the distortion as being a spin induced effect. Thus we rely solely on the single term approximation for our analysis.

### B. GRAPHICAL ANALYSIS

In the graphs which follow we examine how well the single term asymptotic approximation corresponds to its "exact value" as determined by a 41 point Legendre quadrature on the temperature correction terms.

We are not only interested in how well the approximation fares in an absolute sense but even more importantly how well it fares as compared to the exact result when each is added to the zero-temperature term to yield the contribution to the total susceptibility for a particular LL at any given temperature and scattering rate.

To accomplish this the graphs which follow are presented in groups of three. The A graphs in each set show the exact temperature contribution to  $\chi$  and its single term approximation (  $\chi_T$  and  $\chi_{TA}$  respectively ) plotted on the same vertical axis with the magnetic field plotted along the horizontal axis. The A graphs will be an indication of how accurate the asymptotic approximations are in an absolute sense.

The B graphs show the zero-temperature contribution to  $\chi$  and the exact temperature contribution, which we call  $\chi_0$  and  $\chi_T$  respectively, plotted on the same vertical axis with the field plotted along the horizontal axis. The B graphs will indicate the relative importance of the temperature terms as compared to the zero-temperature terms.

The C graphs show the total susceptibility<sup>5</sup>  $\chi = \chi_0 + \chi_T$  and the total approximate susceptibility  $\chi_A = \chi_0 + \chi_T^A$  plotted on the same vertical axis with the field again plotted along the horizontal axis. The C graphs will indicate how effective the approximate formulas are in reproducing the exact susceptibility.

In all cases, the susceptibilities displayed along the vertical axis will be plotted in units of  $D = \frac{e \sqrt{m^*}}{h^2 c} \text{ cm}^3$  while the horizontal axis will be in gauss.

The data chosen is that which is applicable to the  $n=3$  level crossing for electrons in Bismuth<sup>(9)</sup>, viz;

$$m/m^* = 106.383 \quad G = .545 \quad \bar{\mu} = .01897 \text{ ev.}$$

As we shall see, the critical factor which determines how accurate the asymptotic approximations are is the ratio of the temperature  $T$  to the Dingle temperature  $T_d$ .

---

5. Ofcourse the total susceptibility at any field value is a sum of the contributions from all LL's at that particular field value but the main contribution is due to the particular LL which is about to cross the FS. It is only in this region ( $\alpha \sim 0$ ) that the asymptotic expansions are expected to fail. Rather than plotting the total susceptibility, we are examining the contribution to the total susceptibility of a particular LL in the region where that LL is crossing the FS.

From our graphical analysis we've found that for physically reasonable Dingle temperatures of the order of  $.6^{\circ}\text{K}$ , the asymptotic approximations are extremely effective in reproducing the total susceptibility line shape for all temperatures less than  $.3^{\circ}\text{K}$ . They become less effective as the temperature increases past this point and in order to see the effects introduced we begin the graphical analysis right at the point ( $.3^{\circ}\text{K}$ ) where the asymptotic approximations are on the verge of losing their effectiveness.

In figs. 6 A,B,C,  $T = .3^{\circ}\text{K}$  and  $T_d = .6^{\circ}\text{K}$ . For the  $n = 3$  level, the crossing occurs at 4394 gauss and graph 6A shows that once we are approximately 70 gauss past the crossing point ( $|\alpha| = 3 \times 10^{-4} \text{ eV}$ ,  $k_B T = 2.6 \times 10^{-5} \text{ eV}$ ) the discrepancy between the exact temperature result and the approximation to it is negligible.

Figure 6B shows that for  $T = .3^{\circ}\text{K}$  and  $T_d = .6^{\circ}\text{K}$ , the zero temperature term sharply dominates the temperature term so that any minor discrepancy between  $\chi_T$  and  $\chi_{TA}$  will tend to be masked by the overpowering  $\chi_0$  term.

This effect is shown in fig. 6C in which it is not possible with the given resolution ( two curves are plotted ) to see any distinction between  $\chi$  and  $\chi_A$  for  $T = .3^{\circ}\text{K}$  and  $T_d = .6^{\circ}\text{K}$ .

In fig. 7 A,B,C, the scattering rate has remained at  $.6^{\circ}\text{K}$  while the temperature has been increased to  $.4^{\circ}\text{K}$ .

Figure 7B shows that the relative importance of  $\chi_T$  to  $\chi_0$  is increasing while fig. 7A indicates that the approximation to  $\chi_T$  is less accurate in the crossing region although still extremely good for  $|\alpha| > 3 \times 10^{-4} \text{ eV}$ .

These two effects conspire to produce an observable though still small distinction between  $\chi$  and  $\chi A$  as evidenced by fig. 7C.

In figs. 8 A,B,C the temperature has been increased to  $.5^\circ\text{K}$  with the Dingle temperature still remaining fixed at  $.6^\circ\text{K}$ . Figure 8C shows the distinction between  $\chi$  and  $\chi A$  becoming more pronounced but the line shape is still reasonable accurate.

In figs. 9 A,B,C, the temperature is greater than the Dingle temperature (  $T=.7^\circ\text{K}$ ,  $T_d = .6^\circ\text{K}$  ) and we see that not only is the error caused by the approximation large in magnitude ( fig. 9A ) but it begins to introduce some spurious structure into the line shape exhibited in fig. 9C which resembles that caused by spin splitting.<sup>6</sup>

These first four sets of graphs indicate that the transition region occurs for ratios of  $T/T_d = 2/3$  when  $T=.4^\circ\text{K}$  and  $T_d=.6^\circ\text{K}$ .

In the next two sets of graphs, we examine the same ratio (2/3) of  $T/T_d$  but in figs. 10 A,B,C we have  $T=.2^\circ\text{K}$  and  $T_d=.3^\circ\text{K}$  and in figs. 11 A,B,C we have  $T=.8^\circ\text{K}$  and  $T_d=1.2^\circ\text{K}$ .

From these graphs we can conclude that the ratio of  $T/T_d = 2/3$  is indeed the transition region for the asymptotic approximations to be useful over a wide range of low temperatures ( up to  $.8^\circ\text{K}$  at least ) with correspondence being slightly better at lower temperatures since the temperature corrections become less important with decreasing temperature.

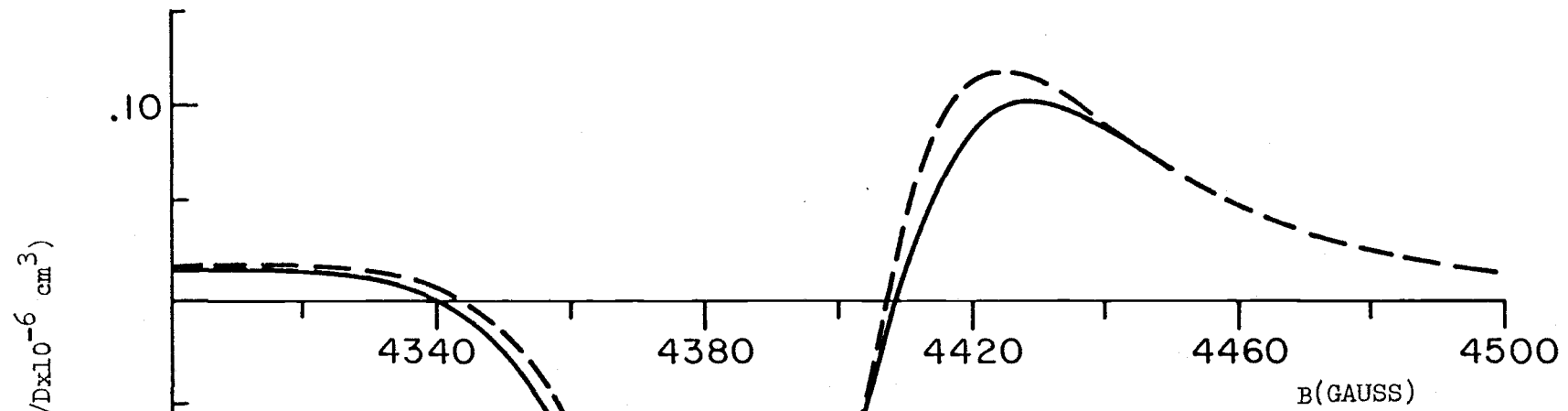
Finally in figs. 12 A,B,C we look at an extreme case of  $T=.3^\circ\text{K}$

---

6. This effect is similar to what occurs when a more than one term expansion is used.

and  $T_d = .1$  °K and we see that the asymptotic approximation greatly overshoots the exact temperature term (fig. 12A) while the temperature correction term itself contributes a significant portion of the total susceptibility (fig. 12B). It is also apparent from fig. 12B that the temperature terms tend to lower the amplitude and broaden the line shape of the total susceptibility. Figure 12C shows how in this extreme region ( $T/T_d = 3$ ) the asymptotic approximation is totally ineffective in reproducing the line shape in the vicinity of the crossing region but still remains accurate once we are sufficiently far from the peaks.

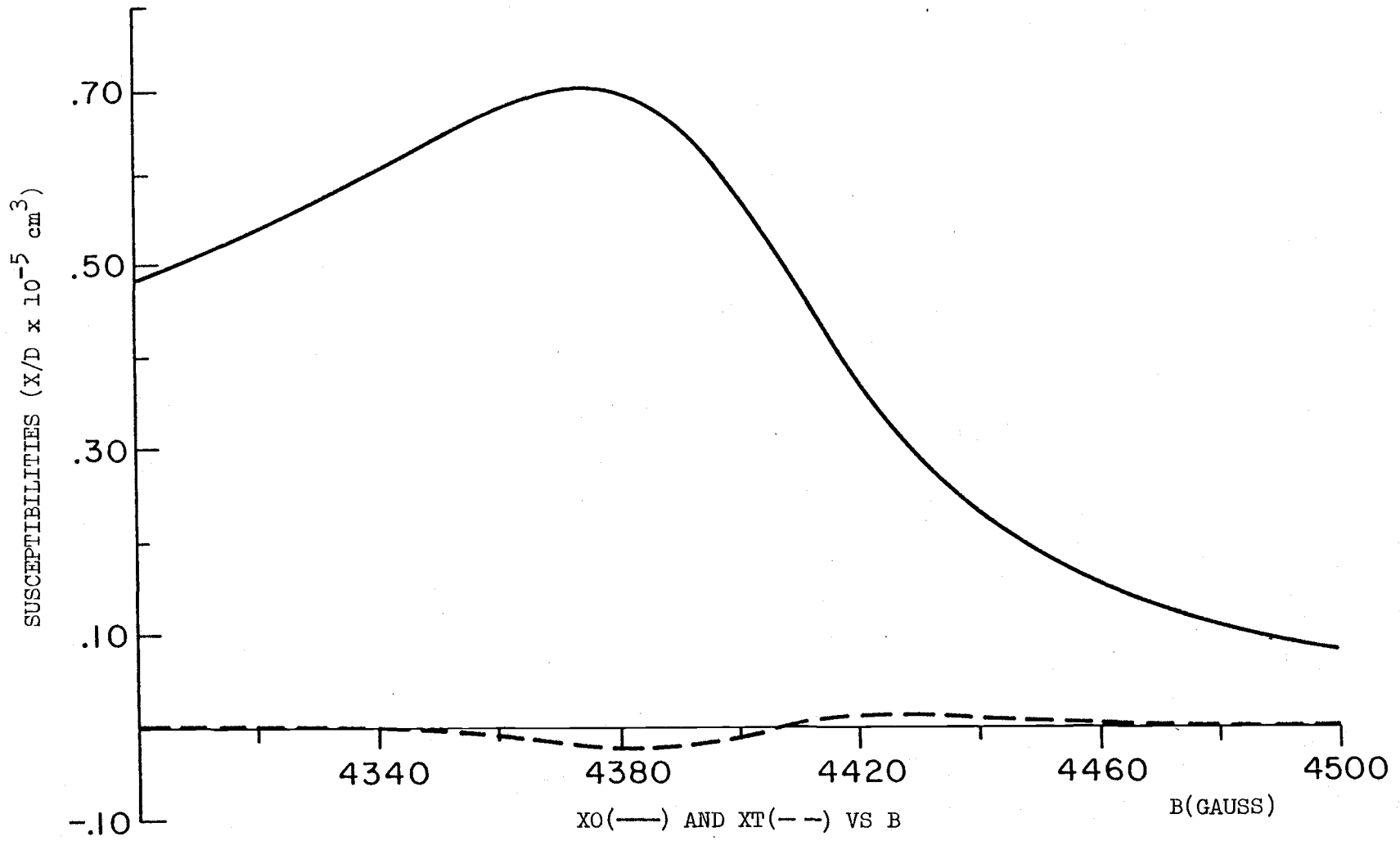
Similar sets of graphs have been examined for different  $n$  values and we conclude from these that the only distinction between  $n$  values is in how far past the peak one must be before the asymptotic approximations are effective independent of the ratio of  $T/T_d$ . With decreasing  $n$  values one must move further past the peak in order for the approximations to become of value. The ratio of  $T/T_d = 2/3$  still appears to be the crucial ratio in the vicinity of the crossing point.



XT(—) AND XTA(--) VS B

T=.3°K T<sub>d</sub>=.6°K N=3

Fig. 6A

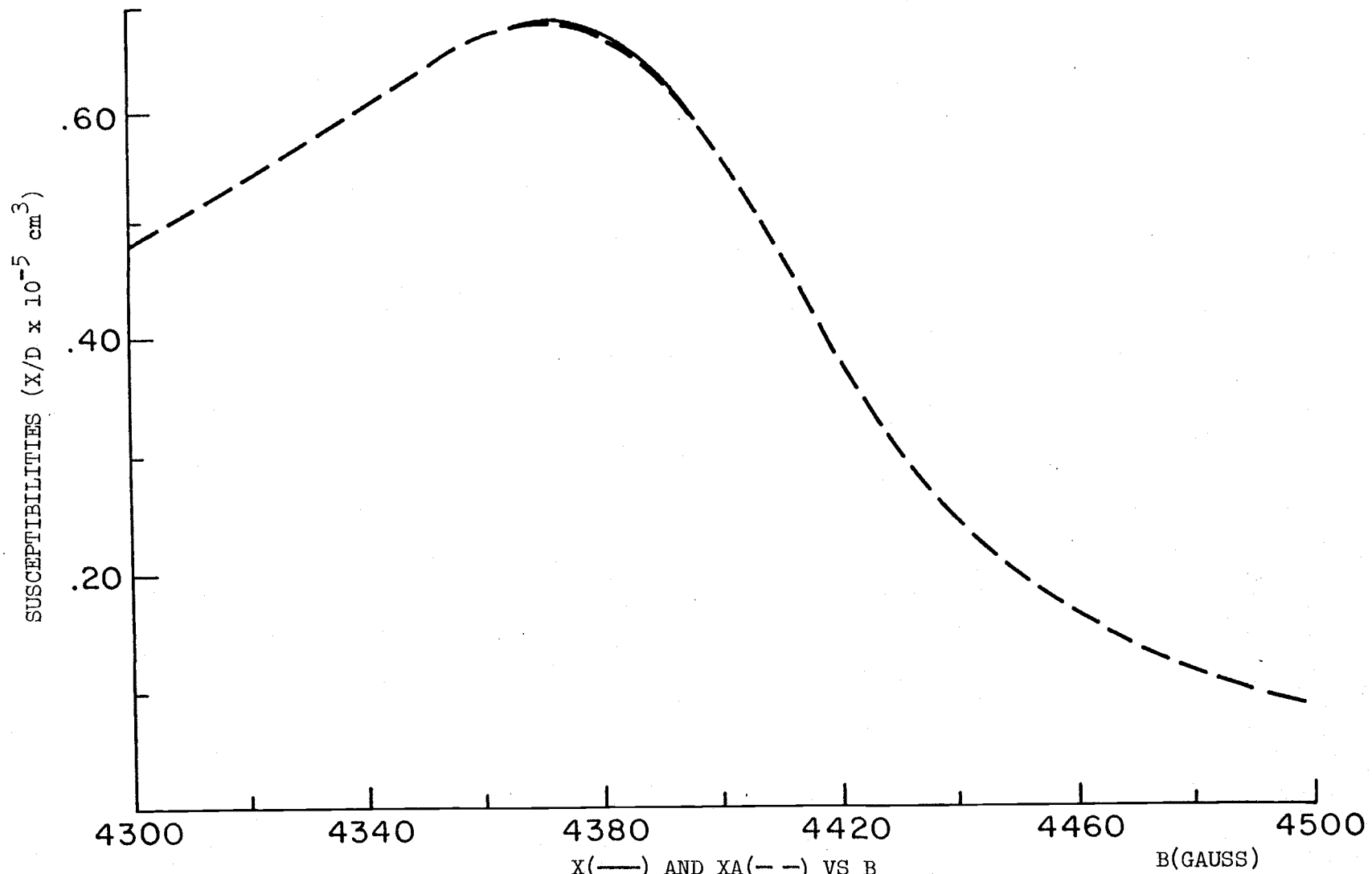


X<sub>0</sub>(—) AND X<sub>T</sub>(-- --) VS B

T = .3°K T<sub>d</sub> = .6°K N = 3

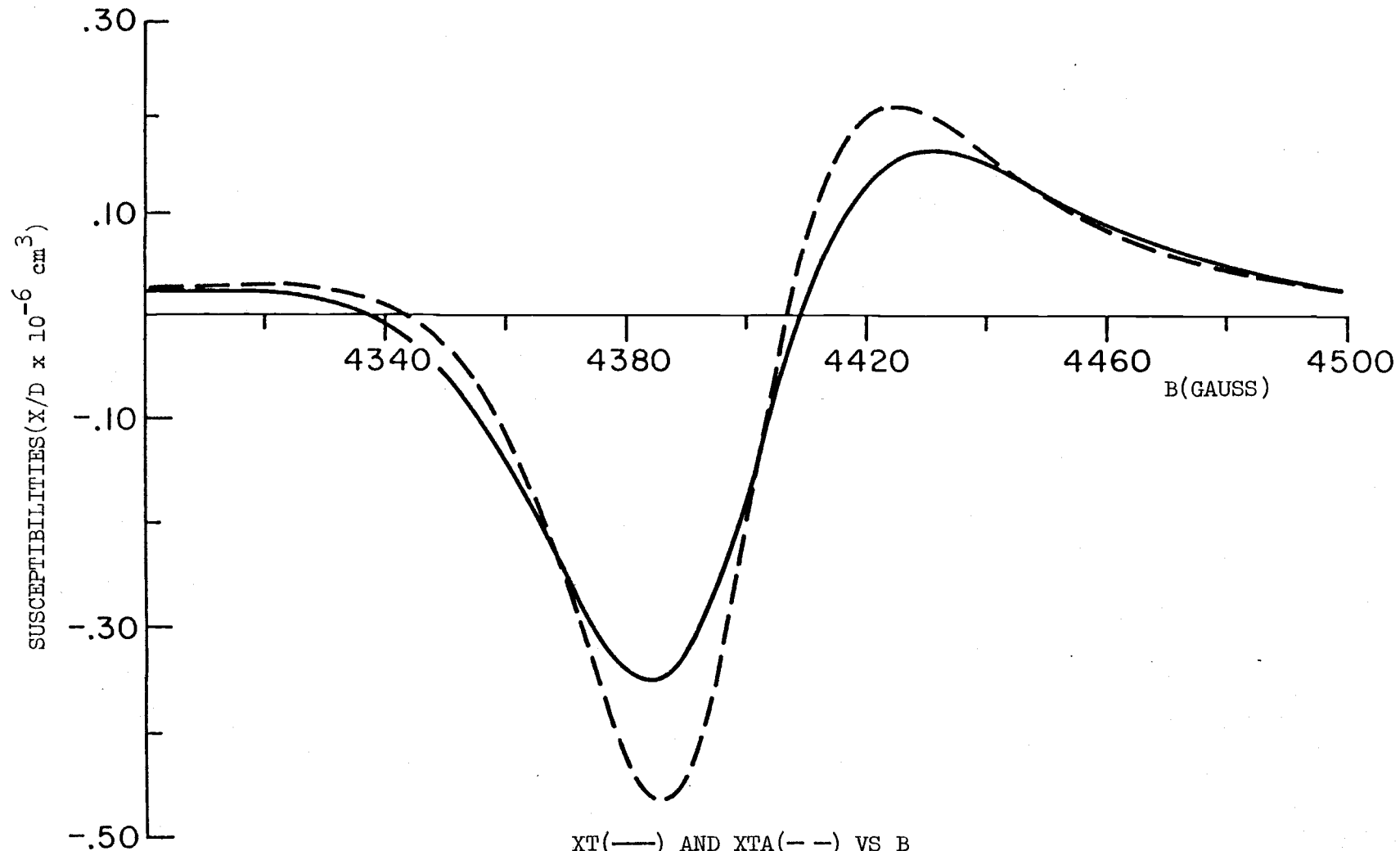
Fig. 6B





$T = .3^{\circ}\text{K}$   $T_d = .6^{\circ}\text{K}$   $N = 3$

Fig. 6C



XT(—) AND XTA(--) VS B

$T = .4^{\circ}\text{K}$   $T_d = .6^{\circ}\text{K}$   $N=3$

Fig. 7A

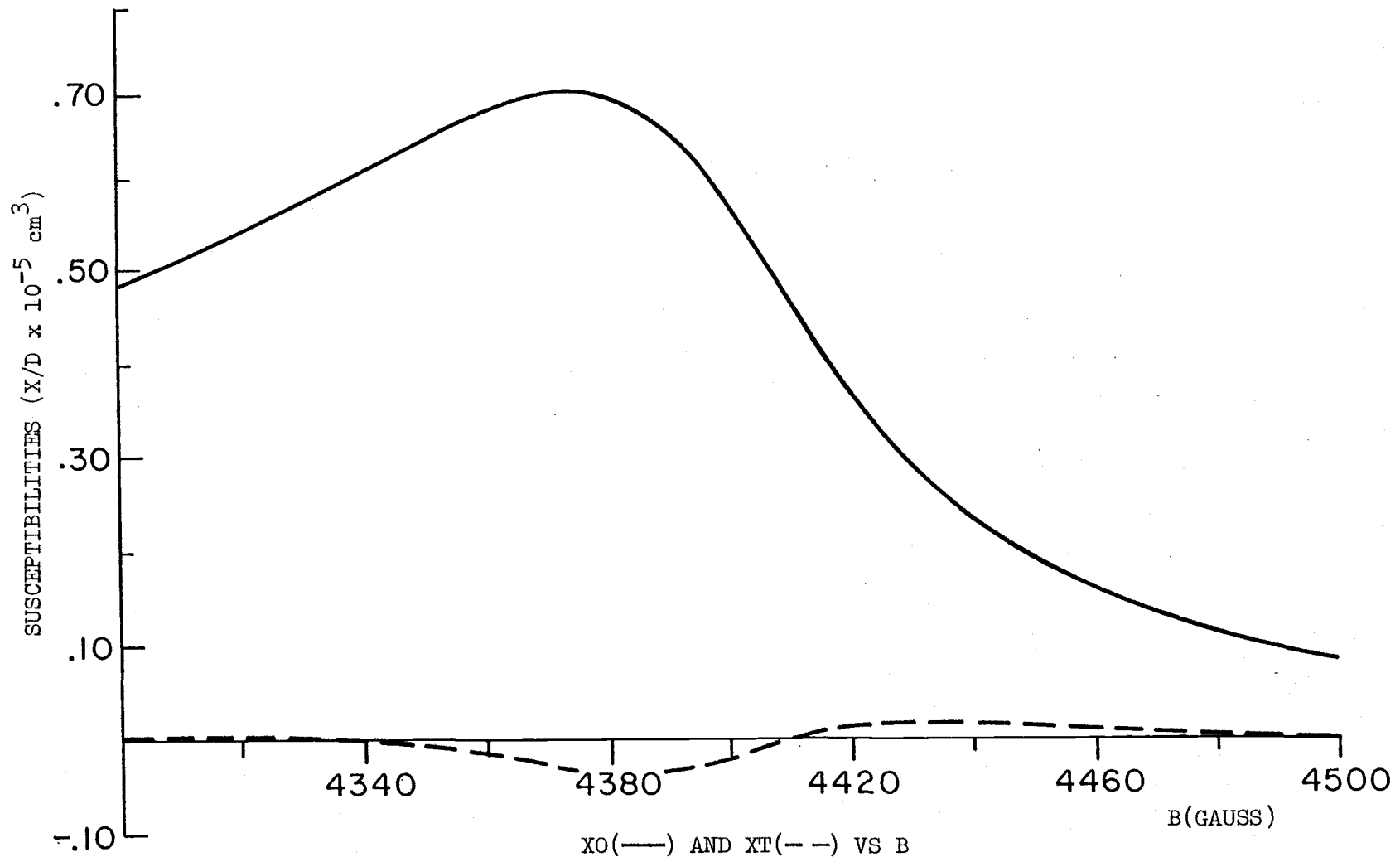
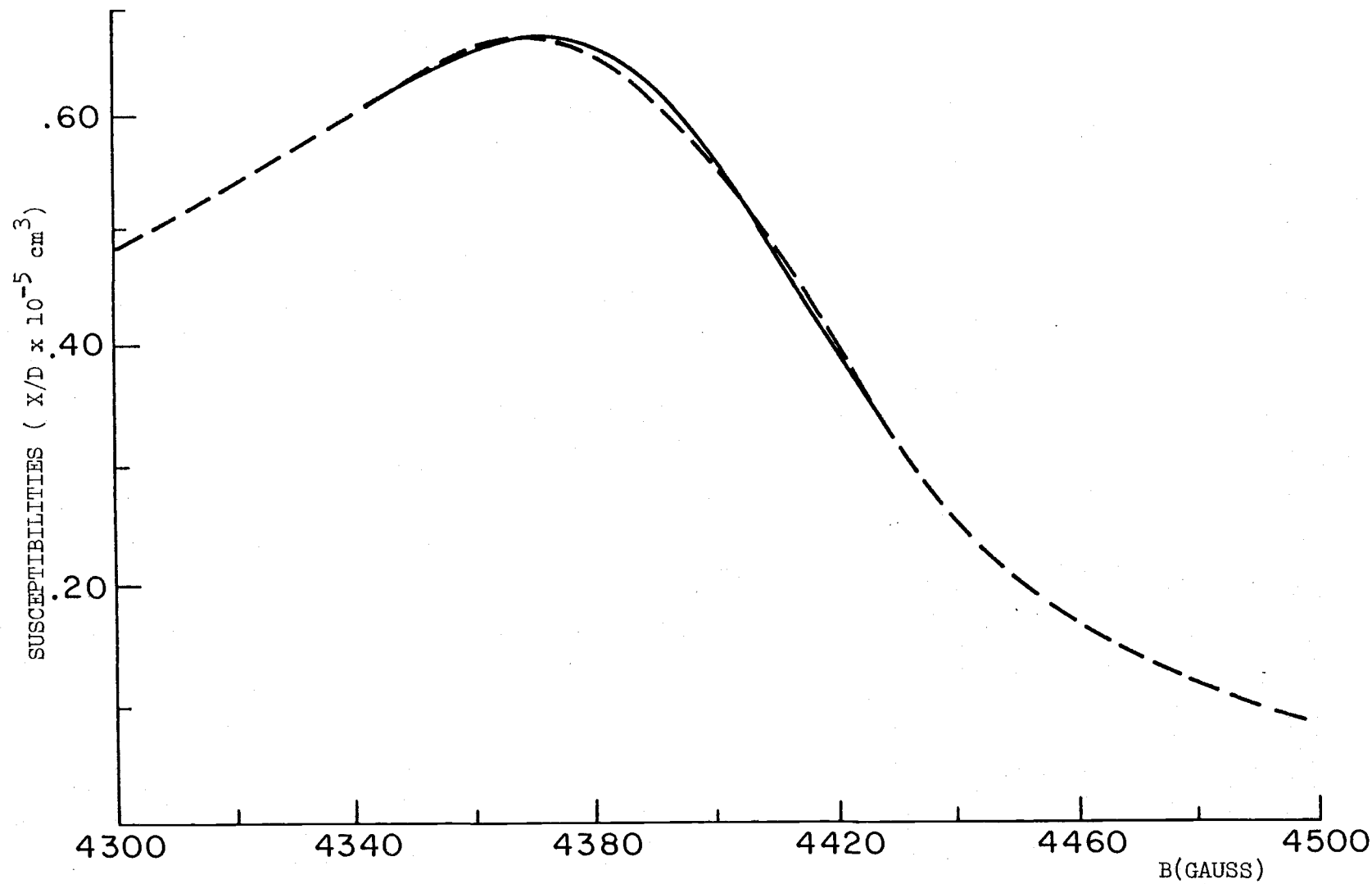


Fig. 7B



X(—) AND XA(---) VS B

$T = .4^{\circ}\text{K}$   $T_d = .6^{\circ}\text{K}$   $N=3$

Fig. 7C

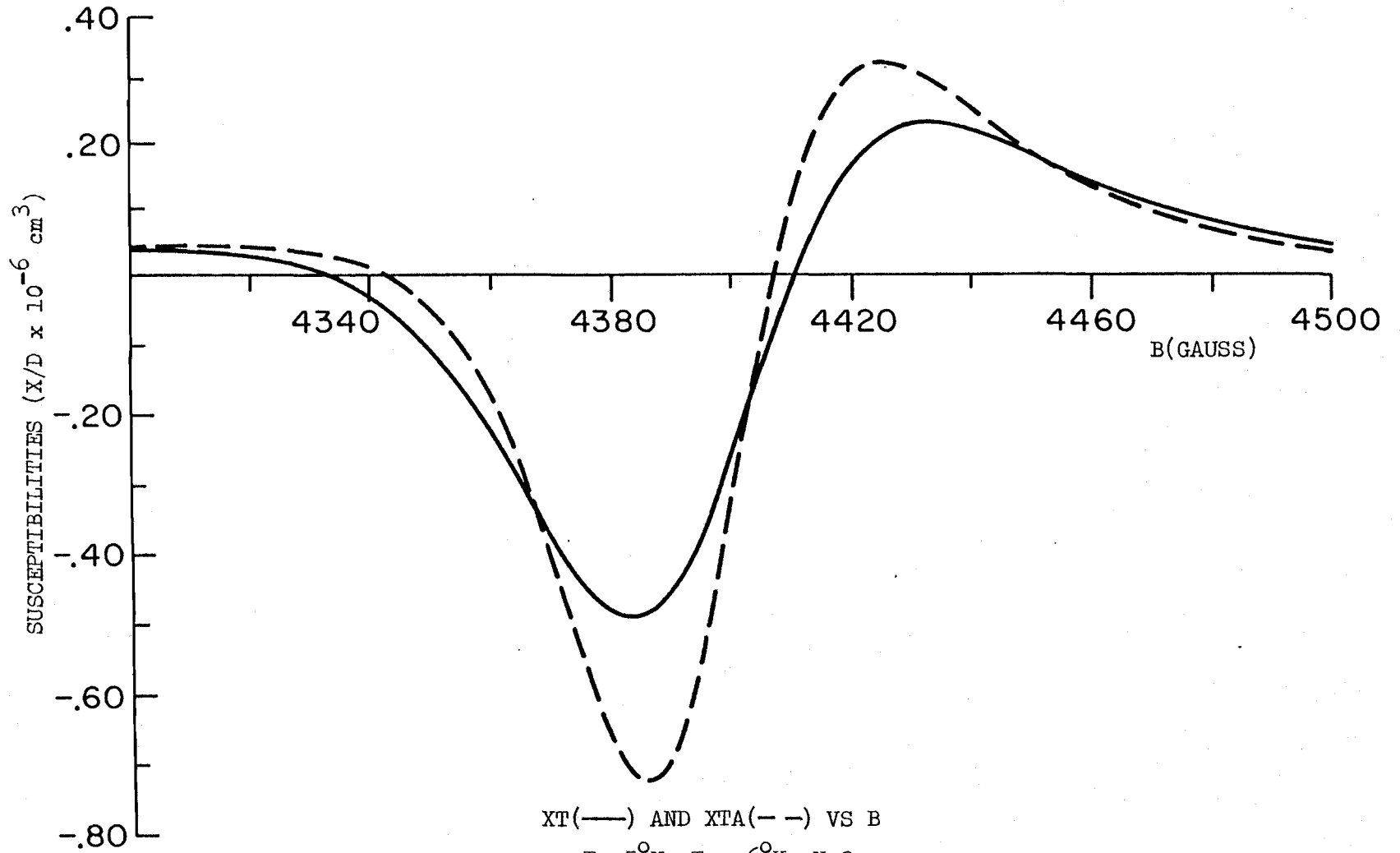
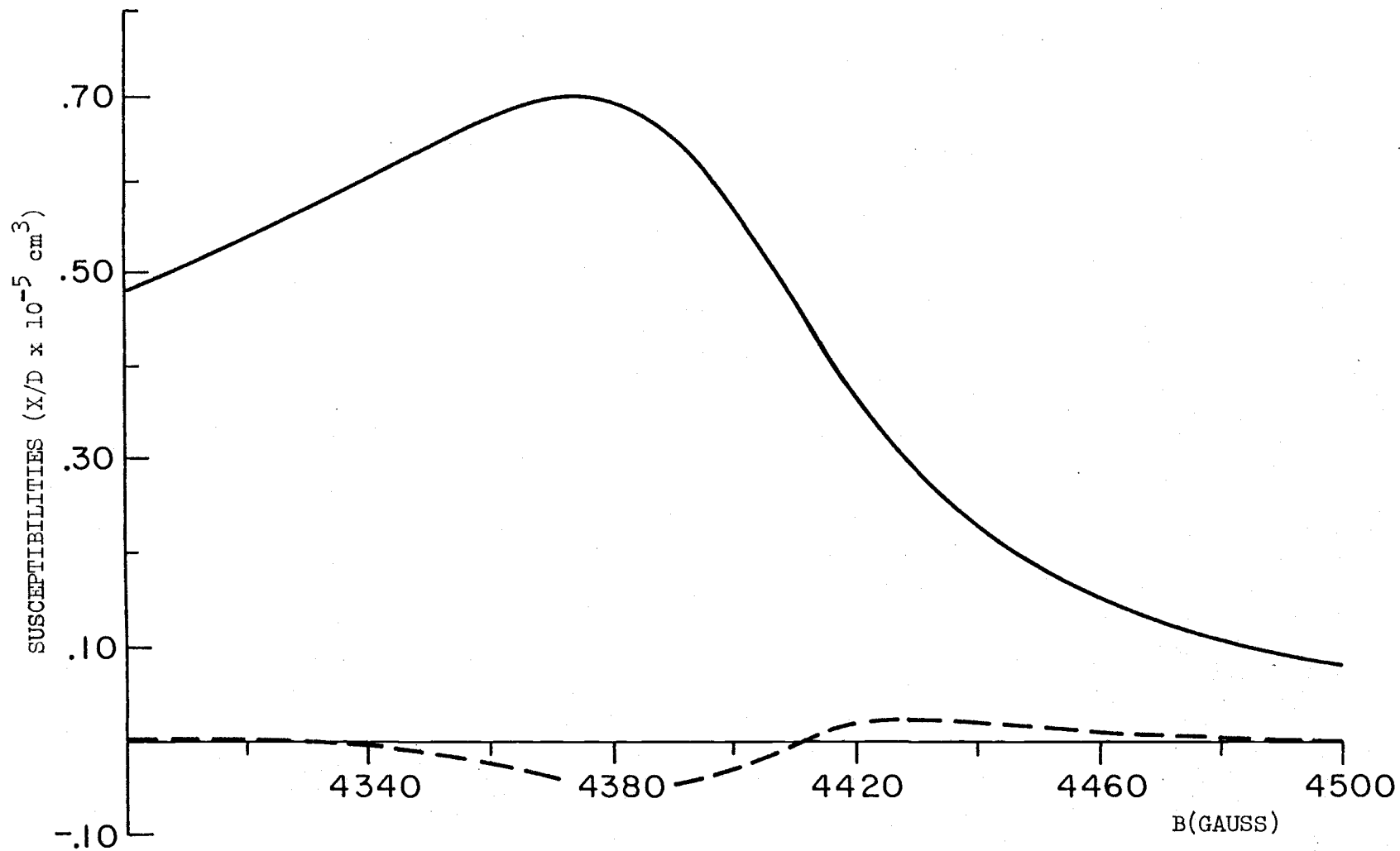


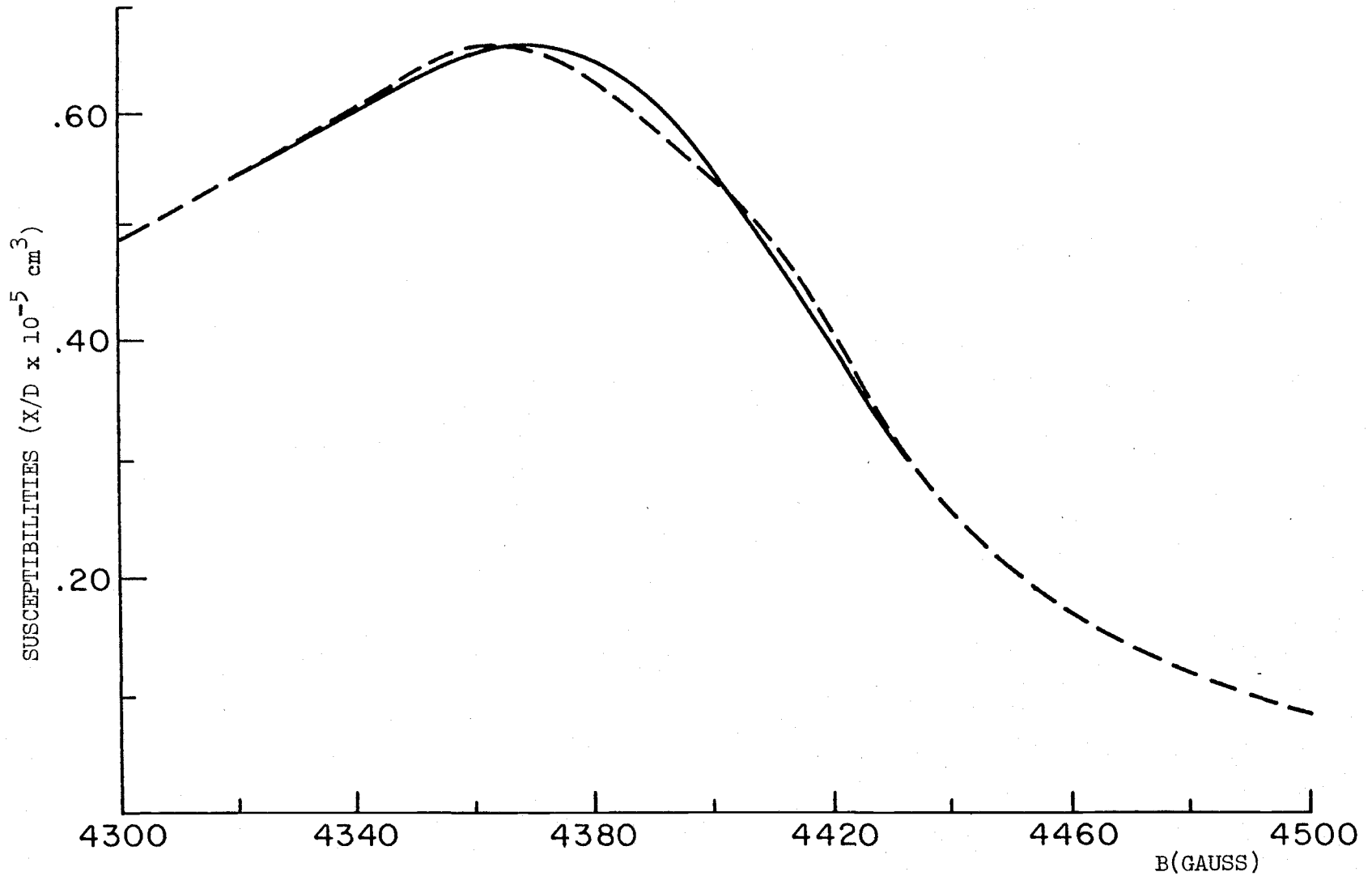
Fig. 8A



XO(—) AND XT(- -) VS B

T=.5°K T<sub>d</sub>=.6°K N=3

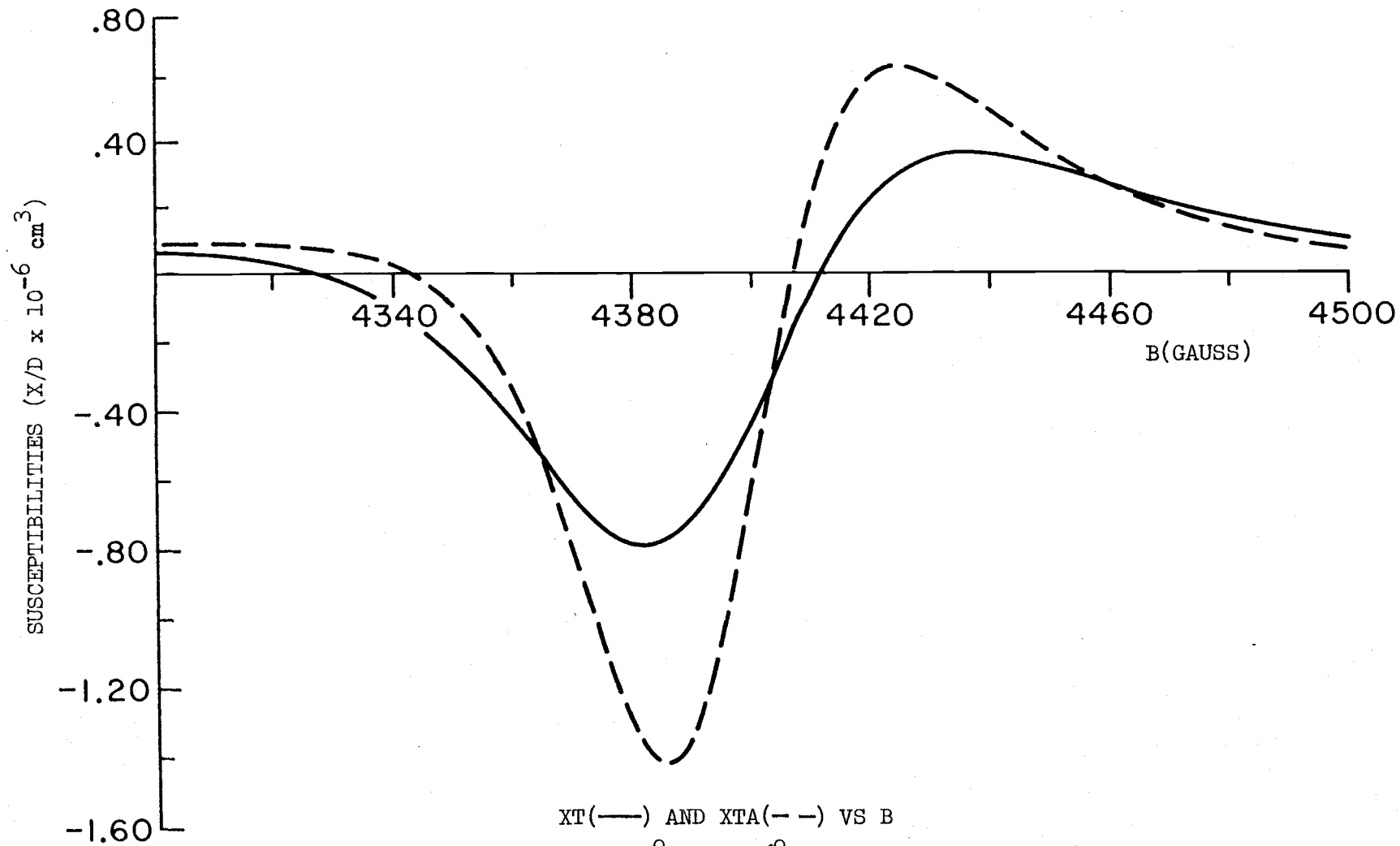
Fig. 8B



X(—) AND XA(---) VS B

T=.5°K T<sub>d</sub>=.6°K N=3

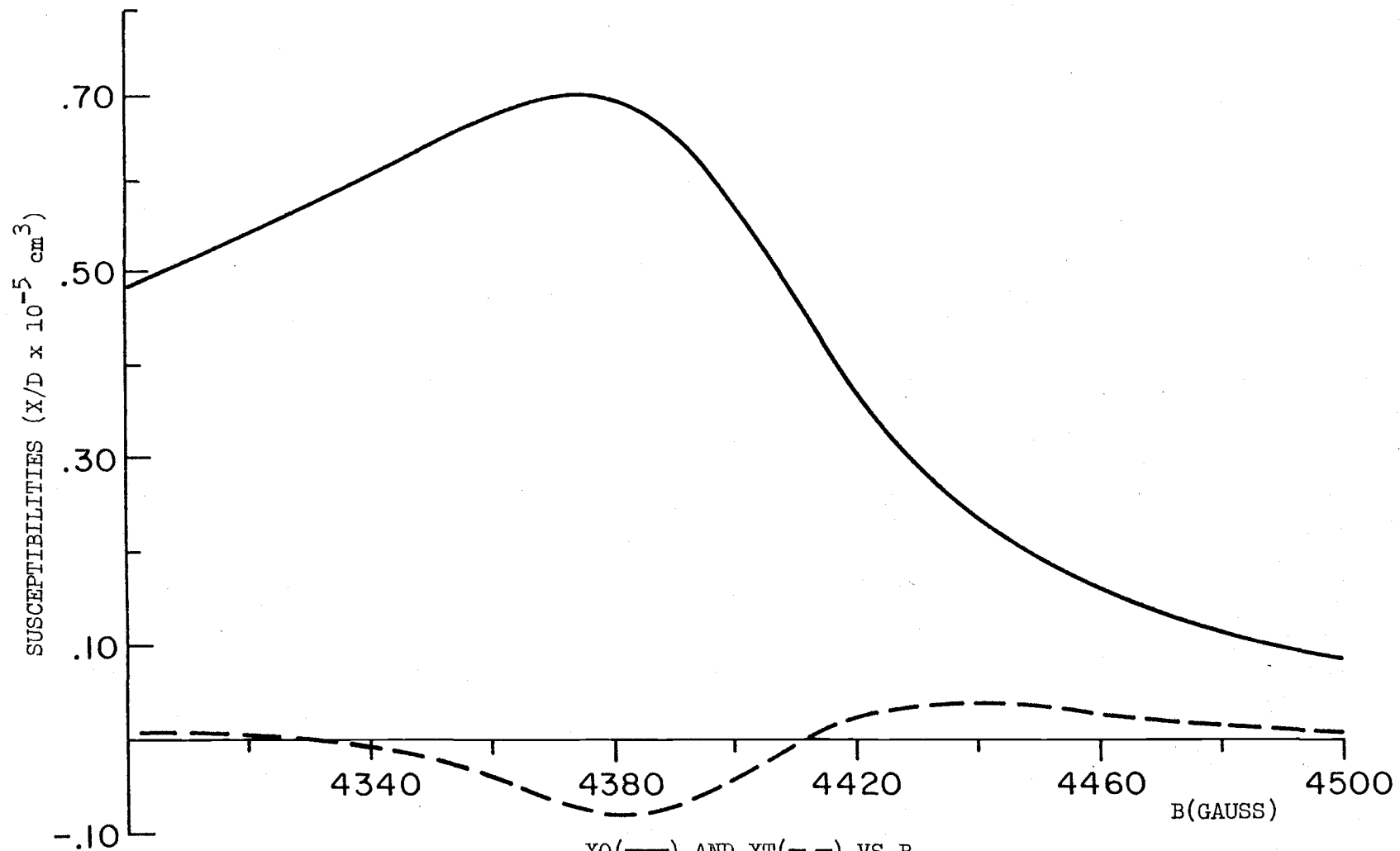
Fig. 8C



XT(—) AND XTA(-- ) VS B  
 $T = .7^{\circ}\text{K}$   $T_d = .6^{\circ}\text{K}$   $N=3$

Fig. 9A

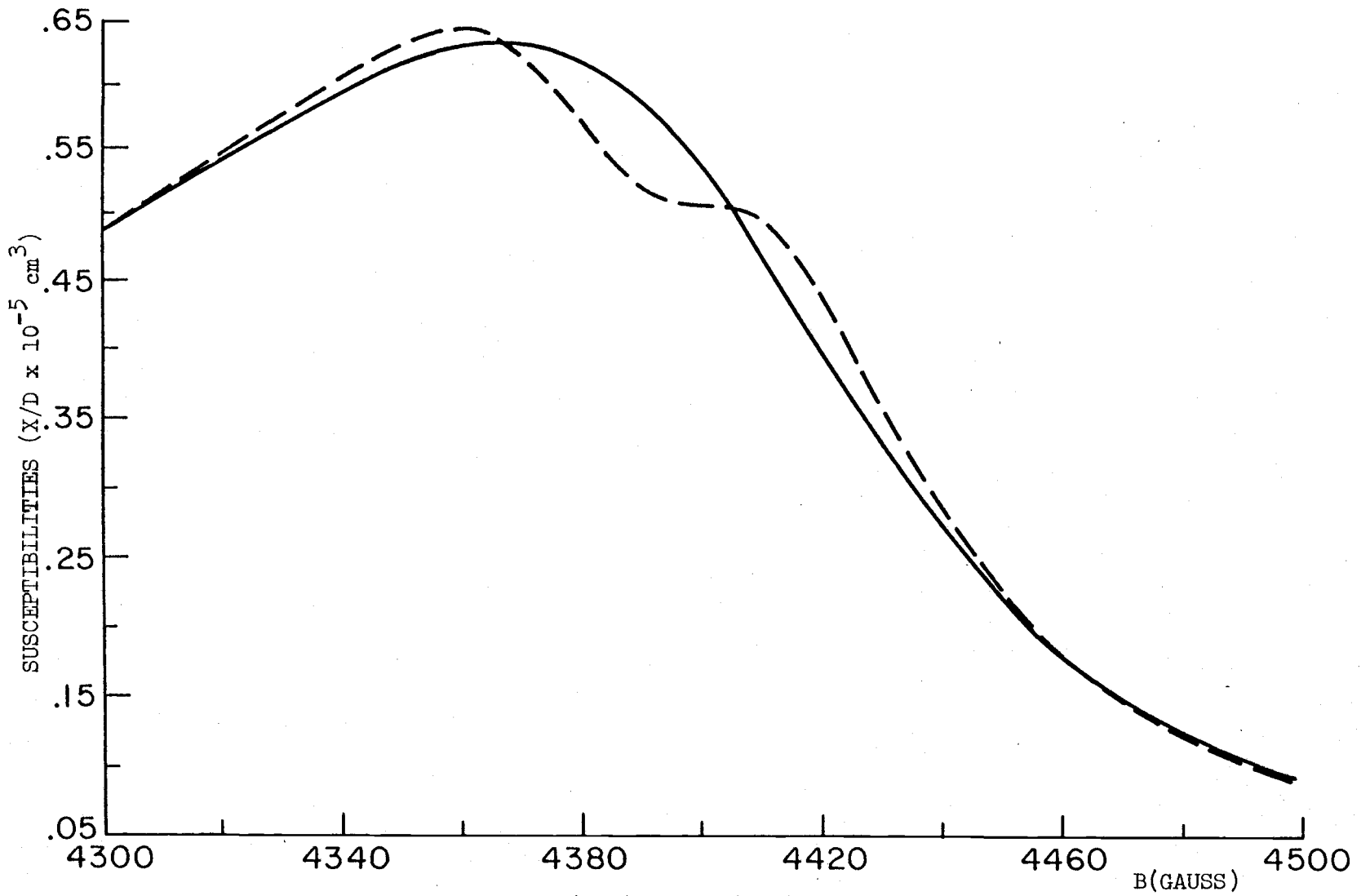




X0(—) AND XT(---) VS B

$T = .7^{\circ}\text{K}$   $T_d = .6^{\circ}\text{K}$   $N=3$

Fig. 9B



X(—) AND XA(--) VS B

$T = .7^{\circ}\text{K}$   $T_d = .6^{\circ}\text{K}$   $N=3$

Fig. 9C

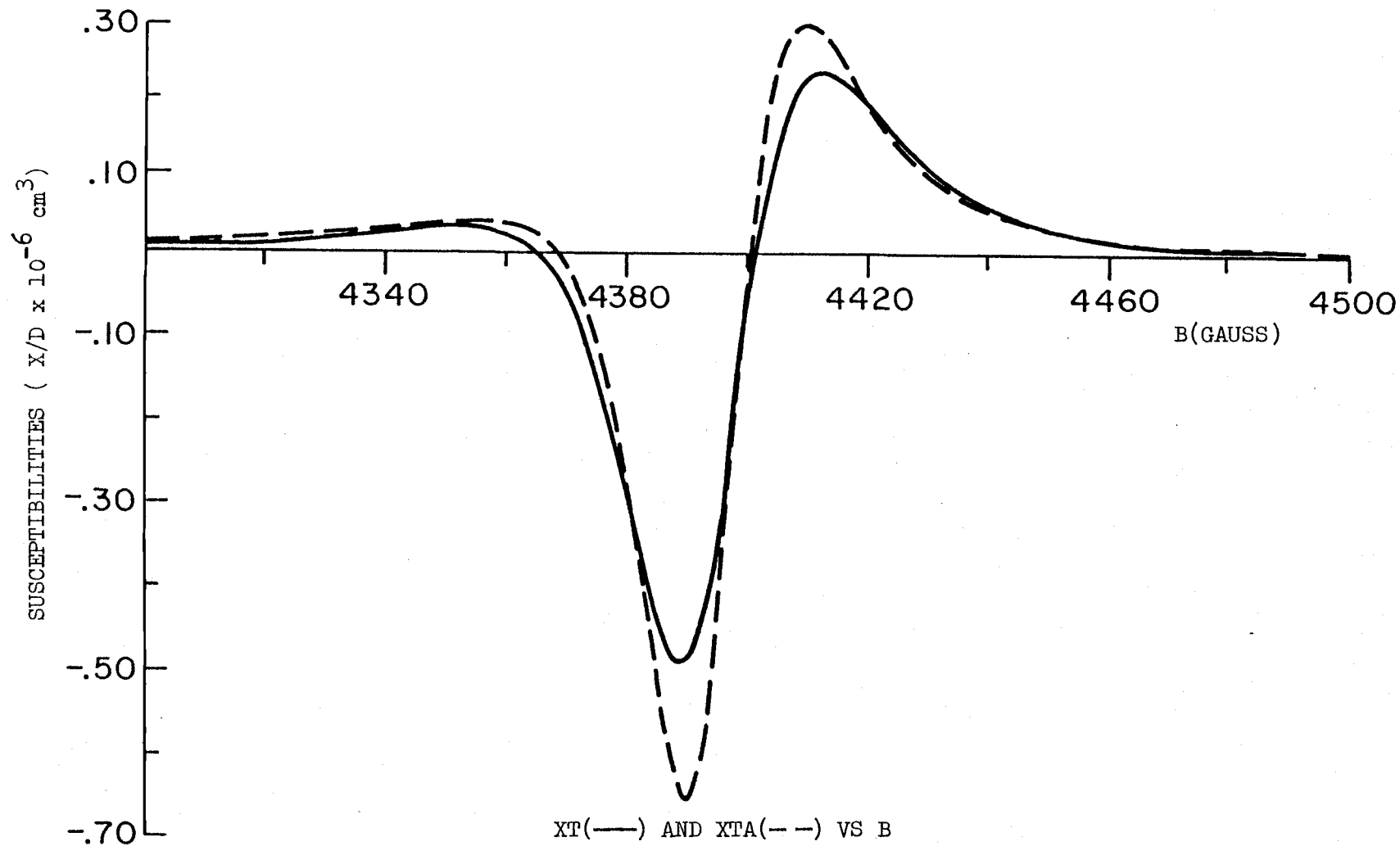
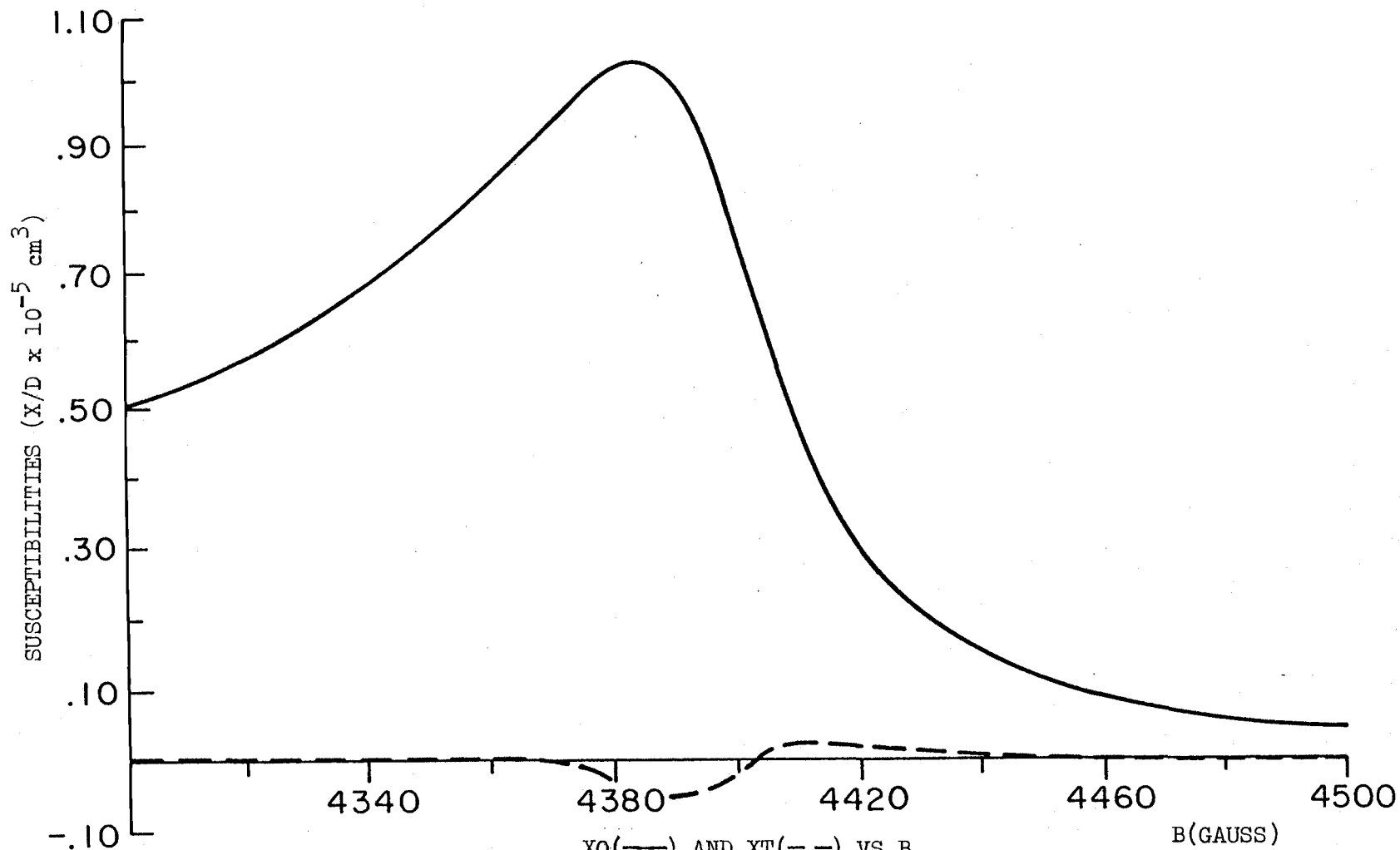


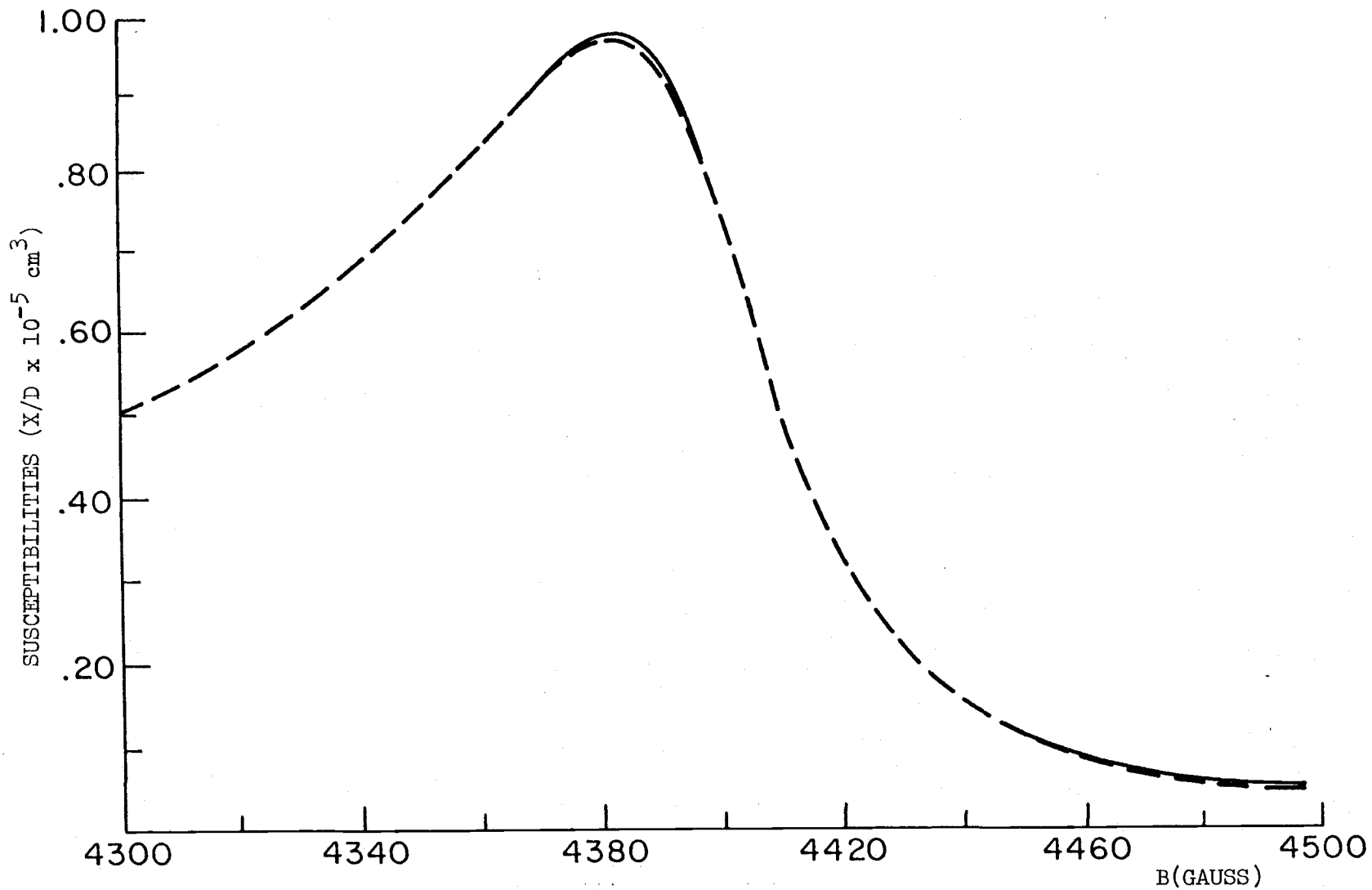
Fig. 10A



XO(—) AND XT(---) VS B

$T = .2^{\circ}\text{K}$   $T_d = .3^{\circ}\text{K}$   $N = 3$

Fig. 10B



X(—) AND XA(---) VS B

T=.2°K T<sub>d</sub>=.3°K N=3

Fig. 10C

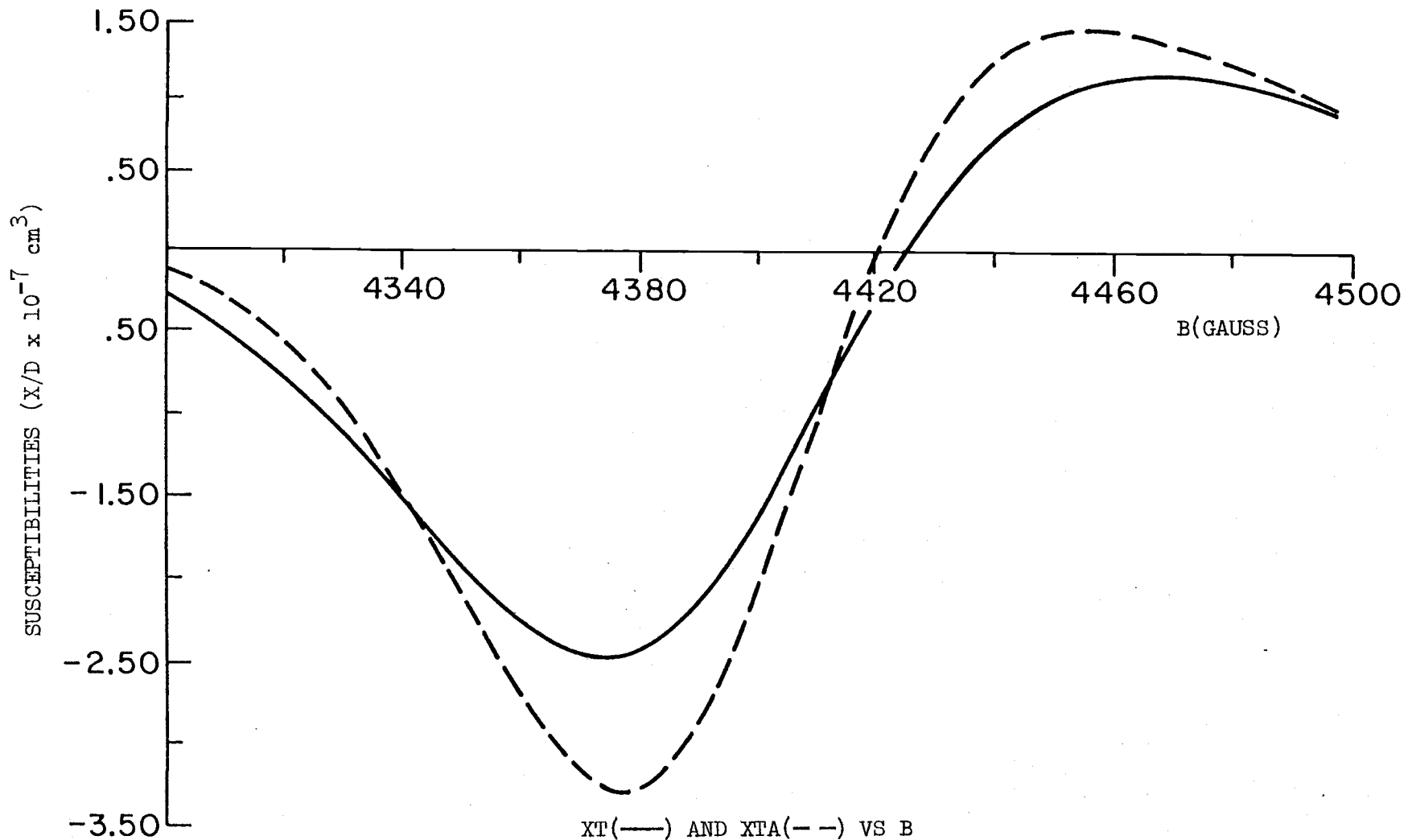
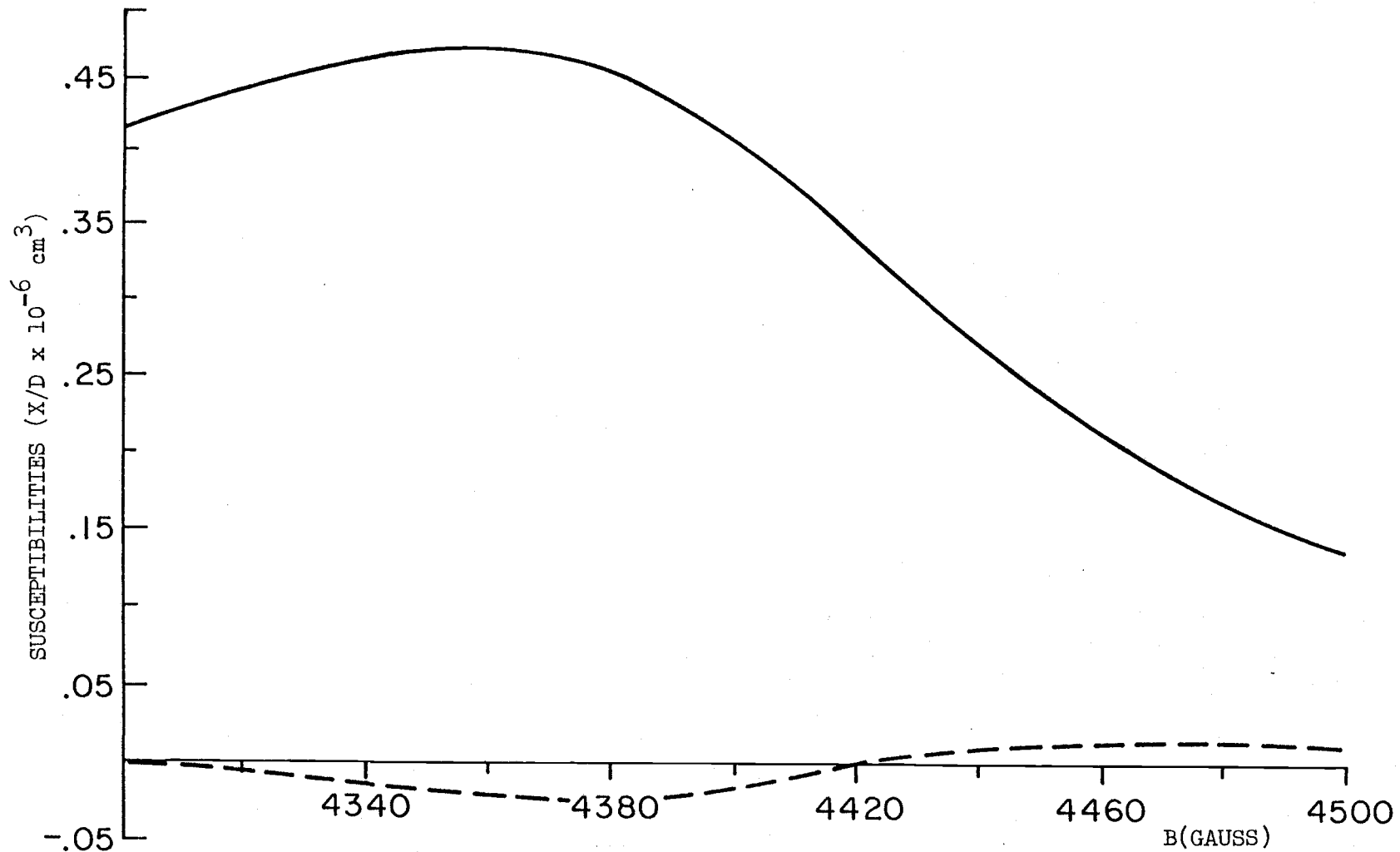


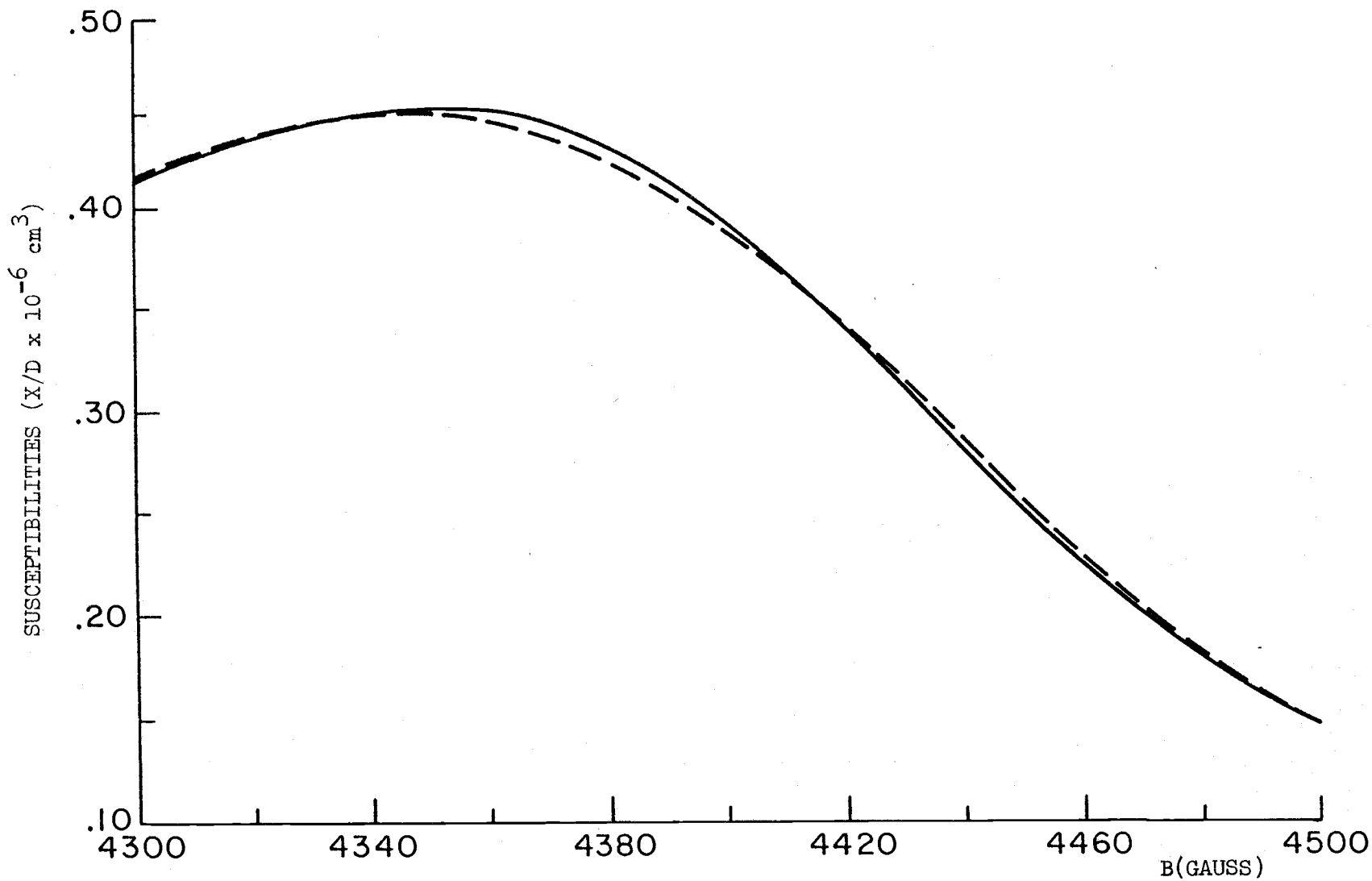
Fig. 11A



X0(—) AND XT(--) VS B

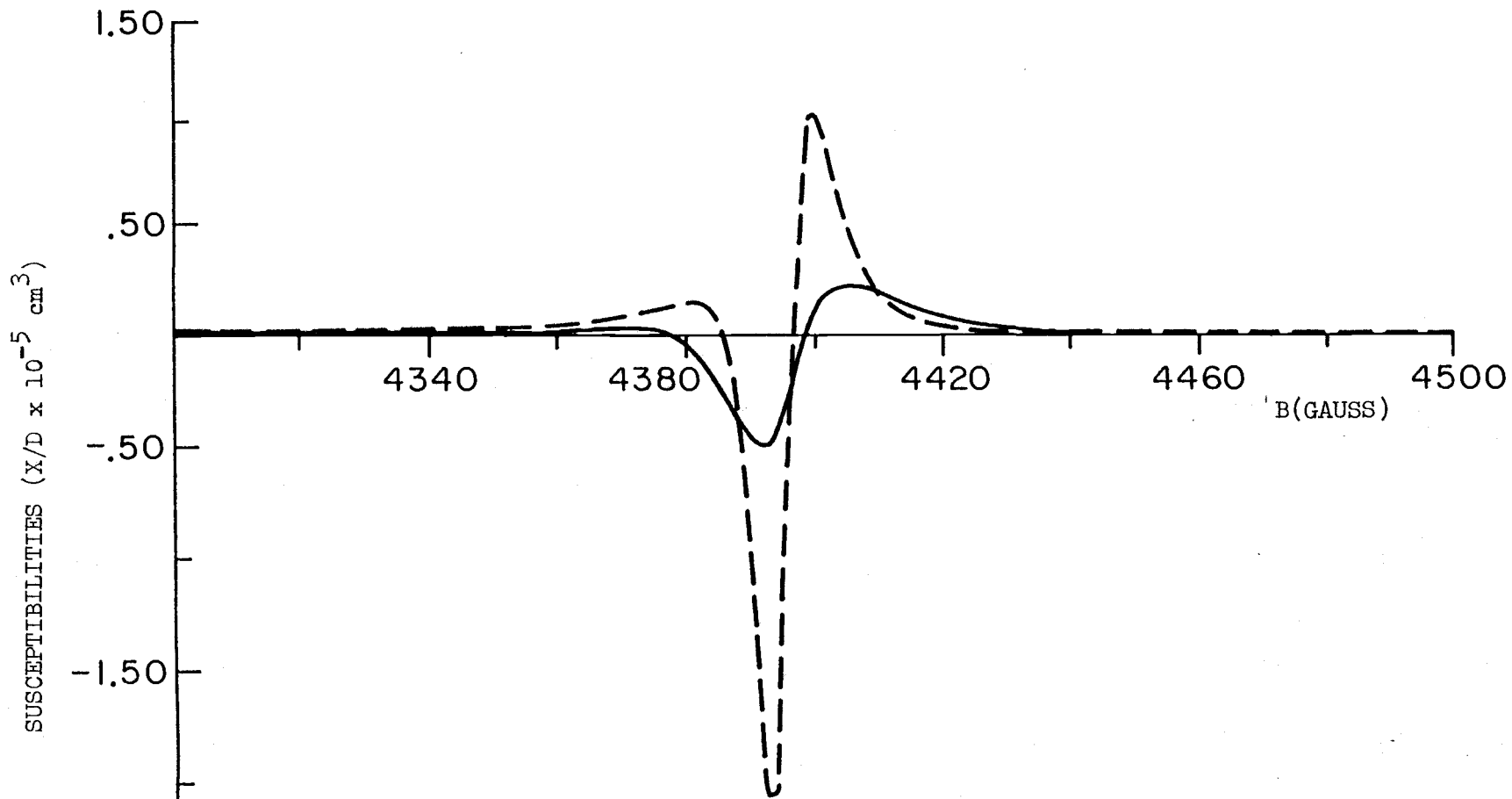
T=.8°K T<sub>d</sub>=1.2°K N=3

Fig. 11B



X(—) AND XA(---) VS B  
 T=.8°K T<sub>d</sub>=1.2°K N=3  
 Fig. 11C

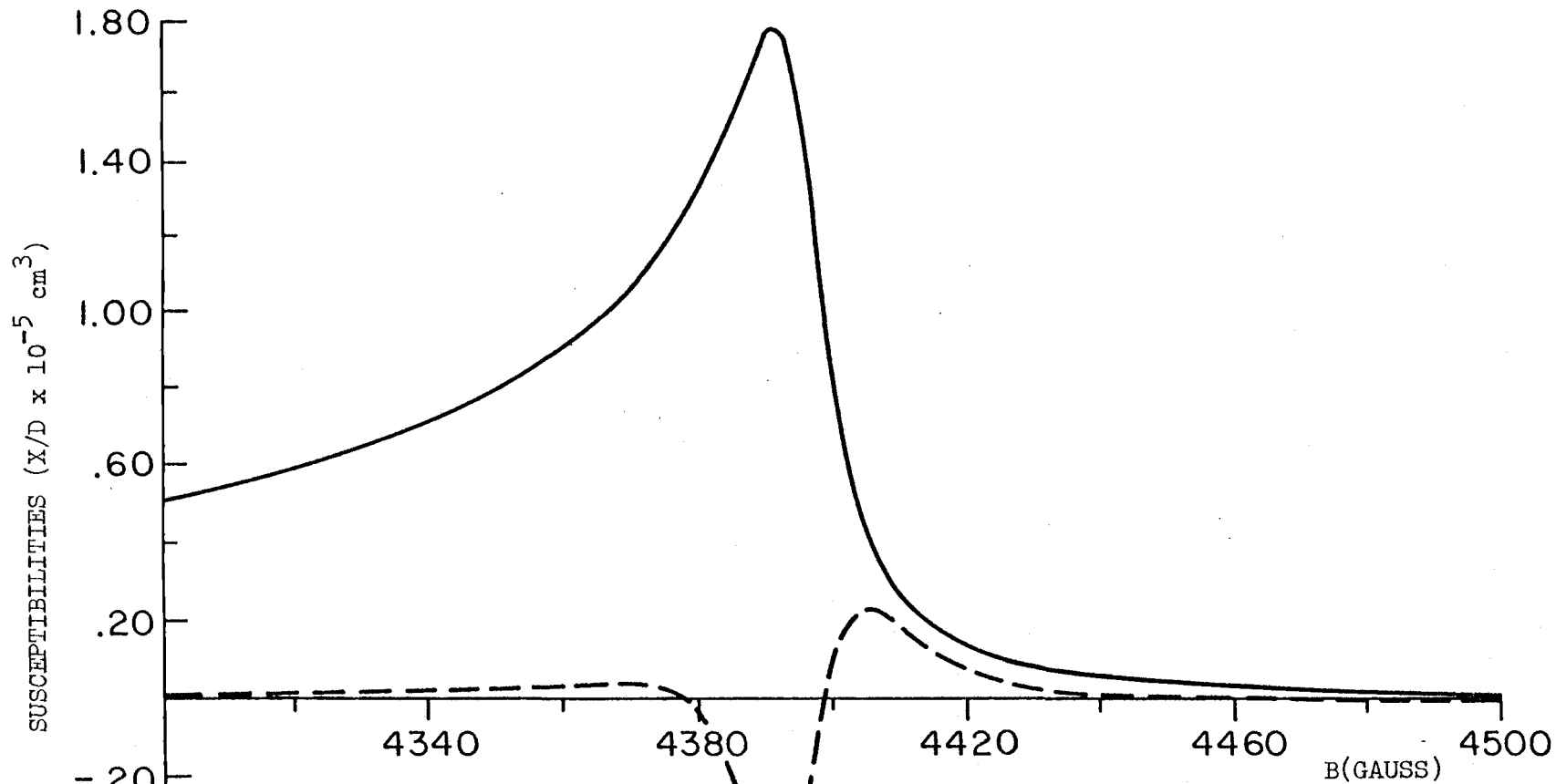




XT(—) AND XTA(--) VS B

$T = .3^{\circ}\text{K}$   $T_d = .1^{\circ}\text{K}$   $N=3$

Fig. 12A



XO(—) AND XT(- -) VS B  
 T=.3°K T<sub>d</sub>=.1°K N=3

Fig. 12B

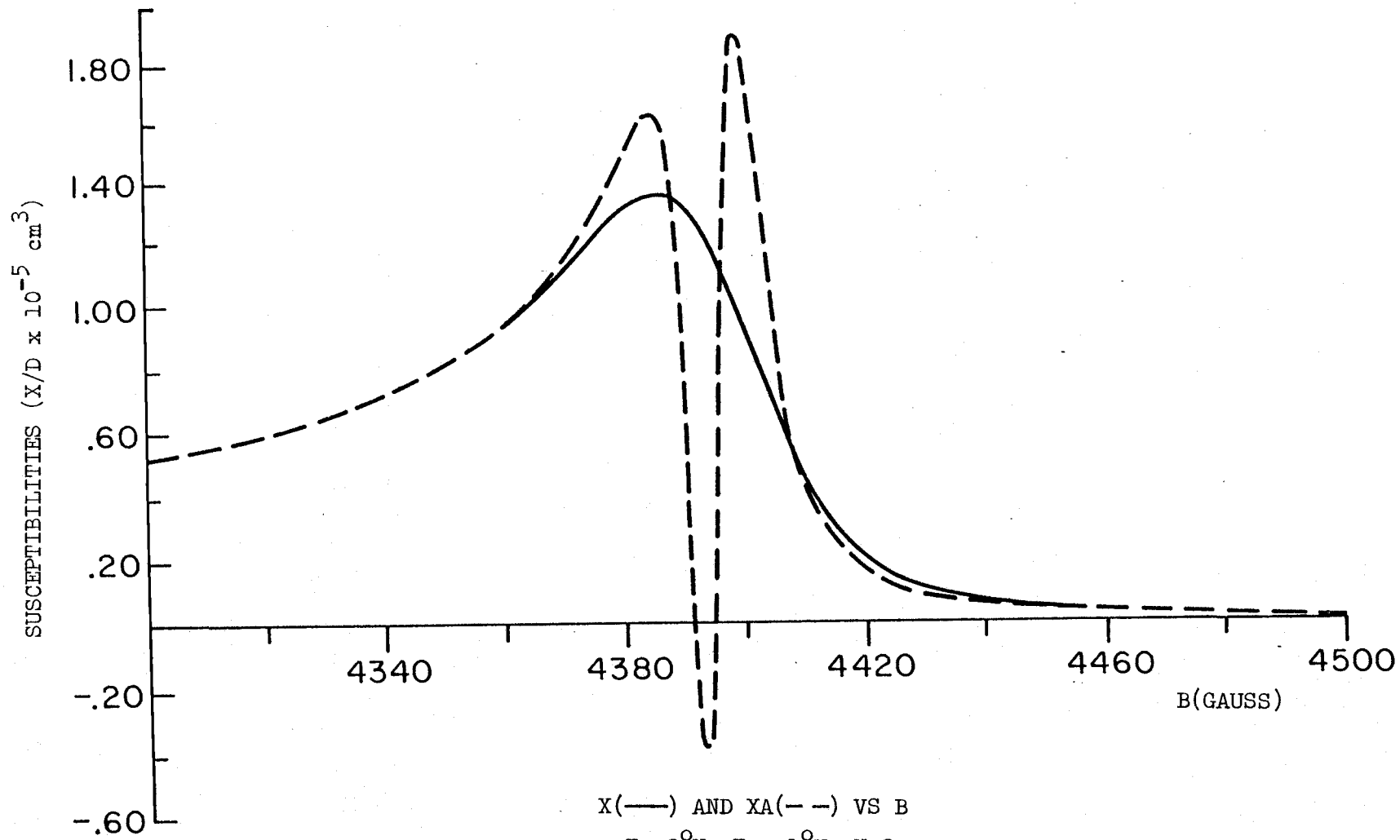


Fig. 12C

## V. SELF-ENERGY CALCULATION

### A. INTRODUCTION

The development of chapter three and the graphical analysis of chapter four shows how sensitive the line shape of the susceptibility is to the electron-impurity and perhaps other forms of the self-energy.

It should be noted that in our approach it has not been necessary to invoke the short range or "weak field" approximations<sup>(21,23)</sup> which would allow one to calculate the scattering matrix elements in plane wave states. In fact, a characteristic of our result is that  $\Sigma$  will explicitly depend upon the LL quantum number  $n$ . It should not be surprising then that each QL peak may indicate a different and therefore field dependent scattering rate. The scattering rate may also have an internal field dependence, apart from its overall  $n$  dependence, which may cause a departure from the constant Lorentzian broadening which has been assumed in previous analysis of the QL (see appendix D).

Exploring this aspect of the problem is extremely difficult since one would ideally like to calculate the scattering rate (imaginary part of  $\Sigma$ ) using the exact LL basis states in conjunction with a somewhat plausible model potential.

Among some of the factors which contribute to the difficulty of such a calculation are:

1. Purely mathematical difficulties involved in calculating matrix elements using the LL basis (see eq.2-7).

2. Physical considerations concerning the nature of the impurity system which determine the degree of sophistication required of the self-energy approximation, e.g.

a. the existence of bound states or strongly repulsive states of the impurity potential.

b. the range of the scattering potential and,

c. the concentration of the scattering centers.

The mathematical difficulties which one will encounter are fairly obvious and have been considered by both Brailsford<sup>(8)</sup> and Dworin<sup>(27)</sup>.

Brailsford attempted to calculate the self-energy in the Born approximation using an arbitrary spherically symmetric potential but was not able to obtain a result valid for all field strengths and potential ranges. Dworin developed a more formal approach to the T-matrix series but he also was unable to reduce it to a useable form.

Even though the Born approximation is a difficult enough calculation, it is still the simplest approximation one can make to the self-energy and in that respect may not be adequate to reflect the physics of certain situations. This will occur, for example, if the impurity potentials can support bound states. In this circumstance the investigations which have been done on impurity band studies<sup>(28,29)</sup> have indicated the need to introduce a self-consistent T-matrix approximation to reflect the existence of bound states. The nature of the self-consistent T-matrix approximation is such that it is

not mathematically feasible to carry it out using a realistic potential. The usual approach then is to invoke either a delta function or a separable potential in order to simplify the analysis<sup>(28)</sup>. One aspect of this simplification is that it removes a crucial convergence factor from certain sums which occur in the analysis. To prevent the divergences from occurring, a cut-off is introduced into the sum (similar to the Slater-Koster model) which is either related to the strength of the bound state<sup>(30)</sup> or to the range of the potential<sup>(29)</sup>.

Even if the potentials could not support a bound state, a self-consistent approximation may still be required if the range of the potential is long enough to cause multiple scattering events to be of significance. Again one is confronted with the necessity to invoke the delta function approximation to carry out the analysis and range effects are later recovered through the cut-off in a manner analogous to that described for the bound state problem<sup>(28,29)</sup>. It should be noted that although the delta function has the advantage of simplifying the analysis, it has the distinct disadvantage of removing all explicit quantum number dependence from the self-energy.

One final comment which is applicable to all self-energy calculations regardless of their complexity is that one must always perform an ensemble average of the impurity centers over the volume of the crystal. This has the effect of introducing a "cumulant averages"<sup>7</sup> as a prefactor multiplying each diagram<sup>(31)</sup>. This in turn

---

7. These are complicated polynomial functions of the concentration.

greatly complicates the summing of diagrams which then can only be carried out exactly in the limit of small concentration. A coherent potential approximation<sup>(32)</sup>, which is essentially a double self-consistent approximation, has been developed to deal with the case of high concentration factors.

From the above discussion it should be apparent that a Born approximation may not be sophisticated enough to adequately describe the self-energy in the QL. But on the other hand more sophisticated approaches demand that one relinquish straightforward information concerning range effects and quantum number dependence by substituting the delta function for more realistic potentials.

We shall attempt in the following analysis to perform a Born approximation calculation using a realistic potential with range effects in full LL states. We shall find that, as opposed to Brailsford who was able to evaluate the self-energy only in the limits of weak fields or ultra short range delta function potentials, we are able to evaluate the self-energy for all values of range and field parameters. The evaluation is expressible in closed form in some regions of the parameters (as an approximation) and as a simple quadrature in others. In those regions where a simple analysis is possible, we find general agreement with the experimental results to date concerning the field dependence of the self-energy<sup>(7)</sup>.

The above discussion may be put into sharper focus by introducing Feynmann diagrams to represent the contributions of various terms to the self-energy.

The diagrammatic analysis may be generated most easily by noting that the full self-energy for the random collection of impurity scattering centers is of the form<sup>(17)</sup>

$$\Sigma^1 = V_T + V_T G_0 V_T + \dots \quad (5-1)$$

where  $V_T$  is the full potential due to all scattering centers and

$$V_T(\bar{n}) = \sum_{i=1}^N V(\bar{n} - \bar{n}_i) \quad (5-2)$$

where  $V(\bar{n} - \bar{n}_i)$  is the potential due to a single impurity at position  $\bar{n}_i$ .

The Born approximation consists in taking only the first two terms in eq. 5-1 and performing an ensemble average over all scattering centers. We shall describe what occurs in the Born approximation so that its diagrams may serve as a prototype for the more sophisticated approximations we wish to describe.

As is shown in detail below, the ensemble averaging yields an expression for  $\Sigma^1$  (retaining only first order terms in the concentration) of the form,

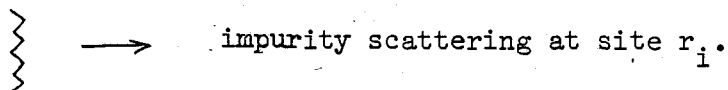
$$\Sigma^1(\bar{x}, \bar{y}) = c \int d^3 n_i V(n_i) + c \int d^3 n_i V(\bar{x} - \bar{n}_i) G_0(\bar{x}, \bar{y}) V(\bar{y} - \bar{n}_i) \quad (5-3)$$

In terms of diagrams this expression may be represented as,

$$\Sigma^1 = \begin{array}{c} \text{zigzag line} \\ \downarrow \\ \bullet \end{array} + \begin{array}{c} \text{zigzag line} \\ \downarrow \\ \text{horizontal line} \\ \downarrow \\ \bullet \end{array}$$



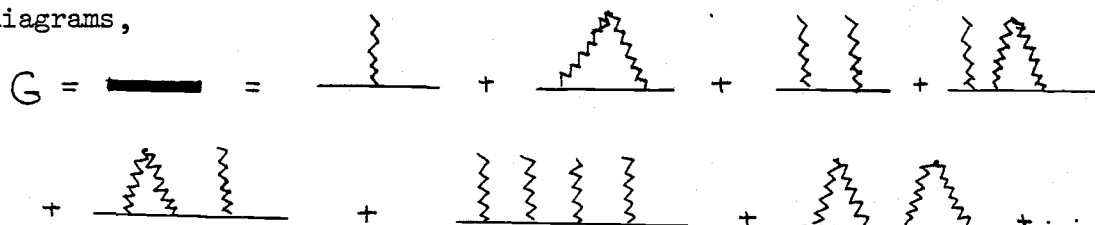
where,



(5-5)

Since  $G = G_0 + G_0 \Sigma G$ , this implies that the expression for  $G$  within the Born approximation includes the following types of

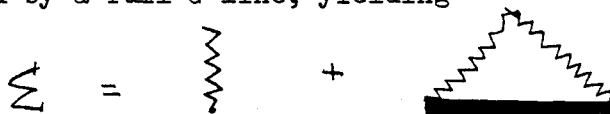
diagrams,



(5-6)

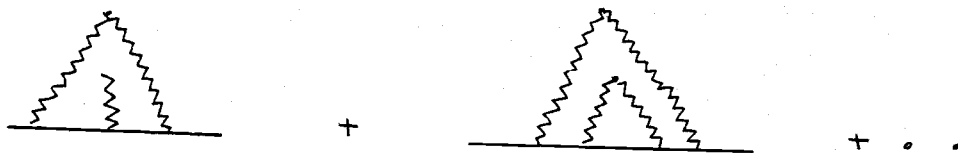
where **[thick line]** indicates the full Green's function. As mentioned previously, each diagram will be multiplied by a cumulant averages coefficient ( not shown ) which arises from the ensemble averaging. These coefficients will all reduce to  $c$  in the limit that  $C \ll 1$ .

In the self-consistent Born approximation, the  $G_0$  line is replaced by a full  $G$  line, yielding



(5-7)

Now the diagrams for  $G$  will include the following type,



(5-8)

It is these diagrams which bring in the multiple scattering aspect of the problem.

The T-matrix approximation for single impurity scattering assumes that  $\Sigma'$  is of the form

$$\Sigma' = \text{[vertical wavy line]} + \text{[triangle with one wavy line]} + \text{[triangle with two wavy lines]} + \dots$$

(5-9)

while the self-consistent T-matrix formulation replaces the  $G_0$  line with the full  $G$  line, leading to the inclusion of the following diagrams,



(5-10)

### B. BORN APPROXIMATION

We shall assume in the Born approximation that the self-energy is given by,

$$\Sigma' = V_T + V_T G_0 V_T$$

(5-11)

Since the first term is real, it will only contribute to a shift in the chemical potential and therefore our attention will be concentrated upon the second diagram in eq. 5-11.

In order to facilitate the ensemble average over scattering centers which must be performed, we write

$$\Sigma'(\alpha, \alpha') = \langle \alpha | \bar{n} \rangle G_0(\bar{n}, \bar{n}') \langle \bar{n}' | \alpha' \rangle V_T(\bar{n}) V_T(\bar{n}') \quad (5-12)$$

where the obvious spatial integrations are left implied.

In terms of the Fourier transforms of the atomic potentials we have,

$$V_T(\bar{n}) V_T(\bar{n}') = \sum_{i,j}^N \int V(\bar{k}) V(\bar{k}') e^{i\bar{k} \cdot (\bar{n} - \bar{r}_i)} e^{i\bar{k}' \cdot (\bar{n}' - \bar{r}_j)} d^3k d^3k' \quad (5-13)$$

The ensemble average of  $V_T(\bar{n}) V_T(\bar{n}')$ , which we designate as  $\langle V_T(\bar{n}) V_T(\bar{n}') \rangle_E$ , is therefore related to the ensemble average of  $\langle e^{-i\bar{k} \cdot \bar{r}_i} e^{-i\bar{k}' \cdot \bar{r}_j} \rangle_E$  where  $\bar{r}_i$  and  $\bar{r}_j$  cover exactly the same set of scattering centers.

We may thus write,

$$\langle \sum_{i,j} e^{-i\bar{k} \cdot \bar{r}_i} e^{-i\bar{k}' \cdot \bar{r}_j} \rangle_E = \langle \sum_i e^{-i(\bar{k} + \bar{k}') \cdot \bar{r}_i} \rangle + \langle \sum_{i \neq j} e^{-i\bar{k} \cdot \bar{r}_i} e^{-i\bar{k}' \cdot \bar{r}_j} \rangle \quad (5-14)$$

We first consider,

$$\begin{aligned}
 \langle \sum_i e^{-i(\bar{k}+\bar{k}') \cdot \bar{r}_i} \rangle_E &= \langle \sum_i \int d^3 r \delta(\bar{r}-\bar{r}_i) e^{-i(\bar{k}+\bar{k}') \cdot \bar{r}} \rangle_E & 76. \\
 &= \int d^3 r e^{-i(\bar{k}+\bar{k}') \cdot \bar{r}} \langle \sum_i \delta(\bar{r}-\bar{r}_i) \rangle_E = c \delta(\bar{k}+\bar{k}')
 \end{aligned}$$

(5-15)

where  $c$  = concentration of the scattering centers.

The contribution of the first term in eq. 5-15 to  $\Sigma'$  is therefore,

$$c \langle \alpha | \bar{r} \rangle G_0(\bar{r}, \bar{r}') \langle \bar{r}' | \alpha' \rangle \int d^3 k V(\bar{k}) V(-\bar{k}) e^{i\bar{k} \cdot (\bar{r} - \bar{r}')}$$

(5-16)

But it is easy to show that,

$$\int d^3 k V(\bar{k}) V(-\bar{k}) e^{i\bar{k} \cdot (\bar{r} - \bar{r}')} = \int d^3 r_i V(\bar{r} - \bar{r}_i) V(\bar{r}' - \bar{r}_i)$$

(5-17)

Therefore, the contribution of the first term to  $\Sigma'$  after ensemble averaging is,

$$\Sigma'(\alpha, \alpha') = \langle \alpha | \bar{r} \rangle \langle \bar{r} | \bar{\Sigma}' | \bar{r}' \rangle \langle \bar{r}' | \alpha' \rangle$$

(5-18)

where

$$\langle \bar{r} | \bar{\Sigma}' | \bar{r}' \rangle = \int d^3 r_i V(\bar{r} - \bar{r}_i) G_0(\bar{r}, \bar{r}') V(\bar{r}' - \bar{r}_i)$$

(5-19)

Diagrammatically these terms may be represented as,

$$\overline{\Sigma} = \text{[Diagram: A triangle with a jagged, sawtooth-like top edge and a solid horizontal base.]}$$

(5-20)

It can be shown in an exactly similar fashion that the second term in eq. 5-14 gives rise to a self-energy term which is of the order  $c^2$ . We shall ignore these contributions and take eq. 5-20 as the Born approximation to the self-energy.

Before we can make any further progress in the analysis of the self-energy we need to calculate  $G_0(r, r')$ . In terms of LL states, this quantity may be expressed as,

$$G_0^0(r, r') = \sum_{\alpha} \frac{\langle r | \alpha \rangle \langle \alpha | r' \rangle}{i p_{\alpha} - \bar{\epsilon}_{\alpha}}$$

(5-21)

This calculation, which is detailed in appendix E, follows the lines introduced by Dworin<sup>(27)</sup> but necessarily incorporates a different set of arguments to make the extension to the Matsubara Green's function.

The results of the calculation show that,

$$G_0^0 = \sum_{\sigma=\pm 1} \frac{1}{4\pi \hbar^2 c^*} \frac{e^{i k_{\alpha} |\bar{r} - \bar{r}'|}}{|\bar{r} - \bar{r}'|} e^{-\frac{i\delta}{2} (x' - x)(y' + y)}$$

(5-22)

where,

$$k_e^2 = \frac{i \mu_e + \mu + G \hbar \omega_c}{c^*} \quad \text{arg } k_e > 0$$

$$\gamma = \frac{m \omega}{\hbar}, \quad c^* = \frac{\hbar^2}{2m^*}, \quad \omega_c = \frac{e B}{m c}, \quad G = g/4$$

When this expression is incorporated into the one for  $\Sigma^1$  the result may be expressed as,

$$\Sigma^1(\alpha, \alpha') = \frac{c}{4\pi c^*} \int V(r) \frac{e^{i k_e |r-r'|}}{|r-r'|} e^{-\frac{i \gamma}{2} (x'-x)(y'+y)} S_{\alpha\alpha'}(r, r') V(r')^* \times d^3 r d^3 r'$$

(5-23)

where,

$$S(\alpha, \alpha') = \int e^{-\gamma(x'-x)y} \psi_{\alpha}^*(\bar{r} + \bar{r}_i) \psi_{\alpha'}(\bar{r}' + \bar{r}_i) d^3 r_i$$

(5-24)

The calculation of  $S(\alpha, \alpha')$  was first performed by Dworin<sup>(27)</sup>, and is outlined in appendix F. We present there an alternate derivation which utilizes integral representations in a manner which makes this calculation much simpler than the one originally presented in ref. 27.

The results of the calculation show that,

$$S(\alpha, \alpha') = \delta_{k_x, k_x'} \delta_{k_z, k_z'} \left( \frac{n'!}{n!} \right)^{1/2} e^{i k_z (z' - z)} e^{i \delta y (x' - x)} \\ \times e^{i \frac{\delta}{2} (x' - x)(y' - y)} \left( i \rho \sqrt{\delta/2} e^{-i\phi} \right)^{n-n'} e^{-\delta \rho^2/4} L_n \left( \frac{\delta \rho^2}{2} \right)$$

$$\rho = \left[ (x - x')^2 + (y - y')^2 \right]^{1/2} \quad (n > n')$$

For  $n < n'$ , the roles of  $n$  and  $n'$  are exchanged. (5-25)

The crucial point to note here is the appearance of the term  $e^{-i\phi(n-n')}$ , where  $\phi$  is the azimuthal angle associated with the vector  $\vec{r} - \vec{r}'$ .

When we calculate  $\Sigma'$  we must integrate the potentials  $V(r)$  and  $V(r')$  over all space together with the above expression in  $\phi$ . If the potential possesses azimuthal symmetry, as we shall henceforth assume, then the integration of the  $\phi$  coordinates will yield zero unless  $n = n'$ . Therefore the self-energy is rendered diagonal in all the Landau level quantum numbers.

Anticipating this diagonality in  $\Sigma'$  and using the diagonal form of  $S(\alpha, \alpha')$ , we may write eq. 5-23 as

$$\Sigma'(\alpha) = -\frac{c}{4\pi c^*} \int V(r) \frac{e^{i k_z |\vec{r} - \vec{r}'|}}{|\vec{r} - \vec{r}'|} e^{i k_z (z' - z)} e^{-\delta \rho^2/4} L_n \left( \frac{\delta \rho^2}{2} \right) V(r') d^3 r d^3 r'$$

(5-26)

We shall continue the analysis by letting the atomic potentials be represented by a shielded coulomb potential;  $V(r) = V_0 \frac{e^{-\alpha r}}{r}$ .

This potential is expressible in terms of its Fourier transform as,

$$V(r) = \frac{V_0}{2\pi^2} \int \frac{e^{i\vec{k}\cdot\vec{r}}}{k^2 + \alpha^2} d^3k \quad (5-27)$$

Using this expression in eq. 5-26 and making the change of variable  $\vec{r}' = \vec{r}'$ ,  $\vec{r} - \vec{r}' = \vec{R}$  (we shall write  $\vec{R}$  as  $\vec{r}$  in what follows) we find that,

$$\begin{aligned} \Sigma_1(\alpha) = \frac{-c V_0^2}{4\pi c^* (2\pi^2)^2} \int \frac{e^{i\vec{k}\cdot(\vec{r} + \vec{r}')}}{k^2 + \alpha^2} \frac{e^{i k_z r}}{r} \frac{e^{i\vec{k}'\cdot\vec{r}'}}{k'^2 + \alpha^2} e^{-i k_z z} e^{-\frac{\gamma p^2}{4}} L_n\left(\frac{\gamma p^2}{2}\right) \\ \cdot d^3k d^3k' d^3r d^3r' \end{aligned} \quad (5-28)$$

The integrals over  $r'$  may be done immediately and yield  $(2\pi)^3 \delta(\vec{r} + \vec{r}')$  which makes the  $k'$  integration trivial.

The result of this is,

$$\Sigma_1(\alpha) = \frac{-c}{c^* 2\pi^2} \int \frac{e^{i\vec{k}\cdot\vec{r}}}{(k^2 + \alpha^2)^2} \frac{e^{i k_z r}}{r} e^{-i k_z z} e^{-\frac{\gamma p^2}{4}} L_n\left(\frac{\gamma p^2}{2}\right) d^3k d^3r \quad (5-29)$$

But (26),

$$\int \frac{e^{i\vec{k}\cdot\vec{r}}}{(k^2 + \alpha^2)^2} d^3k = \frac{\pi^2 e^{-\alpha r}}{\alpha} \quad (5-30)$$



This can be further reduced by noting that, <sup>(33)</sup>

$$\int_{-\infty}^{\infty} \frac{e^{-(\alpha - i k_{\perp}) (\rho^2 + z^2)^{1/2}} e^{-i k_{\perp} z}}{(\rho^2 + z^2)^{1/2}} d\phi dz = 4\pi K_0 \left[ \rho \sqrt{k_{\perp}^2 + (\alpha - i k_{\perp})^2} \right]$$

$$\equiv 4\pi K_0 (\rho \tau_{\perp})$$

(5-32)

Therefore, with our particular choice for the atomic potentials we have been able to reduce the self-energy to a form which involves only one final integration, viz.

$$\Sigma(\alpha, i \rho_{\perp}) = -\frac{2c\pi}{\alpha c^*} \int_0^{\infty} \rho e^{-\frac{\alpha}{4} \rho^2} L_n \left( \frac{\alpha \rho^2}{4} \right) K_0(\rho \tau_{\perp}) d\rho$$

(5-33)

Since our main concern in this work is with the susceptibility near the quantum limit we shall be interested in  $\Sigma'$  for small values of  $n$ . We may then expand the Laguerre polynomials in their series form,

$$L_n(z) = \sum_{m=0}^n C_m(n) z^m$$

(5-34)

where,

$$C_m(n) = (-1)^m \frac{n!}{(n-m)!}$$

This puts  $\Sigma'$  into the form,

$$\Sigma'(\alpha, i p_0) = -\frac{2c\pi}{\alpha c^*} \sum_{m=0}^n \frac{C_m(n) \delta^m}{2^m} \int_0^\infty p^{2m+1} e^{-\delta p^2/4} K_0(p\tau_0) dp \quad (5-35)$$

But, (26)

$$\int_0^\infty p^{2m+1} e^{-\delta p^2/4} K_0(p\tau_0) = \frac{(m!)^2 2^{2m}}{\delta^{m+1/2} \tau_0} e^{\tau_0^2/2\delta} W_{-(m+1/2), 0}(\tau_0^2/\delta) \quad (5-36)$$

where  $W_{-(m+1/2), 0}(z)$  is the Whittaker function which is defined in terms of the more familiar confluent hypergeometric function as, (17)

$$W_{-m+1/2, 0}(z) = e^{-z/2} \sqrt{z} U(m+1, 1, z) \quad (5-37)$$

Setting  $k_z=0$  and  $p_0 = p_0$  as required by our formalism finally yields,

$$\Sigma'(n, p_0) = \frac{c\pi}{\alpha} \sum_{m=0}^n \frac{(-1)^m 2^m n!}{(n-m)! \sqrt{\delta} \tau_0} e^{\tau_0^2/2\delta} W_{-(m+1/2), 0}(\tau_0^2/\delta) \quad (5-38)$$

We now recall that,

$$\tau_0 = \alpha - i k_0$$

where,

$$k_0^2 = \frac{i \gamma_0 - \mu + \sigma G k \omega}{c^*} \quad (5-39)$$

Since for the range of parameter values of interest to us,  $\mu$  dominates the other terms in the numerator of  $k_0^2$  by a factor of 100, we will approximate  $k_0^2$  by  $\mu/c^* = k_F^2$ , where  $k_F$  is defined by the last expression.

We note that neglecting the imaginary part of  $k_0^2$  is equivalent to neglecting the temperature dependence of  $\Sigma'$ .

Now,

$$\left| \frac{\tau_0^2}{\delta} \right| = \frac{\alpha^2 + k_F^2}{\delta} \quad (5-40)$$

Furthermore, as the  $n^{\text{th}}$  LL passes through the FS,  $\delta$  is given by,

$$\delta_n = \frac{k_F^2}{2n+1 + 2\sigma GM} \quad (5-41)$$

Therefore, in terms of  $n$  alone, the value of  $|\tau_0^2/\delta|$ , at that field value where the  $n^{\text{th}}$  LL is crossing the FS is,

$$\left| \tau_0^2/\delta \right| = \left( 1 + \frac{\alpha^2}{k_F^2} \right) (2n+1) \quad (5-42)$$

We see that there are two circumstances under which  $|\tau_0^2/\delta| \gg 1$ ,

- a.  $\alpha \gg K_F$  - short range potential, any n value.
- b.  $n \gg 1$  - long range potential, large n value.

When either situation applies, we may approximate the Whittaker function by, (17)

$$W_{-(m+\frac{1}{2}),0}(z) \sim e^{-z/2} \frac{1}{z^{m+1/2}} \quad (5-43)$$

This enables the self-energy to be expressed as,

$$\Sigma^1(n) = -\frac{2c\pi}{\alpha c^*} \sum_{m=0}^n \frac{(-1)^m n!}{(n-m)!} \left(\frac{2\delta_0}{\tau_0^2}\right)^m \frac{1}{\tau_0^2} \quad (5-44)$$

We note that since  $\tau_0^2/2\delta > n$ , eq. 5-44 under conditions a or b is highly convergent in m and may be well approximated by the first two terms in the series.

Thus,

$$\Sigma^1(n) = -\frac{2c\pi}{\alpha c^*} \left[ \frac{1}{\tau_0^2} - \frac{2\delta n}{\tau_0^4} \right] \quad (5-45)$$

The real and imaginary parts of  $\Sigma^1$  are found to be,

$$\Sigma_R^1(n) = -\frac{2c\pi}{\alpha c^*} \frac{1}{(\alpha^2 + K_F^2)^2} \left[ \alpha^2 - K_F^2 - 2\delta n \left\{ \frac{(\alpha^2 - K_F^2)^2 - 4\alpha^2 K_F^2}{(\alpha^2 + K_F^2)^2} \right\} \right]$$

$$\Sigma_I(n) = \frac{-2c\pi}{\alpha c^*} \frac{1}{(\alpha^2 + K_F^2)^{\alpha}} \left[ 2\alpha K_F - 2\delta n \left\{ \frac{4\alpha K_F (\alpha^2 - K_F^2)}{(\alpha^2 + K_F^2)^{\alpha}} \right\} \right]$$

(5-46)

For case a we may neglect  $k_f$  with respect to  $\alpha$  and find that,

$$\Sigma_R = -\frac{2c\pi}{\alpha^3 c^*} \left[ 1 - \frac{c(K_F/\alpha)^2}{(n+1/2) - \sigma GM} \right] \approx -\frac{2c\pi}{\alpha^3 c^*}$$

$$\Sigma_I = -\frac{4c\pi K_F}{\alpha^4 c^*} \left[ 1 - \frac{2c(K_F/\alpha)^2}{(n+1/2) - \sigma GM} \right] \approx -\frac{4c\pi}{\alpha^4 c^*}$$

(5-47)

For case b,  $n \gg 1$  we find that,

$$\Sigma_R = -\frac{2c\pi}{\alpha K_F^2 c^*} \left[ 1 + \frac{n}{(n+1/2) - \sigma GM} \right]$$

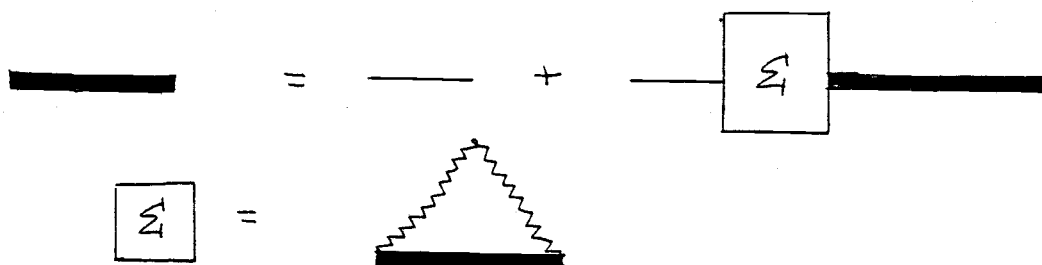
$$\Sigma_I = -\frac{4c\pi}{K_F^3 c^*} \left[ 1 + \frac{2n}{(n+1/2) - \sigma GM} \right]$$

(5-48)

We may conclude from the above analysis that the self-energy in the Born approximation is not inconsistent with the experimental results in the regions in which we have been able to examine it simply. For the short range potential, whether one is in the quantum limit or not, the self-energy is essentially field independent while for long

range potentials in the LK limit we note that although there does exist some slight field dependence through the quantum number  $n$ , the self-energy is still basically field independent.

A field dependent self-energy is most easily obtained by making use of a self-consistent argument for calculating the self-energy. A self-consistent Born approximation would proceed along the following lines,



(5-49)

These diagrams may be translated as follows,

$$G(\alpha) = \frac{1}{i p_{\alpha} - \bar{\epsilon}_{\alpha} - \Sigma'(\alpha)} \quad \alpha = n, K_x, K_z, \sigma$$

$$\Sigma'(\alpha) = c \sum_{\beta} \frac{|\langle \alpha | V | \beta \rangle|^2}{i p_{\alpha} - \bar{\epsilon}_{\beta} - \Sigma'(\beta)}$$

(5-50)

Therefore, we may write,

$$\Sigma'(\alpha) = c \sum_{\beta} \frac{|\langle \alpha | V | \beta \rangle|^2}{i p_{\alpha} - \bar{\epsilon}_{\beta} - \Sigma'(\beta)} =$$

$$= c \bar{D} B \sum_{n=0}^{\infty} \int_{-\infty}^{\infty} dk_z \frac{|\langle \alpha | V | \beta \rangle|^2}{i \epsilon - \bar{\epsilon}_\beta - \Sigma'(\beta)}$$

$$\bar{D} = e / 4\pi^2 c \hbar$$

(5-51)

if one now assume a delta function potential, then

$$|\langle \alpha | V | \beta \rangle|^2 = V_0 = \text{constant}$$

(5-52)

and,

$$\Sigma' = \frac{c V_0^2 B \bar{D} i \pi}{\sqrt{c^*}} \sum_{\substack{n=0 \\ \sigma=\pm 1}}^{\infty} \frac{1}{[i \epsilon - \bar{\epsilon}_n - \Sigma']}$$

(5-53)

It should be pointed out that the assumption of a delta function potential has effectively removed a crucial convergence factor in eq. 5-53 so that the sum over  $n$  is no longer convergent. To remedy this one can insert a cut-off fact  $N_t$  into the sum to duplicate the effect of a finite range in the potential. Doar<sup>(34)</sup> has analyzed this approach in great detail and developed a relationship between the cut-off number and the Thomas-Fermi screening length. For very long range potentials he finds that a cut-off of  $N_t=1$  is sufficient. An analysis of eq. 5-53 shows that taking the sum up to one will yield an approximate  $(B n_i)^{2/3}$  dependence in the self energy.

A number of points should be noted. First is that the assumption of a delta function potential has eliminated all quantum number

dependence from the self-energy and secondly, range effects must now be reinserted in a somewhat less than rigorous fashion.

It should be mentioned that the analysis of Doar<sup>(34)</sup> was ostensibly a full self-consistent T-matrix approximation, but as applied by Rode and Lowndes<sup>(7)</sup>, who bring in the assumption that the potential weighted density of states function ( $V_0 Z(\omega)$ ) is  $\ll 1$  and use this to approximate the self-energy up to second order terms in  $V_0$ , it appears that they are weakening the full T-matrix to obtain a self-consistent Born approximation. Even with this relaxation they are still able to generate a  $B^{2/3}$  dependence in  $\Sigma'$  for the long range potential problem in seeming agreement with experimental results.

In view of these facts, we content that there may be some hope that a self-consistent Born approximation utilizing a realistic model potential with range may be able to be performed and may adequately reflect experimental results.

The analysis will be by no means trivial but it is expected that the calculation would build upon and incorporate much of the analysis performed here into an iterative procedure which when applied to eq.5-53 could extract  $\Sigma'$  from it in a self-consistent fashion while still retaining full range and quantum number information.



## VI. DISCUSSION

In the preceding analysis we have concerned ourselves with an examination of the magnetic susceptibility of an electron gas in an impure lattice in the magnetic field region known as the quantum limit. We have worked throughout within an effective mass approximation to the band structure of the solid and have introduced the self-energy function, in a linear approximation, to account for the presence of impurity scattering centers<sup>8</sup>.

Our main result is embodied in eqs. 3-40 and 4-4 which show that for temperatures on the order of .4 °K or less and for corresponding Dingle temperatures of .6 °K or more, there exist simple algebraic expressions which accurately represent  $M$  and  $\chi$  in the quantum limit region. It is hoped that the simplicity of these forms will allow experimentalists to extract information from the line shapes using techniques which complement those already in use. The current methods involve the generation of  $\chi$  vs B curves and the extraction of Dingle temperature information from the steep slope on the high field side of the quantum limit peak. This slope is highly sensitive to the scattering rate (being infinite for a pure system) and appears to be the prime reason why the experimentalist concerns himself with a measurement of  $\chi$  rather than  $M$ . The higher the derivative taken, the more structure one introduces into the observed effect.

In principle though, there is no reason why the magnetization could

---

8. The self-energy may be extended to include other effects as well, e.g. realistic band structure effects or electron-phonon interactions.

not be measured as well as the susceptibility. It is true that for high scattering rates the shape of the magnetization curve is not very rich in detail and its high field slope does not have the sensitivity to variations in  $\Sigma$  that the susceptibility displays. But it is precisely in this region of high  $T_d$  in which the present analysis is most useful. Thus quantities such as the maximum peak height and B-axis crossing points may be used to extract information from the line shapes which may supplement and substantiate the more traditional slope measurements.

Of course, one would need to have available the individual contributions to the susceptibility from each LL isolated from all the others.

This would seem to be feasible for the lower LL's in particular since they are widely spaced from each other and it is only the low field "tails" of the higher LL's which effect the shape of the lower ones. In fact one can easily show that the expression

$$\chi_n = -8D[(n+1/2)M - \sigma G] |\alpha_n|^{1/2} \quad - \alpha_n \gg 1 \quad (6-1)$$

adequately predicts the susceptibility in regions far from the peaks. These contributions may be subtracted out on a term by term basis starting with the  $n=0$  level and progressively extracting each level out from the total susceptibility.

This assumes that the ultra-high field  $n=0$  level is available to the experimentalist. If this ideal is not achievable, one can still use the analytic forms obtained to perform a parametric fit of the

observed line shape and then analytically retrieve the individual levels from the susceptibility.

If this procedure could be accomplished for the magnetization as well as for the susceptibility, then it would have the added advantage that one need not concern oneself with the possible ramifications of a B dependence in  $\mu$  since  $m = \left(\frac{\partial m}{\partial B}\right)\mu$ .

Furthermore there exists the possibility of incorporating into the experimental approach to the quantum limit a hybrid technique which can appreciably simplify the analysis even in those temperature regimes in which the algebraic forms are not valid for all field values.

It will be recalled that the algebraic forms will hold if one is sufficiently far from a quantum limit peak or in the near vicinity of a peak if the ratio of  $T/T_d$  is approximately 2/3. In the event that this condition does not hold, one can still use the algebraic forms for the majority of the analysis and reserve the numerical integrations solely for those relatively small number of points in the neighborhood of the peak itself.

The current analysis also has the potential of providing a key for the analysis of spin-dependent scattering effects. These would be most accurately observed in the  $n=0$  level where the spin splitting is largest. These effects would be taken into account in the formalism by treating the self-energy as a matrix.

The simplest possibility to consider would be when  $\Sigma$  was diagonal but different for different spin states. This case would require no substantial modification of our present approach and

could be dealt with almost immediately.

In the event that  $\Sigma'$  is off-diagonal in the spin quantum numbers, we would first have to diagonalize the two by two matrix and then carry the formalism forward from that point. This also would not seem to present any insurmountable difficulties.

The question of electron-phonon interactions at high magnetic fields may also be examined in the QL.

In the LK limit it has been shown<sup>(22)</sup> that  $\Sigma'$  for the electron-phonon interaction is a purely imaginary quantity and is simply proportional to the temperature. This linear dependence on the temperature causes the electron-phonon self-energy to appear as a mass enhancement effect rather than as a temperature dependent scattering rate as one might initially expect.

In high magnetic fields on the other hand, the strict linear dependence of  $\Sigma'$  with T is not guaranteed and it may be possible to observe a temperature dependent scattering rate in the high magnetic field regime.

In view of the above considerations, we feel that there now exists a strong incentive for the experimentalist to perform QL experiments in the regime of extremely low temperatures so that the analysis presented in this work can be put to effective use. It is hoped that the simple algebraic forms applicable to the QL at these low temperatures will enable the QL to become as useful a probe of the solid states as the DHVA effect has been in the LK limit.

## APPENDICES

## BIBLIOGRAPHY

1. L.D.Landau (1930), Z.Phys. 64, 629.
2. W.J. deHaas and P.M. vanAlphen (1930), Proc. Acad. Sci., Amsterdam, 33,1106.
3. E.M. Lifshitz and A.M. Kosevitch (1956), Soviet Physics - JETP 2,636.
4. R.C. Barklie and D. Schoenberg (1975), Phys. cond. Matter 19,175-183.
5. N.W. Ashcroft and D.N. Mermin, Solid State Physics, (Holt, Rinehart, Winston, 1976).
6. R.B. Dingle (1952), Proc. Royal Society, A212,38.
7. J.P. Rode and D.H. Lowndes (1977), Solid State Communications, 32, 3/4.
8. A.D. Brailsford, Phys. Rev., vol. 149,2,1966.
9. J.P. Rode, unpublished thesis, University of Oregon, 1976.
10. J.M. Luttinger and J.C. Ward, Phys. Rev. 118,1417 (1960).
11. R.P. Feynmann, Statistical Mechanics, (W. A. Benjamin, 1972).
12. L.D. Landau and E.M. Lifshitz, Quantum Mechanics, (Pergamon Press, 1958).
13. M.D Rensinck, Am. Journal Physics, 37,9,1969.
14. D. Wagner, Introduction to the Theory of Magnetism, (Pergamon Press, 1972).
15. A. Wasserman, T. Buckholtz, and H.E. DeWhitt, (1970), J. Math. Physics 11,477.
16. A. Wasserman and J. Karniewicz, unpublished notes.
17. M. Abramowitz and I. Stegun, Handbook of Mathematical Functions, (Dover, 1965).
18. A.A. Abrikosov, L.P. Gorkov, and I.E. Dzyaloshinski, Methods of Quantum Field Theory in Statistical Physics, (Dover, 1963).

19. J.M. Luttinger, Phys. Rev. 121,1251 (1961).
20. V. Ambegoankar, "Green's Functions in Many Body Problems" in Astrophysics and the Many Body Problem, vol. 2 of the 1962 Brandeis Summer Institute, ( W.A. Benjamin).
21. M. Fowler and R.E. Prange, (1965) Physics, 1,6.
22. P. Soven, Phys. Rev. B5 (1972),260.
23. S. Englesberg and G. Simpson, Phys. Rev. B2, (1970), 1657.
24. A.W. Wasserman and N. Bharitiya, Phys. Rev., in press.
25. N. Bharitiya, unpublished thesis, Oregon State University, 1976.
26. I.S. Gradshteyn and I.M.Ryzhik, Table of Integrals, Series, and Products, ( Academic Press, 1965).
27. L. Dworin, Annals of Physics, 38,431, (1966).
28. M. Saitoh, H. Fukuyama, Y. Uemura and H. Shiba, (1969) Journ. of Phy. Soc. Jap. 27,1.
29. H. Hasegawa and M. Nakamura (1969) Journ. of Phy. Soc. Jap.26,6.
30. F. Yonezawa, Prog. Theor. Phys. 31 (1964), 357.
31. F. Yonezawa, Prog. Theor. Phys. 40 (1968),734.
32. P. Streda. Czech. J. Phys. B24 (1974) 794.
33. W.Magnus and F. Oberhettinger, Formulas and Theorems For Functions of Mathematical Physics, (Chelsea, N.Y. 1949).
34. J. Doar, unpublished thesis, University of Oregon, (1972).
35. A. Erdelyi, et.al., Tables of Integral Transforms, (McGraw-Hill, 1954).

## APPENDIX A

## SYMBOLS AND NOTATION

$B$  = magnetic flux density

$m$  = mass of the electron

$m^*$  = band effective mass of the electron

$-e$  = charge of the electron

$c$  = speed of light in vacuum

$C$  = impurity concentration factor

$\omega_c$  =  $eB/mc$  = cyclotron frequency

$M$  =  $m/m^*$  = ratio of electron mass to effective mass

$k_b$  = Boltzmann's constant

$g_s$  = electron spin gyromagnetic ratio

$G$  =  $g_s/4$

$\mu_s$  =  $g_s \mu_B \hbar / 4$  = electron spin magnetic moment

$\mu_B$  =  $e \hbar / 2mc$  = Bohr magneton

$\delta$  =  $m \omega_c / \hbar$

$\lambda$  =  $G \hbar \omega_c$

$\lambda^*$  =  $\hbar \omega_c^* / 2$

$D$  =  $e \sqrt{m^*} / \hbar^2 c$

$c^*$  =  $\hbar^2 / 2 m^*$

$\text{Tr}$  = sum over a complete set of states

$T$  = temperature

$T_d$  = Dingle temperature =  $|\mathcal{E}_I| / \pi k_B$

$\beta$  =  $1/k_b T$



$\Omega$  = thermodynamic potential

$M$  = magnetization

$\bar{\chi}$  = susceptibility

$\chi$  = differential susceptibility

$\bar{A}$  = vector potential

$\bar{\epsilon}_n = (n + \frac{1}{2}) \hbar \omega_c - \sigma G \hbar \omega_c - \mu$  = Landau level energy referenced  
to the chemical potential

$\bar{\alpha}_n = \epsilon_n + \epsilon_R - \mu$  = impurity shifted LL energy  
referenced to the chemical potential

$\beta_e = (2l + 1) \pi / \beta$

$\sigma = \pm 1$

## APPENDIX B

## INTEGRAL REPRESENTATION FOR THE LOGARITHM

Consider 
$$\sum_{l=-\infty}^{\infty} \ln [g(i f_l)]$$

where

$$g(i f_l) = \bar{\xi}_\alpha + \xi'(i f_l) - i f_l$$

$$f_l = (2l+1)\pi/\beta$$

(B-1)

The sum over  $l$  may be replaced by two contour integrals, viz.

$$\sum_{l>0} g(f_l) = \frac{1}{2\pi i} \int_{C_1} dz g(z) f(z)$$

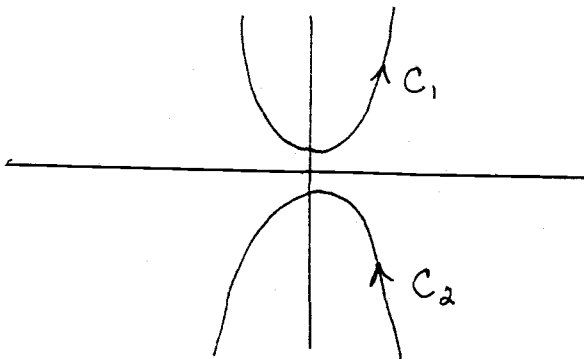
$$\sum_{l<0} g(f_l) = \frac{1}{2\pi i} \int_{C_2} dz g(z) f(z)$$

(B-2)

where  $f(z)$  is a function which has poles at  $z = (2l+1)\pi/\beta$  along the imaginary axis and has a unit residue at these poles. An example of

such a function is  $f(z) = -\beta / (1 + e^{\beta z})$

The contours  $C_1$  and  $C_2$  are chosen as follows,



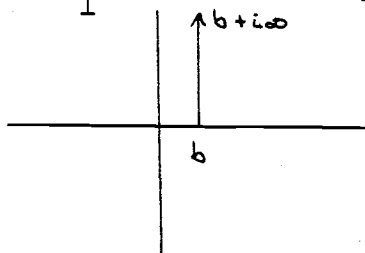
Consider now the following expression,

$$I = \int_{C_1 \text{ OR } C_2} dz f(z) \int_{C'} \frac{e^{-sg} g(z)}{s} ds = 2\pi i \int_{C'} \frac{e^{-sg} g(z)}{s} ds$$

$\begin{matrix} \int_{z_1}^{z_2} \\ \text{OR} \\ \int_{-\infty}^{\infty} \end{matrix}$

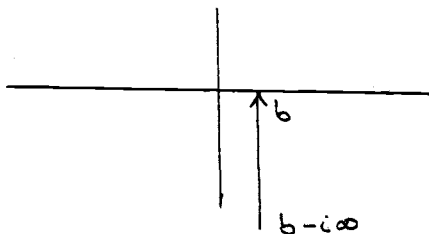
(B-3)

Where for  $C_1$  the contour  $C'$  is taken as,



$$0 < |b| < 1$$

Whereas for  $C_2$  the contour  $C'$  is taken to be,



$$0 < |b| < 1$$

This is necessary in order to insure the convergence of some of the integrals which are to follow.

Integration of the left hand side of eq. B-3 by parts allows us to write,

$$\int_{C'} ds \int_{C_1/C_2} dz f(z) e^{-sg} g(z) = \int_{C'} \frac{ds}{s} \left[ e^{-sg} F \Big|_{z_1}^{z_2} + \int_{C_1/C_2} F s e^{-sg} g' dz \right]$$

(B-4)

where  $F'(z) = f(z)$

Thus,

$$\begin{aligned}
 I &= \int_{c_1}^{c_2} \frac{ds}{s} \int_{c_1/c_2} F(z) e^{-sq(z)} d[q(z)] \\
 &= \int_{c_1/c_2} F(z) dq \left\{ -\frac{e^{-sq}}{q} \Big|_b^{b+i\infty} \text{ or } \Big|_{b-i\infty}^b \right\} \\
 &= \int_{c_1/c_2} F(z) dq \left\{ \frac{1}{q} - C_1 \right\} = \pm \int_{c_1}^{c_2} F(z) d(\ln q)
 \end{aligned}$$

(B-5)

Integrating by parts once again allows us to write,

$$I = \pm \int_{c_1/c_2} f(z) \ln q(z) = 2\pi i \left\{ -\sum_{\rho \in \mathcal{P}} \ln q(i\rho) + \sum_{\rho \in \mathcal{Q}} \ln q(i\rho) \right\}$$

(B-6)

Thus we have shown that,

$$\begin{aligned}
 \sum_{\rho \in \mathcal{P}} \ln q(i\rho) &= -\sum_{\rho \in \mathcal{P}} \int_b^{b+i\infty} \frac{e^{-sq(i\rho)}}{s} ds \\
 \sum_{\rho \in \mathcal{Q}} \ln q(i\rho) &= \sum_{\rho \in \mathcal{Q}} \int_{b-i\infty}^b \frac{e^{-sq(i\rho)}}{s} ds
 \end{aligned}$$

(B-7)

## APPENDIX C

## INTEGRAL EVALUATION

The form of the integral which must be analyzed is,

$$I_{\nu}(\alpha, \Sigma) = \int_b^{b+i\infty} \frac{e^{-st}}{s^{\nu}} ds + \int_{b-i\infty}^b \frac{e^{-st^*}}{s^{\nu}} ds$$

where,

$$t = \alpha + i \Sigma, \quad \Sigma < 0, \quad 0 < |b| < 1$$

(C-1)

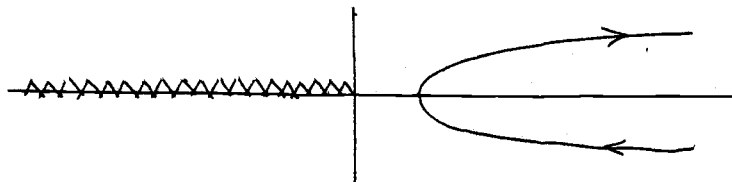
Our basic assumption in dealing with this integral is that it is an analytic function of the parameter  $\nu$ . Therefore we shall deform the contour to lie along the real axis, evaluate the resulting integrals along the real axis for values for which they are convergent and then analytically continue the result to all values of  $\nu$  for the original complex contour integral.

In deforming the contours to lie along the real axis, we make use of the fact that the contributions from the infinite arcs which result from the deformation yield zero in each quadrant if the following conditions hold on  $\alpha$  and  $\Sigma$ .

$$\left| \int_{\text{ARC}} \frac{e^{-st}}{s^{\nu}} ds \right| < \infty \implies$$

$\alpha, \Sigma < 0$	$\alpha > 0, \Sigma < 0$
$\alpha < 0$ $\Sigma > 0$	$\alpha, \Sigma > 0$

Thus for  $\alpha > 0$ , our contour becomes

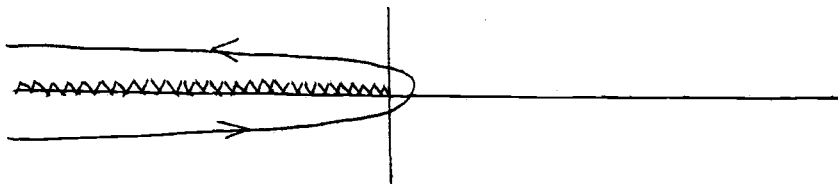


and the integral reduces to

$$\begin{aligned}
 I_\nu &= \int_0^\infty \frac{e^{-xt}}{x^\nu} dx + \int_\infty^0 \frac{e^{-xt^*}}{x^\nu} dx & \nu > 1 \\
 &= -2i \int_0^\infty \frac{e^{-\alpha x} \sin \Sigma x}{x^\nu} dx \\
 &\equiv -2i S_\nu(\alpha, \Sigma) & \alpha > 0
 \end{aligned}$$

(C-2)

while for  $\alpha < 0$ , the contour becomes



and the integral reduces to

$$\begin{aligned}
 I_\nu &= \int_{-\infty}^0 \frac{e^{-xt^*}}{e^{-i\pi\nu} |x|^\nu} dx + \int_0^{-\infty} \frac{e^{-xt}}{e^{-i\pi\nu} |x|^\nu} dx & \nu > 1 \\
 &= 2i \int_0^\infty \frac{e^{\alpha x} \cos \Sigma x}{x^\nu} dx \\
 &\equiv 2i C_\nu(-\alpha, \Sigma) & \alpha < 0
 \end{aligned}$$

(C-3)

Therefore, for all  $\alpha$ , I may be written as,

$$I_{\nu} = 2i \left[ -\Theta(\alpha) S_{\nu}(\alpha, \xi) + \Theta(-\alpha) C_{\nu}(-\alpha, \xi) \right]$$

(C-4)

Now for  $\nu > 1$ , the integrals  $S_{\nu}$  and  $C_{\nu}$  may be done explicitly and yield<sup>(35)</sup>,

$$S_{\nu}(\alpha, \xi) = \Gamma(1-\nu) \left[ (\alpha^2 + \xi^2)^{\frac{\nu-1}{2}} \sin \left[ (1-\nu)\phi_s \right] \right]$$

$$C_{\nu}(-\alpha, \xi) = \Gamma(1-\nu) \left[ (\alpha^2 + \xi^2)^{\frac{\nu-1}{2}} \cos \left[ (1-\nu)\phi_c \right] \right]$$

$$\phi_s = \arg[\alpha + i\xi] \quad , \quad \phi_c = \arg(-\alpha + i\xi)$$

(C-5)

For values of  $\nu = 1/2$  and  $5/2$  we find,

$$\sin \left[ -\frac{3}{2}\phi_s \right] = -\frac{1}{\sqrt{2}} G^{3/2} \frac{|\xi|}{\xi} \left[ |\xi| [G+\alpha]^{1/2} + \alpha [G-\alpha]^{1/2} \right]$$

$$\cos \left[ -\frac{3}{2}\phi_c \right] = -\frac{1}{\sqrt{2}} G^{3/2} \left[ |\xi| [G-\alpha]^{1/2} - \alpha [G+\alpha]^{1/2} \right]$$

$$\sin \left[ \phi_s/2 \right] = \frac{1}{\sqrt{2}} \frac{[G-\alpha]^{1/2}}{G^{1/2}}$$

$$\cos \left[ \phi_c/2 \right] = \frac{1}{\sqrt{2}} \frac{[G+\alpha]^{1/2}}{G^{1/2}}$$

$$G = [\alpha^2 + \xi^2]^{1/2}$$

(C-6)

Therefore,

$$S_{5/2}(\alpha, \xi') = -\frac{4}{3} \frac{\sqrt{\pi}}{\sqrt{2}} \frac{\xi'}{|\xi'|} \left[ |\xi'| (G+\alpha)^{1/2} + \alpha (G-\alpha)^{1/2} \right]$$

$$S_{1/2}(\alpha, \xi') = \sqrt{\pi/2} \frac{(G-\alpha)^{1/2}}{G}$$

$$C_{5/2}(\alpha, \xi') = -\frac{4}{3} \frac{\sqrt{\pi}}{\sqrt{2}} \left[ |\xi'| (G-\alpha)^{1/2} - \alpha (G+\alpha)^{1/2} \right]$$

$$C_{1/2}(\alpha, \xi') = \sqrt{\pi/2} \frac{(G+\alpha)^{1/2}}{G}$$

(C-7)

We may note some useful properties of the above function,

$$S_{\nu}(\alpha, \xi') = -S_{\nu}(\alpha, -\xi')$$

$$C_{\nu}(\alpha, \xi') = C_{\nu}(\alpha, -\xi')$$

$$S_{\nu}(\alpha, \xi) = C_{\nu}(-\alpha, \xi')$$

(C-8)

So that finally  $I_{\nu}$  may be simply written as,

$$I_{\nu}(\alpha, \xi < 0) = 2i \left[ \theta(\alpha) S_{\nu}(\alpha, |\xi'|) + \theta(-\alpha) S_{\nu}(\alpha, |\xi'|) \right]$$

$$= 2i S_{\nu}(\alpha, |\xi'|)$$

$$= 2i C_{\nu}(-\alpha, |\xi'|)$$

(C-9)



## APPENDIX D

## OUTLINE OF RODE'S CALCULATION

The approach taken by Rode<sup>(9)</sup> to calculate  $\chi$  in the QL for an interacting system begins with the expression for the density of states for a system of non-interacting electrons at zero-temperature, viz.,

$$\rho(E) = \frac{e B \sqrt{2m^*}}{h^2 c} \sum_{n,\sigma} [E - \bar{\epsilon}_n]^{-1/2} \Theta [E - \bar{\epsilon}_n] \quad (D-1)$$

As expected from the discrete nature of the LL's,  $\rho(\epsilon)$  diverges whenever  $E = \bar{\epsilon}_n$ .

The density of states function may be used to find  $\Omega$  according to

$$\Omega = - \frac{1}{\beta} \int_{-\infty}^{\infty} \rho(\epsilon) \ln [1 + e^{-\beta(\epsilon - \mu)}] \quad (D-2)$$

Integrating by parts twice allows this expression to be put into the form,

$$\Omega = - \int_{-\infty}^{\infty} \left( - \frac{\partial f}{\partial \epsilon} \right) G(\epsilon) d\epsilon \quad (D-3)$$

where,  $f(\epsilon) = \frac{1}{1 + e^{\beta(\epsilon - \mu)}}$

(D-4)

and

$$G(E) = \int_{-\infty}^E \int_{-\infty}^x f(y) dy dx \quad (D-5)$$

in the limit that  $T \rightarrow 0$ ,  $-\frac{\partial f}{\partial \xi} = \delta(\xi - \mu)$  and we see that

$$\Omega(T=0, T_D=0) = G(\mu) \quad (D-6)$$

The function  $G(E)$  may be calculated explicitly and Rode finds,

$$G(E) = \frac{4e\beta}{3h^2c} \sqrt{2m^*} \sum_{n,\sigma} [E - \bar{\epsilon}_n]^{3/2} \Theta [E - \bar{\epsilon}_n]$$

$$\Omega_0 = G(\mu) \quad (D-7)$$

From  $\Omega_0$  the susceptibility for the zero-temperature, non-interacting system is calculated according to the usual prescription with the result,

$$\chi(T=0, T_D=0) = \frac{4e}{h^2c} \sqrt{2m^*} \left[ \mu_0^a \beta \sum_{n,\sigma} \frac{[(n+1/2)M - \sigma G]^2}{[\mu - \bar{\epsilon}_n]^{1/2}} \right]^2 \quad (D-8)$$

The claim is then that the effects of both temperature and scattering are similar in that they both cause a spreading of the energy and therefore may both be taken into account by using the appropriate convolution function.

For temperature, the appropriate function is

$$\phi_1(\xi) = -\frac{\partial f}{\partial \xi} = \frac{\beta}{2} \frac{1}{[1 + \cosh \beta \xi]} \quad (D-9)$$

while for scattering the choice is,

$$\phi_a(\varepsilon) = \frac{\Gamma}{\pi} \frac{1}{[\varepsilon^2 + \Gamma^2]} \quad (\Gamma = \pi k_B T_D)$$

(D-10)

The claim is then that for non-zero temperature and non-zero scattering, the susceptibility may be obtained from the zero-temperature, zero-scattering susceptibility according to,

$$\chi(\mu, T, T_D) = \int_{-\infty}^{\infty} \int_{-\infty}^{\infty} \phi_1(\varepsilon) \phi_a(\varepsilon') \chi[\mu + \varepsilon + \varepsilon', 0, 0] d\varepsilon d\varepsilon'$$

(D-11)

He finds that either the  $\varepsilon$  or  $\varepsilon'$  integrals may be done first, but that once one is performed, the second appears intractable and thus must be performed by numerical methods.

He chooses to perform the  $\varepsilon'$  integration first and finds from this that the zero-temperature, non-zero scattering susceptibility is,

$$\chi(\mu, T_D, 0) = \sum_{n, \sigma} D C_n^2 B \left[ \frac{(G(\alpha) - \alpha)^{1/2}}{G(\alpha)} \right] - 4 D C_n [G(\alpha) - \alpha]^{1/2}$$

(D-12)

where the notation is the same as in chapter three.

Finite temperature is then incorporated into the calculation by numerically integrating the following convolution integral,

$$\chi(\mu, T_D, T) = \int_{-\infty}^{\infty} \phi_1(\varepsilon) \chi(\varepsilon, T_D, 0) d\varepsilon$$

(D-13)

## APPENDIX E

CALCULATION OF  $G_a^0(r, r')$ 

As stated previously,  $G_a^0(r, r')$  may be expressed in terms of the LL states as

$$\hbar G_a^0(\bar{r}, \bar{r}') = \sum_{\alpha} \frac{\Psi_{\alpha}(\bar{r}) \Psi_{\alpha}(\bar{r}')}{i\gamma_{\alpha} - \bar{\epsilon}_{\alpha}} \quad (\text{E-1})$$

where,

$$\gamma_{\alpha} = (2l+1)\pi/\beta, \quad \bar{\epsilon}_{\alpha} = (n+1/2)\hbar\omega_c^* + c^*k_z^2 + \sigma G\hbar\omega_c - \mu \quad (\text{E-2})$$

and

$$\Psi_{\alpha}(\bar{r}) = \frac{1}{\sqrt{L_x L_z}} \left(\frac{\gamma}{\pi}\right)^{1/4} (2^n n!)^{-1/2} e^{i k_x x} e^{i k_z z} e^{-\gamma/2 (y-y_0)^2} H_n[\sqrt{\gamma}(y-y_0)]$$

$$\gamma = \frac{eB}{\hbar c} = \frac{m\omega}{\hbar}, \quad k_x = \gamma y_0 \quad (\text{E-3})$$

The sum over  $k_x$  may be converted to an integral over  $y_0$  as follows,

$$\sum_{k_x} = \frac{L_x}{2\pi} \int_{-\infty}^{\infty} dk_x = \frac{L_x \gamma}{2\pi} \int_{-\infty}^{\infty} dy_0 \quad (\text{E-4})$$

Thus we have,

$$\sum_{k=0}^{\infty} \frac{\Psi_a(\bar{z}) \Psi_a(\bar{z}')}{i \rho e^{-\bar{z} a}} = A \int_{-\infty}^{\infty} e^{-i \delta y_0 \delta x} e^{-\delta/2(y-y_0)^2} e^{-\delta/2(y'-y_0)^2} H_n[\sqrt{\delta}(y-y_0)] \times H_n[\sqrt{\delta}(y'-y_0)] dy_0$$

(E-5)

where,

$$A = \delta/2\pi L z (\delta/2\pi)^{1/2} \frac{1}{2^n n!} \frac{e^{-i k z \delta z}}{i \rho e^{-\bar{z} a}}$$

$$\delta x = (x' - x), \delta y = (y' - y), \delta z = z' - z$$

A change of variable puts this last expression into the form,

$$\frac{A e^{-i \delta \delta x \cdot \gamma} e^{-\delta/2(\delta y)^2}}{\sqrt{\delta}} \int_{-\infty}^{\infty} e^z (i\sqrt{\delta} \delta x - \sqrt{\delta} \delta y) e^{-z^2} H_n(z) H_n(z + \sqrt{\delta} \delta y) dz$$

(E-6)

We will now focus our attention on the following integral,

$$I = \int_{-\infty}^{\infty} e^{(a-b)z} e^{-z^2} H_n(z) H_n(z+b) dz$$

(E-7)

where,  $a = i\sqrt{\delta} \delta x, b = \sqrt{\delta} \delta y$

By using an integral representation for  $H_n(z+b)$ ,<sup>(17)</sup>

$$H_n(z+b) = \frac{n!}{2\pi i} \int_c \frac{e^{2(z+b)t - t^2}}{t^{n+1}} dt$$

(E-8)

( the contour chosen in eq. E-8 is such that it encloses the origin in a counterclockwise direction ) and completing the square of the terms which result in the exponential, we are able to generate the following form,

$$I = \frac{n!}{2\pi i} \int_c dt \frac{e^{-t^2}}{t^{n+1}} e^{[t + \frac{(a-b)}{2}]^2} e^{abt} \int_{-\infty}^{\infty} e^{-[z - (t - \frac{[a-b]}{2})]^2} H_n(z) dz \quad (E-9)$$

The integral over  $z$  is standard<sup>(26)</sup> and has the value,

$$\sqrt{\pi} \left[ t + \frac{(a-b)}{2} \right]^n 2^n \quad (E-10)$$

When this result is used in eq. E-6, we obtain

$$I = \frac{n!}{2\pi i} \sqrt{\pi} 2^n e^{\frac{(a-b)^2}{4}} \int_c dt \frac{e^{t(a+b)}}{t^{n+1}} \left[ t + \frac{(a-b)}{2} \right]^n dt \quad (E-11)$$

Another change of variable yields the form,

$$I = \frac{n! \sqrt{\pi} 2^n e^{\frac{(a-b)^2}{4}}}{2\pi i} \int_c \frac{e^{-t} \left[ t - \frac{(a-b)(a+b)}{2} \right]^n}{t^{n+1}} dt \quad (E-12)$$

By making use of the following integral representation of the Laguerre function<sup>(17)</sup>,

$$L_n^{(\alpha)}(x) = \frac{1}{2\pi i} \frac{1}{x^\alpha} \int_c \frac{e^{-t} (t+x)^{n+\alpha}}{t^{n+1}} dt \quad (E-13)$$

and performing some algebraic simplifications, we are able to deduce that,

$$\sum_{k_z} \frac{\Psi_a(\bar{z}) \Psi_a^*(\bar{z}')}{i p_a - \bar{\epsilon}_a} = \frac{\gamma}{2\pi L_z} e^{-\frac{\gamma p^2}{4}} L_n^{(\sigma)}\left(\frac{\gamma p^2}{2}\right) e^{-\frac{i\gamma}{2} \delta x (\gamma + \gamma')} \frac{e^{i k_z (z - z')}}{i p_a - \bar{\epsilon}_a} \quad (\text{E-14})$$

The sum over  $k_z$  is equivalent to  $\frac{L_z}{2\pi} \int_{-\infty}^{\infty} dk_z$  and the resulting integral,

$$\int_{-\infty}^{\infty} dk_z \frac{e^{i k_z (z - z')}}{i p_a - [c^* k_z^2 + \bar{\epsilon}_n]} \quad (\text{E-15})$$

where,

$$\bar{\epsilon}_n = (n + 1/2) \hbar \omega_c^* + \sigma G \hbar \omega_c - \mu$$

is most easily done by means of contour techniques. The result of the contour integration is

$$- \frac{i\pi}{c^*} \frac{e^{i \bar{k}_z |z - z'|}}{\bar{k}_z} \quad (\text{E-16})$$

where, 
$$\bar{k}_z = \frac{1}{c^{*1/2}} [i p_a - \bar{\epsilon}_n]^{1/2}$$

The branch of the square root function implied in eq. E-16 is the one which has a positive imaginary part.

Summarizing the results so far, we may state that,

$$\hbar G_z^0(\bar{z}, \bar{z}') = -\frac{i\pi\gamma}{(2\pi)^2 c^*} e^{-\frac{\gamma p^2}{4}} e^{-\frac{\gamma}{2} \delta x (\gamma + \gamma')} \sum_{\substack{n=0 \\ \sigma=\pm 1}}^{\infty} \frac{e^{i k_z |z - z'|}}{\bar{k}_z} L_n^{(\sigma)}\left(\frac{\gamma p^2}{2}\right) \quad (\text{E-17})$$

The sum over  $n$  will be done using the Poisson sum formula which when applied to eq. E-17 yields,

$$\sum_{n=0}^{\infty} e^{-\frac{\gamma p^2}{4}} L_n^{(0)}\left(\frac{\gamma p^2}{2}\right) \frac{e^{i\bar{k}_z |z-z'|}}{\bar{k}_z} = \sum_{\kappa=-\infty}^{\infty} \int_{-1/2}^{\infty} dx e^{-\frac{\gamma p^2}{4}} {}_1F_1(-\kappa, 1, \frac{\gamma p^2}{2}) \frac{e^{i\bar{k}_z(x, \Omega) |z-z'|}}{\bar{k}_z(x, \Omega)} \cdot e^{2\pi i \kappa x}$$

We may expand  ${}_1F_1(-\kappa, 1, z)$  as <sup>(17)</sup>,

$${}_1F_1(-\kappa, 1, z) e^{-z/2} = \sum_{m=0}^{\infty} A_m(x) (1+2x)^{-m/2} J_m(2\sqrt{z(x+1/2)}) \quad (\text{E-18})$$

where the coefficients satisfy the following recursion relation,

$$A_{m+1}(x) = \left(\frac{n}{n+1}\right) A_{m-1} - (2x+1) A_{m-2}$$

$$A_0 = 1, \quad A_1 = 0, \quad A_2 = 1/2 \quad (\text{E-19})$$

An explicit evaluation of the first few shows that,

$$A_3 = -(2x+1) \qquad A_5 = -\frac{13}{10} (2x+1)$$

$$A_4 = \frac{3}{8} - (2x+1) \qquad A_6 = -2(2x+1) + (2x+1)^2 \quad (\text{E-20})$$

We can see from the pattern which is being generated that the order of the coefficients is,

$$A_m(x) \sim O(2x+1)^{L(m)} \quad (\text{E-21})$$

where  $L(m)$  is the largest integer  $\leq m/3$ .

Therefore the total  $x$  dependent coefficient multiply the Bessel function is of the order

$$A_m(x) (1+2x)^{-m/2} \sim O[2x+1]^{L(m)-m/2} \quad (\text{E-22})$$



This argument assures us that for those values of  $x$  for which we expect the integral to have its main contributions, the first term in the series will be adequate to represent  ${}_1F_1(-x, 1, z)$ .

We therefore make the following replacement,

$${}_1F_1(-x, 1, z) e^{-z/2} \approx J_0 \left[ 2\sqrt{z(x+1/2)} \right] \quad (\text{E-23})$$

Furthermore, in applying the Poisson sum formula we see that there are two contributions which arise - the  $k=0$  steady-state term and the  $k \neq 0$  oscillatory term.

From a physical point of view we note that the  $k \neq 0$  terms will produce oscillations with an already oscillatory effect. We therefore chose to neglect the  $k \neq 0$  terms in what follows.

Taking these points into consideration allows us to write,

$$\frac{1}{\hbar} G_{\alpha}^0(\bar{a}, \bar{a}') = \frac{-i\pi\delta}{(2\pi)^2 c^{*1/2}} e^{-\frac{i\gamma}{2}(x'-x)(y'+y)} \int_{-1/2}^{\infty} dx e^{\frac{i [i\gamma_{\alpha} - \bar{\epsilon}_x]^{1/2} |z-z'|/\sqrt{c^*}}{(i\gamma_{\alpha} - \bar{\epsilon}_x)^{1/2}}} \cdot J_0 \left[ \gamma \sqrt{2\delta(x+1/2)} \right] \quad (\text{E-24})$$

The change of variable  $\tau = [2\delta(x+1/2)]^{1/2}$  converts the integral into the following form,

$$\frac{1}{\delta} \int_0^{\infty} \frac{e^{-[\tau^2 - k_{\alpha}^2]^{1/2} |z-z'|}}{i [\tau^2 - k_{\alpha}^2]^{1/2}} \tau J_0(\gamma\tau) d\tau \quad (\text{E-25})$$

where,

$$k_{\alpha}^2 = \frac{\mu - \sigma G \hbar \omega_c + i\gamma_{\alpha}}{c^*} \quad (\text{E-26})$$

Again the branch of the square root which is implied in eq. E-26 is that with the positive imaginary part.

This integral is of standard form<sup>(33)</sup> and is equal to,

$$\frac{1}{i\delta} \frac{e^{i k_d |\bar{r} - \bar{r}'|}}{|\bar{r} - \bar{r}'|}$$

(E-27)

so that we may finally write,

$$\frac{1}{\hbar} G_2^0(\bar{r}, \bar{r}') = \frac{-1}{4\pi c^*} e^{-\frac{i\delta}{a}(x'-x)(y'+y)} \frac{e^{i k_d |\bar{r} - \bar{r}'|}}{|\bar{r} - \bar{r}'|}$$

(E-28)

## APPENDIX F

## CALCULATION OF S (r, r')

The quantity  $S_{\alpha\alpha'}$  has been defined as,

$$S_{\alpha\alpha'}(\bar{n}, \bar{n}') = \int \Psi_{\alpha}(\bar{n} + \bar{n}_i) e^{i\delta\gamma_i(x-x')} \Psi_{\alpha'}(\bar{n}' + \bar{n}_i) d^3 n_i \quad (\text{F-1})$$

which in terms of the LL's themselves may be written as,

$$S_{\alpha\alpha'} = \left(\frac{\delta}{\pi}\right)^{1/2} \left[ \frac{1}{2^{n+n'}} \frac{1}{n!n'} \right]^{1/2} \begin{matrix} \delta_{k_x, k_x'} \\ \delta_{k_z, k_z'} \end{matrix} e^{i k_x(x'-x)} e^{i k_z(z'-z)} \cdot \text{I} \quad (\text{F-2})$$

where

$$\text{I} = \int_{-\infty}^{\infty} e^{-\frac{\gamma}{2}(y+\gamma_i-\gamma_0)^2} e^{-\frac{\gamma}{2}(y'+\gamma_i-\gamma_0)^2} e^{i\delta\gamma_i(x-x')} H_n[\sqrt{\delta}(y+\gamma_i-\gamma_0)] \cdot H_{n'}[\sqrt{\delta}(y'+\gamma_i-\gamma_0)] d\gamma_i \quad (\text{F-3})$$

In this last expression, the trivial  $x_i$  and  $z_i$  integrations have been done and have led directly to the diagonality of S in the  $k_x$  and  $k_z$  quantum numbers.

A change of variable puts I into the form,

$$\text{I} = \frac{1}{\sqrt{\delta}} \int_{-\infty}^{\infty} e^{-z^2/\delta} e^{-\frac{(z+\sqrt{\delta}\delta\gamma)^2}{\delta}} e^{-i\delta[z/\sqrt{\delta} + \gamma_0 - \gamma]\delta x} H_n(z) H_{n'}(z + \sqrt{\delta}\delta\gamma) \cdot dz \quad (\text{F-4})$$

We now replace the Hermite polynomial by its integral representation, complete the square and obtain after some simplification,

$$I = \frac{n!}{\sqrt{\delta}} 2^n \sqrt{\pi} e^{-\frac{\delta(\delta y)^2}{2}} e^{-i\delta(y_0-y)\delta x} e^{A^2/4} I'$$

(F-5)

where,

$$I' = \frac{1}{2\pi i} \int_c \frac{e^{-At} e^{2t\sqrt{\delta}\delta y}}{t^{n'+1}} \left(t - \frac{A}{2}\right)^n dt$$

$$A = \sqrt{\delta}(\delta y + i\delta x) \\ = i\sqrt{\delta} \rho e^{-i\phi}$$

$$\rho = [(\lambda' - \lambda)^2 + (\gamma' - \gamma)^2]^{1/2} \quad \phi = \tan^{-1} \left( \frac{\gamma' - \gamma}{\lambda' - \lambda} \right)$$

(F-6)

Another change of variable converts  $I'$  into the form,

$$I' = \frac{1}{2\pi i} \left(\frac{A}{2}\right)^\nu (-1)^\nu \int_c \frac{e^{-t}}{t^{n'+1}} \frac{[t + A/2(2\sqrt{\delta}\delta y - A)]^{n'+\nu}}{[A/2(2\sqrt{\delta}\delta y - A)]^\nu}$$

$$\nu = n - n'$$

(F-7)

We again recognize the appearance of the integral representation for the Laguerre function and deduce that,

$$I' = (-1)^\nu \left(\frac{A}{2}\right)^\nu L_n^\nu \left[ \frac{A}{2} (2\sqrt{\delta}\delta y - A) \right]$$

(F-8)

where we have assumed that  $n > n'$ .

Combining all of these results, we find that

$$S_{\alpha\alpha'} = \frac{\sqrt{n'!}}{\sqrt{n!}} (-1)^{n-n'} \delta_{k_x, k_x'} \delta_{k_z, k_z'} e^{i k_z \delta k_z} e^{i \gamma y \delta x} e^{\frac{i \delta}{2} \delta x \delta y} \\ \times \left( i \int \sqrt{\delta/2} e^{-i\phi} \right)^{\nu} e^{-\gamma \int^2/4} L_n^{\nu} \left( \gamma \int^2/2 \right).$$

(F-9)

For the case  $n < n'$ , we repeat the procedure but this time we replace  $H_n$  by its integral representation rather than  $H_{n'}$ , with the result that  $n$  and  $n'$  are exchanged in eq. F-9.